



Handling Shadow Effects on Greenness Indices from Multispectral UAV Imagery

A thesis submitted to the School of Forest Science and Resource Management
Sustainable Resource Management Program in partial fulfillment of the requirements for
the degree of Master of Science

By

Sukhveen Kaur

Matriculation No. - 03697968

Supervisor

Dr Marvin Lüpke

Mr Lars Uphus

Chair of Ecoclimatology
Technical University of Munich

15.09.2020

Acknowledgement

I am glad that I can extend my deepest gratitude to all the people without whom this journey to complete this dissertation and my master degree would not have been possible.

First of all, I would like to express my sincere gratitude to my supervisor Mr Lars Uphus for his valuable advice, understanding, time and words of encouragement which motivated me to work harder and accomplish this thesis. I would like to thank you for scrutinizing my work and giving me insightful suggestions which helped me to analyze my thought process and it helped me to take my work to the next level and overcome my shortcomings.

Secondly, I would like to thank my second supervisor Dr Marvin Lüpke for his valuable feedback and words of encouragement to improve my work and complete this thesis on time.

Thirdly, I would like to thank the faculty of Ecoclimatology, Technical University of Munich for giving me an opportunity to work with them and for providing data for my thesis.

Lastly, I would like to thank my family for their words of encouragement and their continuous support to complete my thesis and journey at the Technical University of Munich.

Contents

Acknowledgement	ii
Contents	iii
List of Figures	v
List of Maps	vi
List of Tables	vii
List of Abbreviations	viii
Abstract	ix
Chapter – 1 Introduction	1
1.1. Need for Shadow Detection	2
1.2. Objectives	2
1.3. Scope	2
1.4. Thesis Outline	3
Chapter – 2 Literature Review	6
2.1. Shadows	6
2.2. Shadow Detection Methods	7
2.2.1. Unsupervised Classification	7
2.2.2. Supervised Classification	8
2.2.3. Threshold Classification	9
2.2.4. Vegetation Indices	9
2.3. Case Study	10
2.3.1. Rapeseed Oil Project, China	10
2.3.2. Vineyard Project, USA	11
2.3.3. Conclusion	12
Chapter – 3 Methodology	13
3.1. Data Identification and Collection	13
3.2. Methodology	15
3.2.1. Unsupervised Classification	19
3.2.2. Supervised Classification	19
3.2.3. Threshold Classification	20
3.2.4. Vegetation Indices Threshold Classification	21
Chapter – 4 Results	22

4.1. Unsupervised Classification	22
4.2. Supervised Classification	34
4.3. Threshold Classification.....	40
4.4. Vegetation Indices Threshold Classification.....	54
Chapter – 5 Discussion	66
Chapter – 6 Conclusion.....	70
Bibliography	72
Annexure 1: Unsupervised Hartigan-Wong Clusters	75
Annexure 2: Unsupervised Lloyd Clusters	78
Annexure 3: Area of the Samples	81
Annexure 4: Overview of Accuracy of Shadow Detection Methods	82
Declaration of Originality	85

List of Figures

Figure 1: Thesis Outline (Own Illustration).....	5
Figure 2: Formation of Shadows (Zhang et al. 2014).....	6
Figure 3: Subset of May 30, 2019 (MicaSense RedEdge-M and Pix4D).....	14
Figure 4: Methodology (Own Illustration)	15

List of Maps

Map 1:	Sample Sets – 30.05.2019 Subset.....	16
Map 2:	Sample Sets – 30.05.2019.....	17
Map 3:	Sample Sets – 11.04.2019.....	18
Map 4:	Hartigan-Wong – Unsupervised Classification.....	24
Map 5:	Lloyd – Unsupervised Classification.....	25
Map 6:	Forgy – Unsupervised Classification.....	26
Map 7:	MacQueen- Unsupervised Classification.....	27
Map 8:	Hartigan-Wong – Unsupervised Classification 30.05.2019.....	29
Map 9:	Lloyd – Unsupervised Classification 30.05.2019.....	30
Map 10:	Hartigan-Wong – Unsupervised Classification 11.04.2019.....	32
Map 11:	Lloyd – Unsupervised Classification 11.04.2019.....	33
Map 12:	Maximum Likelihood – Supervised Classification 30.05.2019.....	35
Map 13:	Random Forest – Supervised Classification 30.05.2019.....	36
Map 14:	Maximum Likelihood – Supervised Classification 11.04.2019.....	38
Map 15:	Random Forest – Supervised Classification 11.04.2019.....	39
Map 16:	Blue Band – Threshold Classification 30.05.2019.....	42
Map 17:	Green Band – Threshold Classification 30.05.2019.....	43
Map 18:	Red Band – Threshold Classification 30.05.2019.....	44
Map 19:	Red Edge Band – Threshold Classification 30.05.2019.....	45
Map 20:	NIR Band – Threshold Classification 30.05.2019.....	46
Map 21:	Blue Band – Threshold Classification 11.04.2019.....	49
Map 22:	Green Band – Threshold Classification 11.04.2019.....	50
Map 23:	Red Band – Threshold Classification 11.04.2019.....	51
Map 24:	Red Edge Band – Threshold Classification 11.04.2019.....	52
Map 25:	NIR Band – Threshold Classification 11.04.2019.....	53
Map 26:	CCCI – Threshold Classification 30.05.2019.....	56
Map 27:	EVI – Threshold Classification 30.05.2019.....	57
Map 28:	GCC – Threshold Classification 30.05.2019.....	58
Map 29:	NDVI – Threshold Classification 30.05.2019.....	59
Map 30:	CCCI – Threshold Classification 11.04.2019.....	62
Map 31:	EVI – Threshold Classification 11.04.2019.....	63
Map 32:	GCC – Threshold Classification 11.04.2019.....	64
Map 33:	NDVI – Threshold Classification 11.04.2019.....	65

List of Tables

Table 1:	Vegetation Indices and application.....	10
Table 2:	Accuracy of Shadow Detection Methods.....	12
Table 3:	Sample Size for Training and Validation.....	15
Table 4:	Confusion Matrix – Unsupervised 30.05.2019 Subset.....	22
Table 5:	Confusion Matrix – Unsupervised 30.05.2019.....	28
Table 6:	Confusion Matrix – Unsupervised 11.04.2019.....	31
Table 7:	Confusion Matrix – Supervised 30.05.2019.....	34
Table 8:	Confusion Matrix – Supervised 11.04.2019.....	37
Table 9:	Confusion Matrix – Threshold 30.05.2019.....	40
Table 10:	Confusion Matrix – Threshold 11.04.2019.....	47
Table 11:	Confusion Matrix – Vegetation Indices 30.05.2019.....	54
Table 12:	Confusion Matrix – Vegetation Indices 11.04.2019.....	60

List of Abbreviations

CCCI	Canopy Chlorophyll Content Index
ET	Evapotranspiration
EVI	Enhanced Vegetation Index
GCC	Green Chromatic Coordinate
HW	Hartigan-Wong
LAI	Leaf Area index
NDVI	Normalized Difference Vegetation Index
NIR	Near-Infrared
RGB	Red, Green, Blue
TUM	Technical University of Munich
UAV	Unmanned Aerial Vehicle
VI	Vegetation Index

Abstract

To monitor and predict variation in phenology, the unmanned aerial vehicle (UAV) has become an evident source to collect data at any required time. The high-resolution data contains information on shadows which are usually treated as an error or misinterpreted by the user which leads to loss or suboptimal utilization of the information. Therefore, it is necessary to detect these shadows. Hence, the objectives of the study were to identify the best method to detect shadows and identify which vegetation indices (VIs) were sensitive to shadows. Unsupervised classification, supervised classification, threshold classification for the multispectral UAV bands and threshold classification for VIs were compared through the results of the two datasets that were obtained in spring 2019. The unsupervised and supervised classification methods showed higher accuracy levels as compared to the threshold classification for bands and VIs. As for the vegetation indices, Canopy Chlorophyll Content Index (CCCI) and Normal Difference Vegetation Index (NDVI) were more sensitive to shadows as compared to Enhanced Vegetation Index (EVI) and Green Chromatic Coordinate (GCC). While comparing shadow detection methods, it was observed that a few parameters such as the size of the study area, time, objectives and desired land covers to be detected need to be given due consideration to decide which method would be best to detect shadows. The results showed a variation in the physical characteristics of shadows throughout the spring season which affected the accuracy of the methods to detect shadows. It also showed that spectral characteristics of shadows were similar to the spectral characteristics of the dormant forest and tree trunks before spring leaf development started, while this changed during the peak season of the spring when the shadows showed similarity with forest. To conclude, this thesis identified the best method to detect shadows and response of vegetation indices to shadows which can be used to provide new insights in studying variation in the phenology.

Chapter – 1

Introduction

Buisson et al. (2017) stated “phenology is the study of the timing of recurring biological events in plants and animals, the causes of their occurrence concerning biotic and abiotic forces, and interactions among phases of the same or different species.” During the early phase of the evolution of phenology, scientists studied only one species at a time, but in the 1970s, the study focus expanded to the ecosystems. In the last three decades, the issue of climate change became a concern for ecologists because they observed changes in the seasonal lifecycle of the vegetation in response to changes in climate variables, disturbances and land management activities (Gordo and Sanz, 2005). In turn, that alters the length of the reproductive phase of vegetation which affects the nutrient utilization and soil resource utilization which in turns affects nutrient content over time, microbial activities, and land surface qualities which may lead to nutrient imbalance and toxicity (Nord and Lynch, 2009).

Phenology data helps to track the amount of vegetation and helps to predict changes in patterns at a landscape and global scale (Buisson et al. 2017). To build a bridge between the ground data and global-scale data, landscape-scale studies were introduced which covers range of ecosystem and land uses over a larger spatial area. To study phenology on a landscape-scale, remote sensing became a reliable source to obtain information. In the 2000s, drones or unmanned aerial vehicle (UAV) gained popularity as it can capture imageries at high spatial resolution with quick flights, easy operation and lower cost compared to full-sized satellite operations e.g. satellite collects data for a spot once in one revolution and would return to same spot only during the second revolution. In recent years, UAVs became an evident instrument to study vegetation phenology and environmental applications because it can produce quantitative remotely sensed information using multispectral and thermal sensors (Berni et al. 2009).

However, a generally considered major problem in remotely sensed imagery is the presence of shadows, because it hinders the accuracy of information extraction, land cover mapping and change detection from the imageries. Shadows become more evident with an increase in spatial resolution of the aerial imagery and could be treated either as a piece of useful or useless information (Shahtahmassebi et al. 2013).

1.1. Need for Shadow Detection

Shadows have become a common problem in remotely sensed imageries because some users overlook the information that can be obtained from the shadows and leave it unread while some treat it as an error in the image processing. Therefore, shadows are either removed or masked from the imageries to minimize the obstruction in the extraction of the rest of the land cover information. But in case the user tries to extract information manually then shadows can easily be misinterpreted because shadows contain incomplete spectral information about the earth cover which can be used to estimate the characteristics of the stand-alone earth surface objects (Shahtahmassebi et al. 2013). In all the cases, handling shadows requires a lot of time, cost and labour and therefore, researchers are constantly researching methods to detect shadows to minimize the loss or suboptimal utilization of the information. Hence, it is necessary to find the best techniques to detect shadows for the optimum utilization of the information for this study.

1.2. Objectives

The foremost objective of this study was to identify and study different methods to detect shadows using spectral characteristics of each band of the multispectral UAV imageries. This helped to identify the best method to detect shadows.

The second objective was to calculate vegetation indices (VIs) using all the multispectral bands and then use it to detect shadows. This helped to identify the VIs that were able to detect shadows and the VIs that misinterpreted the information.

1.3. Scope

As climate change is a rising concern, Landklif aims to study biodiversity and ecosystem functions in different climate zones of Bavaria and find adaptation and mitigation strategies for climate change (Landklif, n.d.). One of the ten Landklif projects studies the effects of climate change on variation in phenology at four scales namely, satellite, UAV, wildlife cameras (which deliver similar data as ‘phenocams’ in other studies) and manual observations. The data for which was collected for nine different forest stands over a climate and land use gradient throughout Bavaria. Out of the nine forest stands across Bavaria, this study focuses on the forest stand near Parsberg.

The UAV multispectral imageries were collected on three different days of the spring, 2019 which were April 11, 2019, April 30, 2019 and May 30, 2019. Out of these three datasets, only two dataset (April 11, 2019 and May 30, 2019) contained shadows which were therefore selected for this study.

1.4. Thesis Outline

Given below is the detailed thesis structure that was followed during the study.

Stage 1: Set objectives – The objectives of the study were set based on the aim to find the best method to detect shadows in the remotely sensed imagery for the spring season, 2019. The objectives of the study were to identify different methods to detect shadows, calculate VIs and then identify each VI response to shadows.

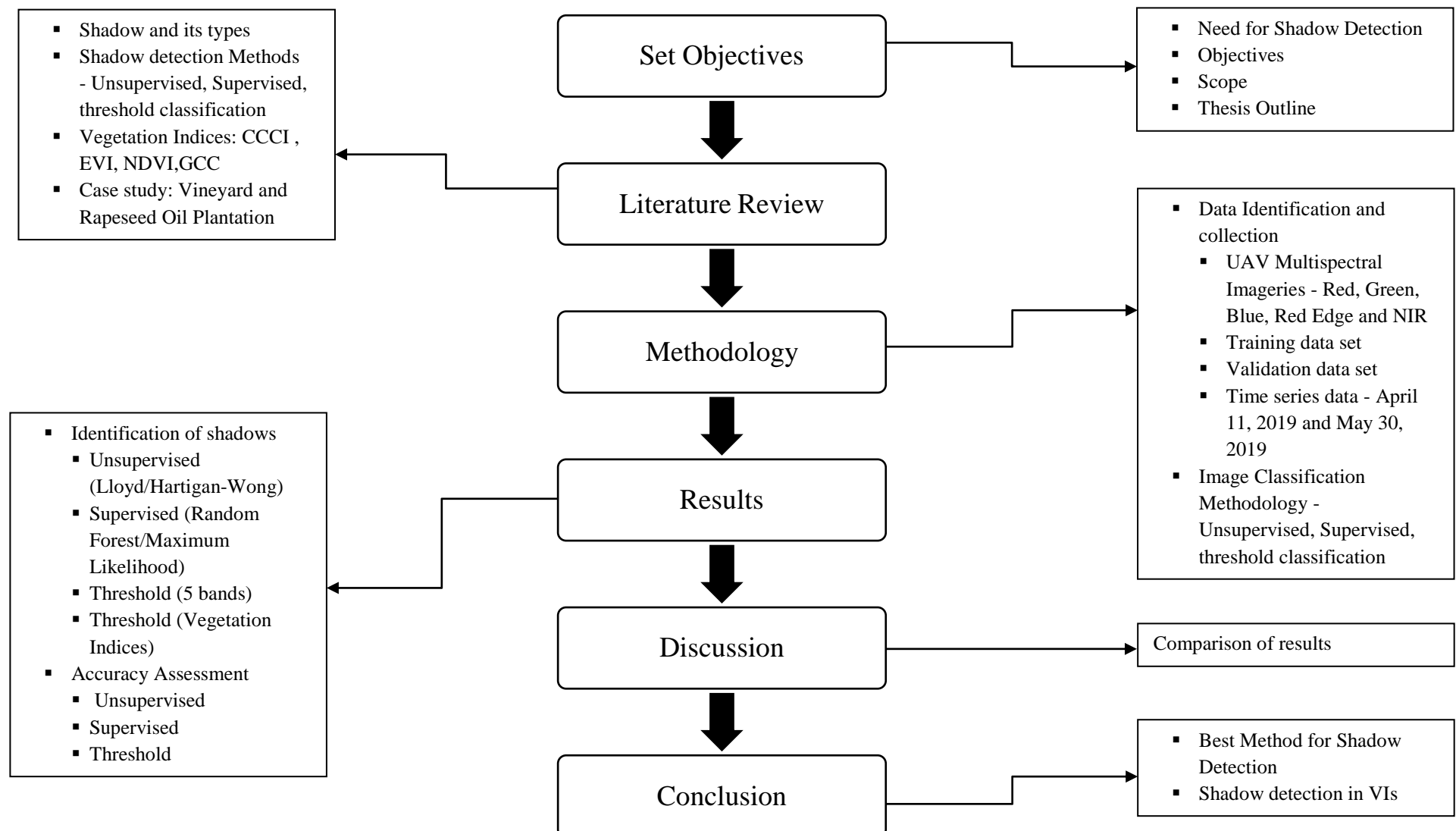
Stage 2: Literature Review – The literature was obtained from journals, books, published articles on internet library and live projects. It helped to understand the concept of the shadow, different methods and algorithms to detect shadows using five bands' spectral signature characteristics. It also covers the theoretical explanation of VIs and application of Canopy Chlorophyll Content Index (CCCI), Enhanced Vegetation Index (EVI), Green Chromatic Coordinate (GCC) and Normalized Difference Vegetation Index (NDVI).

Stage 3: Methodology – It lists the requirements such as 5 bands for two datasets, preparation of training and validation samples for the datasets. It helps to prepare a framework to implement shadow detection methods namely, unsupervised classification, supervised classification and threshold classification and calculate VIs. Also, it would help to reproduce this study in the future.

Stage 4: Analysis Results – The shadows were detected using unsupervised classification (Hartigan-Wong (HW) and Lloyd algorithm), supervised classification (random forest (RF) and maximum likelihood (MLC) algorithm), threshold classification for five bands and VIs and compare it based on their accuracy obtained from the confusion matrix (refer Figure 1).

Stage 5: Discussion – The results were discussed based on the accuracies by the visual interpretation, comparing different methods which helped in identifying the best method.

Stage 6: Conclusion – The last stage of dissertation showed the best method to detect shadows in the multispectral imagery based on the overall accuracy, class-specific accuracy and time required to execute each shadow detection method. It also showed the vegetation indices (VIs) that can detect shadows and the VIs that were not sensitive to shadows and misinterpreted the information.

**Figure 1: Thesis Outline** (Own Illustration)

Chapter – 2

Literature Review

This chapter reviews the literature on the concept of shadows, methods to detect shadows, vegetation indices (VIs) theory, formula applications and case studies to provide a better understanding of the characteristics of shadows in aerial imageries, parameters to filter data, and best practices.

2.1. Shadows

Shadow is a dark patch formed when an object partially or completely obstructs the path of illumination (Pons et al. 2019). There are two types of shadows: cast shadow and self-shadow. The cast shadow is the dark patch formed due to the obstruction of the path of illumination by an object while the self shadow is the part of the object devoid of the direct illumination (refer

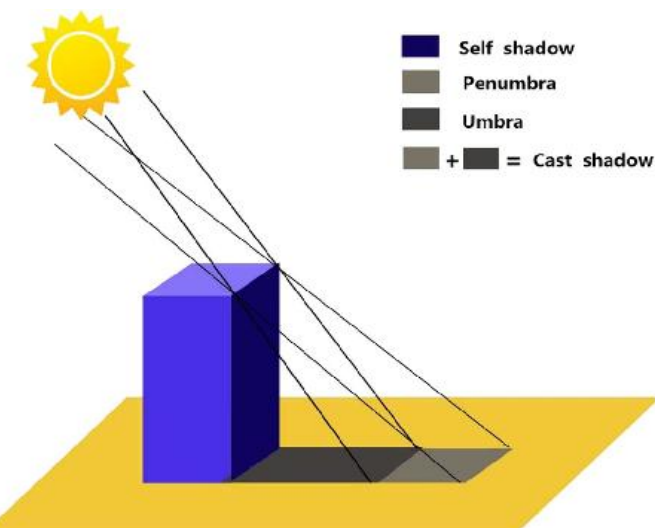


Figure 2: Formation of Shadows (Zhang et al. 2014)

Figure 2). In daily application, the solar eclipse is due to cast shadow while the night on earth is due to the self shadow. The cast shadow has a fully shaded nucleus region which is called the umbra while the partially shaded external region is called the penumbra.

Shadows are created due to hindrance in the direct illumination by urban material, mountain, natural components and cloud in remotely sensed imageries (Pons et al. 2019). Therefore, shadows become an unpreventable part of the remotely sensed image which appears with low brightness, high hue and fuzzy boundaries. Shadows can be of great advantage in analyzing the characteristics of the structure of the objects like height and location by estimating the shadow length and tree crowns. But on the other hand, it can lead to misinterpretation of the information leading to misclassification or loss or distortion of the data (Sanin et al. 2012).

Hence, the study focuses on the cast shadows formed by the trees on various land covers such as pathway, dormant forest, grassland, cropland and forest.

2.2. Shadow Detection Methods

Shadow detection methods can broadly be grouped into two categories: feature-based and model-based. The feature-based method uses the intensity, chromaticity, physical property, geometry, texture and temporal information of the earth surface to give a certain value to the pixels to enable identification of shadows (Shi et al. 2012). The model-based method constructs a model using simulation, objects and light source that are not affected by the image quality and material reflectance and therefore, it requires the user to have prior knowledge of the study region on aspects like illumination angle, time of recording, NDVI index and illumination source which is difficult to obtain in most of the cases. Both the methods require a further input of the in-built algorithm based on which the results within one method can differ. This study focuses on feature-based shadow detection methods because imagery is the only required input without any additional details as it would be required in the model-based method. The shadows can be detected using three feature-based classifications namely; unsupervised classification, supervised classification and threshold classification.

2.2.1. Unsupervised Classification

Unsupervised Classification is a computer-based method in which pixels are grouped into clusters with similar spectral signature values. The clustering of pixels is based on the mean class and covariance matrices. Unsupervised classification focuses on minimizing the variation within a cluster. In this method, the user doesn't require any prior knowledge of the study area and can define the desired number of clusters, the number of iteration, sample size and algorithm for the classification. This method can be used by applying four algorithms such as Hartigan-Wong (1979), Lloyd (1982), Forgy (1965) and Macqueen (1967) (Slonim et al. 2013).

Hartigan-Wong (HW) algorithm works using a local minimum of the sum of squares of the distance between the centres of the clusters. This method is time-saving as it automatically updates the centroid when the point is moved. Lloyd is the simplest and commonly used k-means algorithm in unsupervised classification. It considers the set of observations and groups them into k number of clusters as it minimizes the sum of the squares of the distance between the centroids. Forgy method is also an alternative of k-means unsupervised classification. The difference in this method is that it selects k-random points from data based

on the user's input to create k number of clusters. MacQueen algorithm is also one of the simplest k-means unsupervised methods of classification as it creates a certain number of clusters based on the partitional clustering technique using the mean or center of the data points of the clusters (Slonim et al. 2013).

The study experiments using Hartigan-Wong, Lloyd, Forgy and Macqueen methods of unsupervised classification on a subset from the May 30, 2019 dataset and the two methods out of the four with the better results were selected and used on the main datasets of April 11, 2019 and May 30, 2019. The accuracy of each method was determined using a validation dataset.

2.2.2. Supervised Classification

Supervised Classification is a user-oriented method and therefore, requires prior knowledge of the land cover of the study area. The user is required to generate reference datasets for training based on prior knowledge. The samples are selected from the study area ensuring that the pixel values contain natural spectral values without any disturbances. The classification is performed based on number and type of classes, training set, validation set, mode of classification and algorithm defined by the user. Supervised classification uses the spectral value of the pixels and compares it with a threshold of spectral value of the defined classes and then predicts the class to which the pixel belongs. This method can be executed using two algorithms: Maximum Likelihood (MLC) and Random Forest (RF) (Al Ajmi, 2009).

Random Forest is a simple and diverse method of supervised classification as it can produce the result for classification and regression model. It creates a multitude of decision trees from randomly selected training samples and assigns classes based on the majority of the votes from all the decision tree has made (Liu et al. 2020). It uses meta-algorithm which improves the stability and accuracy of the overall result. Maximum Likelihood algorithm calculates the probability that the given pixel belongs to a certain class based on the assumption that the statistics for each class was distributed normally. If the probability is low than the user-defined class threshold then the pixels remain unclassified (Al Ajmi, 2009).

The study experiments with both the methods (RF and MLC) and use it on datasets of April 11, 2019 and May 30, 2019. The accuracy was estimated using a validation dataset through the built-in function.

2.2.3. Threshold Classification

Threshold classification is a technique to create ranges of values corresponding to the desired type of class by using the spectral values or band ratios i.e. VIs. The user defines the pixel value range bracket for each class through the process of hit and trial technique to find the most accurate range. It is one of the simplest methods of image classification as it doesn't require any prior knowledge of the study area. This method produces results in a short time but the only difficulty is to identify the appropriate threshold values and the difficulty level increases with increase in the size of the study area (Shahtahmassebi et al. 2013).

The study experimented using threshold method which utilized the information from the five bands individually because each band has different minimum-maximum values range based on which the threshold was identified for each land cover class. The accuracy of the threshold classification method was estimated using a validation dataset.

2.2.4. Vegetation Indices

Vegetation Indices (VIs) are the mathematical expressions or transformation of two or more wavebands of the image that enhances the spectral properties of the earth surface (Gilabert et al. 2010). VIs help to study vegetation characteristics such as leaf area, chlorophyll content, nitrogen content, greenness values, water content, biomass, etc. based on which the health, abundance and yield of the vegetation can be calculated. The greenness or productivity of the vegetation helps to study phenology at a landscape and global scale. The VIs can be measured for a few months or years enables to track vegetation changes and study phenology including the factors affecting the vegetation phenology (St Peter et al. 2018).

There are more than 150 vegetation indices which can be grouped into seven major categories. Based on the properties it can calculate for instance broadband greenness, narrowband greenness, light use efficiency, canopy nitrogen, dry or senescent carbon, leaf pigments, and canopy water content. This is possible because VIs are not solely dependent on the red, green and blue bands but also uses other electromagnetic bands such as near-infrared, red edge, etc. The common range of values for the vegetation indices lies between either -1 to +1 or 0 to +1. The study focuses to use only four vegetation indices for both the datasets.

Table 1: Vegetation Indices and its application (Source: Index database, n.d.)

Vegetation Index	Formulas	Applications
CCCI	$\frac{NIR-Red\ Edge}{NIR+Red\ Edge}$ $\frac{NIR-Red}{NIR+Red}$	Crop management - nitrogen content status and vegetation management - chlorophyll content
EVI	$2.5 * \frac{NIR-Red}{NIR + 6*Red - 7.5*Blue + 1}$	Vegetation analysis using biomass content, calculates leaf area index
GCC	$\frac{Green}{Red+Green+Blue}$	Monitor phenology, phenology parameters and canopy greenness
NDVI	$\frac{NIR-Red}{NIR+Red}$	Crop yield, parameters, management, forest management, vegetation biomass, cellulose, starch, stress and water content.

Table 1 shows the vegetation indices, mathematical expression and its application. The quantitative interpretation of the remotely sensed information on vegetation is difficult and becomes limited when individual bands or only a few bands are analyzed. Therefore, it is recommended to combine bands in different combinations to achieve the desired study objectives. Hence, the study focuses on Canopy Chlorophyll Content Index (CCCI), Enhanced Vegetation Index (EVI), Green Chromatic Coordinate (GCC) and Normalized Difference Vegetation Index (NDVI) because these indices are universally used to study vegetation (refer Table 1). Furthermore, the selected VIs use the spectral information saved in all the bands (Red band, Green band, Red band, Red Edge and Near-Infrared band (NIR)), utilizing all the information from the five bands of the multispectral image.

2.3. Case Study

It is important to review recently completed projects or on-going projects to gain a deeper understanding of different shadow detection methods, methodology and other applications of methods. It helps to identify the risks, uncertainty and loop holes in the procedures and helps to find solutions to various the research gaps.

2.3.1. Rapeseed Oil Project, China

The objectives of the rapeseed oil project were to compare different methods of classification to find flower cover area, relation between VIs and number of flowers and compare the estimation performance of individual UAV variables with variable importance estimations. The study compared unsupervised, RGB-based threshold, RGB-based back propagation

neural network (BPNN), RGB-based support vector machine (SVM) and hue saturation value (HSV) method but the main focus was on unsupervised classification. It also covered ten VIs in order to estimate the number of flower heads. Two datasets with a total of 209 samples were collected for over a period of two years from 2016 to 2017 using an octocopter UAV. The different methods used in the Rapeseed Oil project used RGB UAV imageries for image classification and for calculating eight VIs while multispectral imageries were used to calculate only two other VIs.

The vegetation indices like SRI (simple ratio index) and NSDI (normalized difference spectral index) were calculated for the multispectral imagery. The flower head count was calculated using unsupervised classification. The highest correlation to flower head count was 0.91 and 0.85 for the VI from RGB imagery.

It also showed that on combining the vegetation indices with the image classification can produce better results to count the flower heads. It also brings in light the idea of combining RGB and multispectral imageries with other methods of classification to calculate flower heads which provided a new insight to the phenotypic research (Wan et al. 2018).

2.3.2. Vineyard Project, USA

The objective of vineyard project was to review four methods of detecting shadows in UAV imagery of a vineyard in California, United States of America. The study compared unsupervised, supervised, index and physical classification methods. The data was collected for the time period of three years from 2014 to 2016. The result showed that over the years, the accuracy of the shadow detection was above 80% for each method (refer Table 2). The temporal data showed an increase in accuracy rate for supervised classifications while the accuracy of unsupervised classification and index-based classification dropped by 3% and physical-based methods dropped by approx 1%. The probable reason for the variation in the accuracy was due to the difference in the days on which the data was collected. In 2014, the data was collected at the end of the summer in August while in 2015, it was collected during the summer in June and July and in 2016, it was collected at the end of the spring in May. Hence it can be said that the spectral reflectance must have varied since the plants were at different stages of development during the period of the study which lead to variation in the accuracy over the years.

Table 2: Accuracy of Shadow Detection Methods (Source: Aboutalebi et al. 2017)

Year	Supervised	Unsupervised	Index-Based	Physical Based
2014	80.57	93.47	96.75	87.19
2015	82.94	91.65	93.2	87.49
2015	83.06	91.37	93.4	87.63
2016	84.10	90.39	93.14	86.38
Average	82.67	91.72	94.12	87.17

But after comparing the NDVI and LAI (leaf area index) values for shaded and non-shaded regions, it was concluded that the supervised and index based methods were superior to other methods. The statistical assessment (ANOVA) showed that the average values of NDVI and LAI (leaf area index) for non-shaded areas was higher than the shaded areas. The impact of shadows on evapotranspiration (ET) was observed by calculating the soil heat flux, latent heat flux, sensible heat flux and net radiation for the shaded and non shaded regions using energy models. The energy balance model further showed that shadows lead to larger water stressed areas. Therefore, shadows can significantly influence the procedure and produce biased results in the ET models (Aboutalebi et al. 2017).

2.3.3. Conclusion

Therefore, it can be derived that there are different methods to detect shadows but which method would be well suited depends on the aim of the study. The accuracy of shadow detection can vary between the different observation dates and also after re-running the methods because the classification was by default conducted using the probability of sharing a similarity in the spectral signatures (Aboutalebi et al. 2017). As mentioned in the rapeseed oil project, it is important to not to depend on RGB imageries solely but also to use other multispectral bands so that all the spectral information stored in all the bands can fully be exercised to achieve the objectives of the study (Wan et al. 2018). Hence, to find the best method to detect shadows, it becomes necessary that all the methods are implemented for each temporal dataset utilizing the five bands to obtain unbiased results and compare them fairly in quantitative and qualitative terms.

Chapter – 3

Methodology

This chapter gives an overview of the type of data, structure of the data required for the study along with the methodology for each shadow detection method.

3.1. Data Identification and Collection

Once the objectives and literature review were set then the next step was to identify the data required for the study and its sources.

Site selection: Out of the nine Landklif TP5 sites, the forest stand near Parsberg is one of the biggest sites spread across 14.20 hectares approximately. 50% of the study area consists of beech trees while 10% coniferous, 10% ash, 10% maple, 10% elm, 5% oak and 5% is under the other species. The beech part is mainly in juvenile stage but also consists of single mature and heavily defoliating trees which have an average height of 35-40 meters while the rest of the forest has an average height of 20-25 meters.

Spectral Data: After selecting the study area, the next step was to identify and collect spectral data. The department of Ecoclimatology, TUM collected multispectral imageries for the nine regions using ‘MicaSense RedEdge-M’ multispectral camera installed on a UAV for the period of the spring season in 2019.

The collected imageries were then processed in Pix4D for generating georeferenced orthophotos for each dataset. The orthophotos were generated by setting image scale, point density and number of matches for the processing of all the UAV imageries. The image scale for the initial processing was set to 1 under custom option because it was the original image size and was system recommended. The image scale for the point cloud densification was set to 0.5 to speed up the process. The point density was set to optimal option and the minimum number of matches was set to 3 while the rest of the parameters were set as by-default options under the Pix4D software system (Pix4Dmapper, n.d.).

The processed multispectral imageries consist of 5 bands namely: Blue, Green, Red, Red Edge and NIR. One dataset was acquired in the middle of the spring season, on April 11, 2019, when the seasonal foliage was not out yet while the other selected dataset was acquired

at the end of the spring season, on May 30, 2019, when most of the leaves were fully developed.

Sample Sets: A subset of May 30, 2019 dataset was created to develop different methods to detect shadows and also to test variation within a method itself (refer Figure 3). The subset site covers 1.41 hectares consisting of four land cover classes: shadows, forest, grassland and pathway (refer Map 1).

The collected multispectral imageries helped to estimate the different categories of the land cover and variation in the land features for April and May datasets. In the May 30, 2019 dataset, we can visually observe five classes, namely, shadows, forest, grassland, pathway and cropland (refer Map 2) while in the April 11, 2019 dataset, we observed two additional classes namely tree trunks and dormant forest (refer Map 3).

For each dataset, training and validation datasets were created by drawing polygons corresponding to the visible land cover classes which were created across the study area. These sample sites that were demarcated for each dataset contains pure and natural spectral values for each visible land cover class. Table 3 shows the number of sample sites selected for the corresponding to all the datasets and visible land cover classes. It also shows a variation in land cover classes over the change in the dataset size. The map 1, 2 and 3 shows the location of the sample site on the RGB image and also all the land cover classes visible on RGB image.

In the subset of May 30, 2019 dataset, the total area of training polygons for shadows was 35.56 m^2 while the total area of validation polygons for shadows was 18.19 m^2 . In the May 30, 2019 dataset, the total area of training polygons for shadows was 93.97 m^2 while the total area of validation polygons for shadows was 99.42 m^2 . In the April 11, 2019 dataset, the total area of training polygons for shadows was 19.82 m^2 while the total area of validation polygons for shadows was 9.65 m^2 (refer Annexure 3).



Figure 3: Subset of May 30, 2019 (MicaSense RedEdge-M and Pix4D)

Table 3: Sample Size for Training and Validation (Source: Own Illustration, ArcMap (refer map 1, 2, 3))

Class	Land cover	Training Samples			Validation Samples		
		30 May Subset	30 May	11 April	30 May Subset	30 May	11 April
1	Shadows	12	22	12	12	17	10
2	Forest	7	16	13	7	12	8
3	Grassland	10	9	11	10	10	8
4	Pathway	5	8	9	5	8	10
5	Cropland	x	9	7	x	7	7
6	Tree Trunks	x	x	22	x	x	18
7	Dormant Forest	x	x	20	x	x	16

3.2. Methodology

The methodology of the study divides the entire process into various small segments based on the methods to detect shadows and VIs. The required data for each process was only the multispectral imagery which helped to detect shadows and calculate VIs.

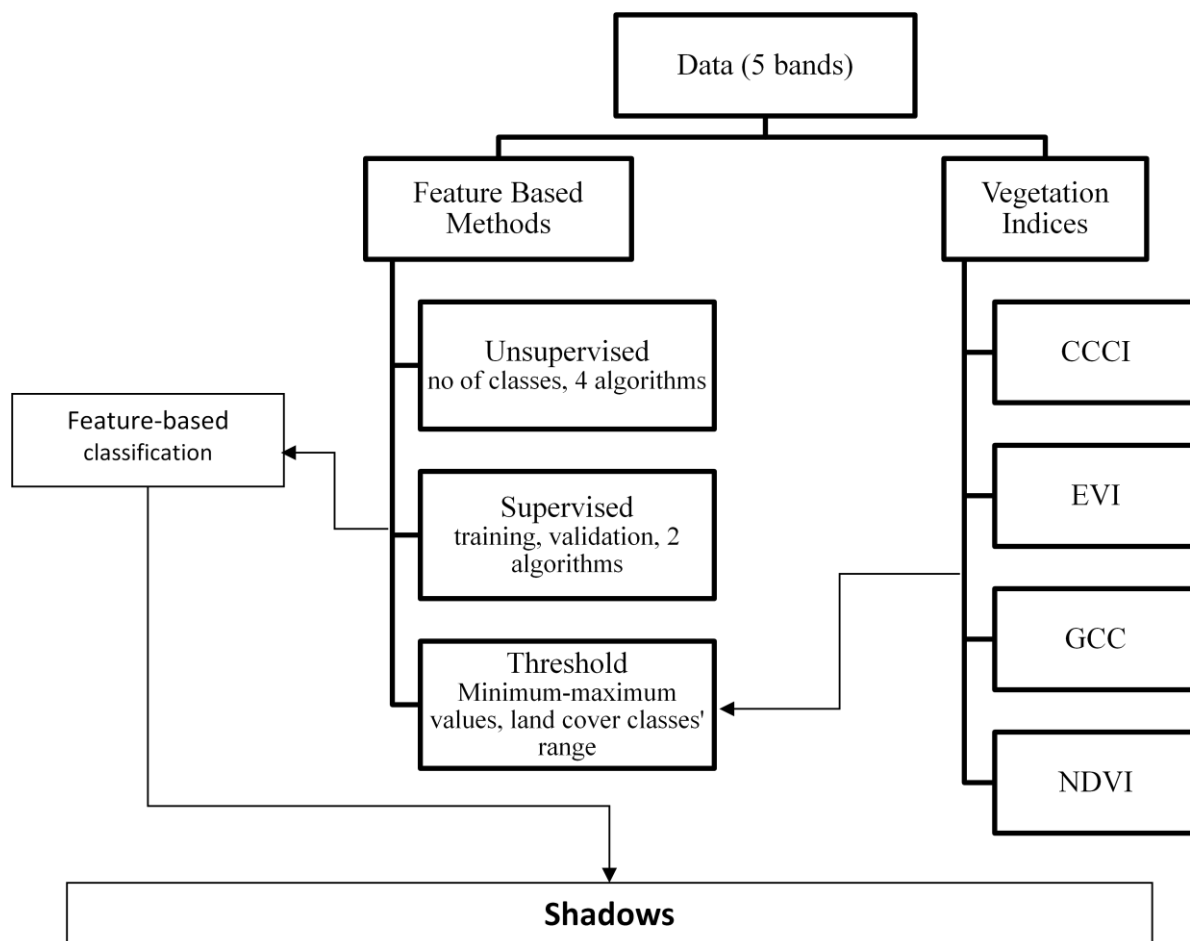
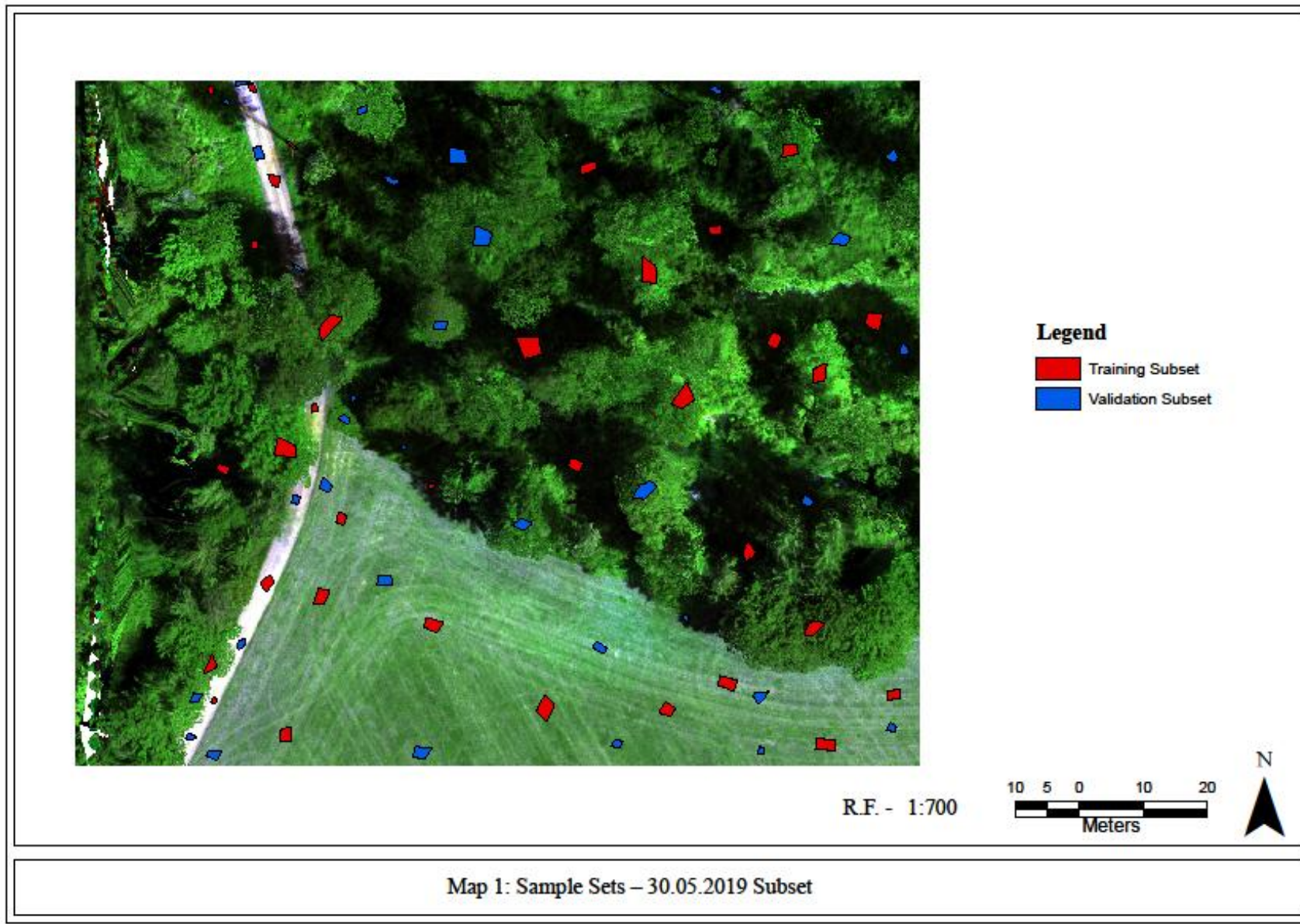
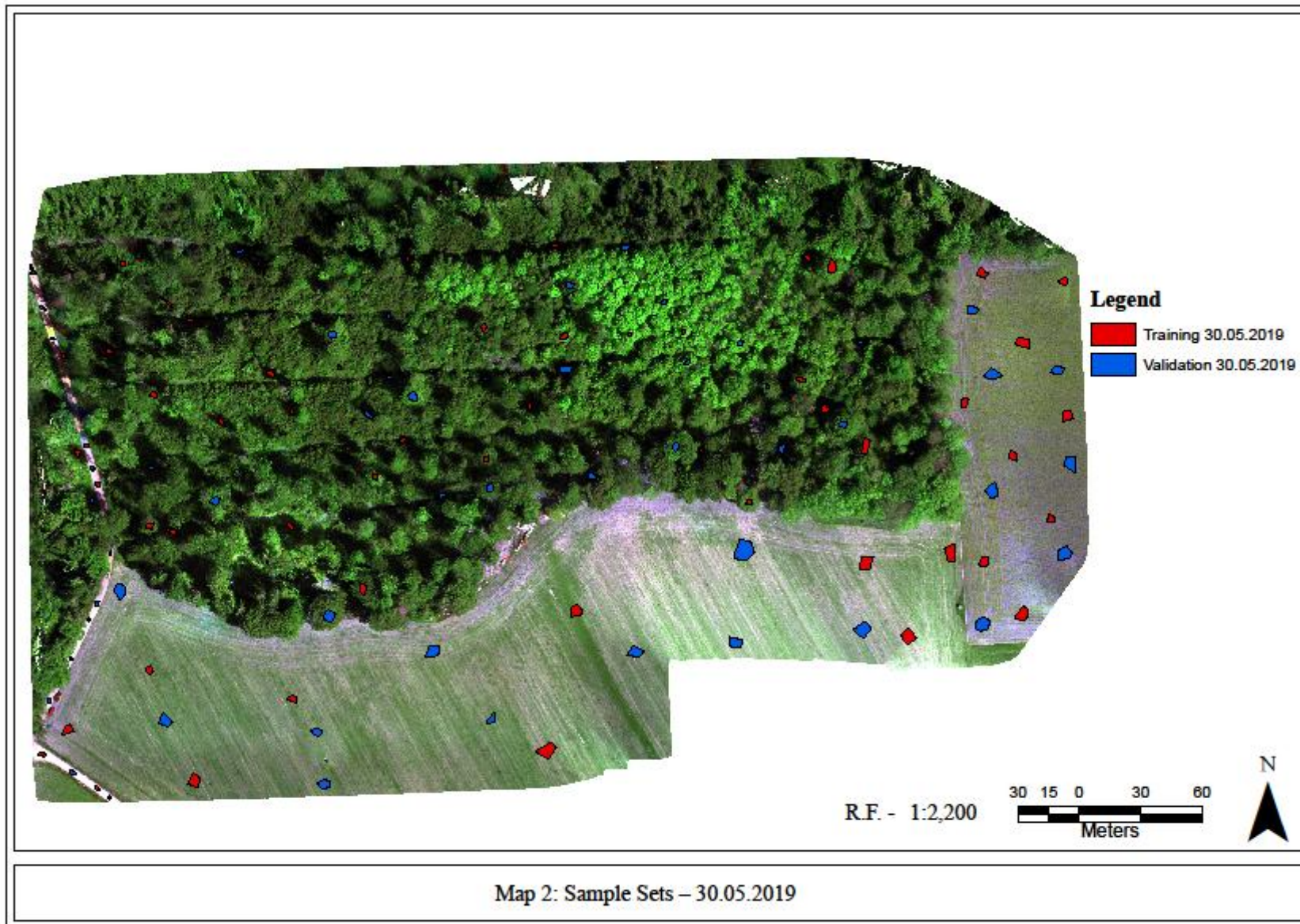
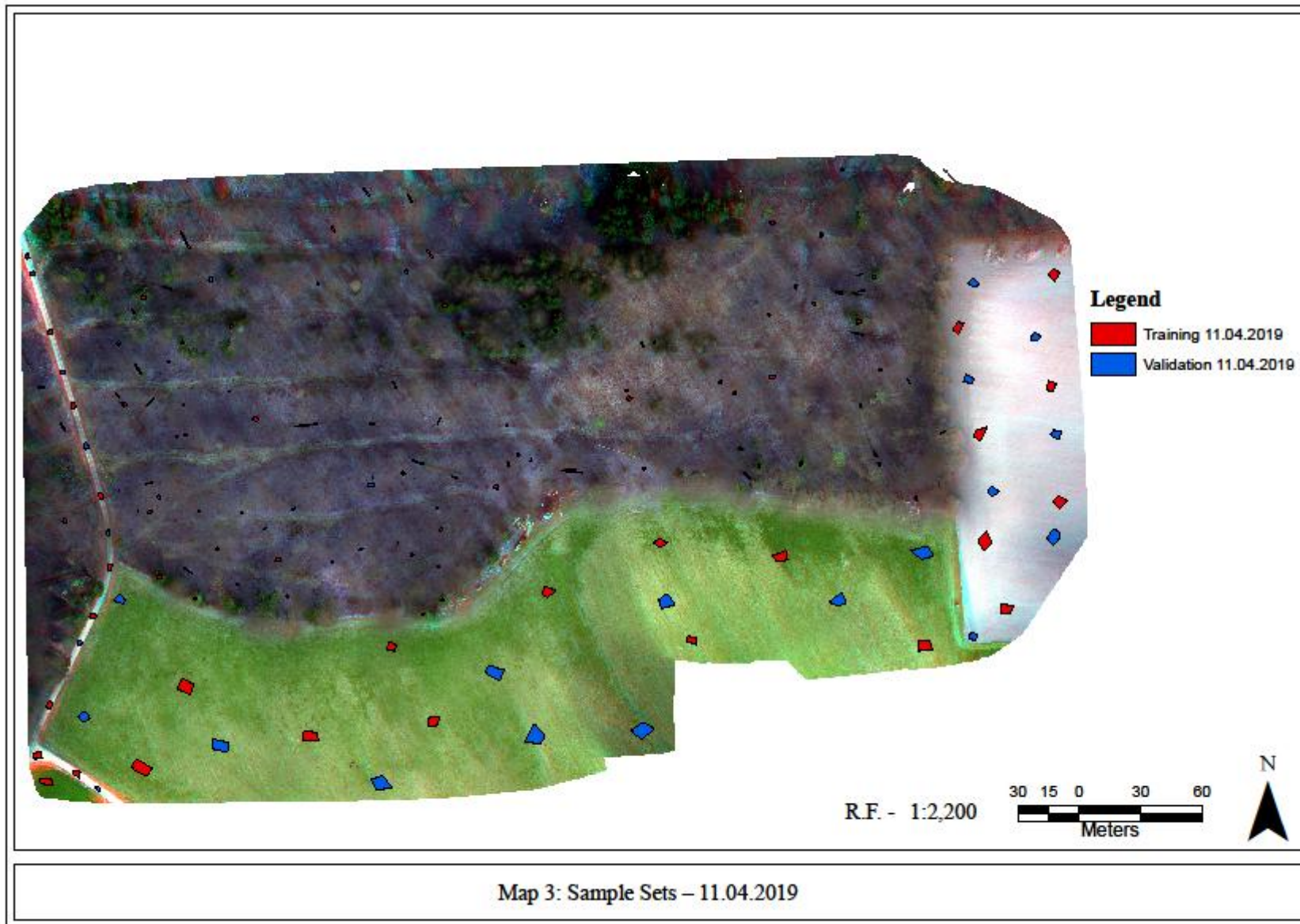


Figure 4: Methodology (Own Illustration)







The first step was to input data for each shadow detection method and calculation of VI which was the 5 bands (Blue, Green, Red, Red Edge and NIR) of the UAV multispectral imageries. The second step was to test each feature-based shadow detection methods namely: unsupervised classification, supervised classification and threshold classification (refer Figure 4). Afterwards, different algorithms were applied for each of these methods. The produced results from each method showed shadows as one the land cover classes for each dataset along with the other visible classes as seen in the RGB imageries.

3.2.1. Unsupervised Classification

Unsupervised classification uses a stacked dataset consisting the five UAV multispectral bands which were stacked in the following order: blue band, green band, red band, red edge band and NIR band (refer Figure 4). In R 3.5.3, unsupervised classification was performed using RStoolbox::unsuperClass command which allows the user to define the number of samples, classes, iterations, and algorithm model (Hartigan-Wong, Lloyd, Forgy and MacQueen) (R Core Team, 2013).

The first step was to identify the number of the desired classes in which the datasets would be classified into. The unsupervised classification was performed for two to ten clusters to check the difference between clustering of pixels for these different numbers of clusters for the subset of May 30, 2019 dataset. The number of the classes chosen for each dataset was selected based on the best number of classes in which the unsupervised method was able to detect shadows as one of them in the best way. Once the number of classes for each dataset was decided then the next step was to identify the algorithms that would work best to detect shadows. Therefore, all the four algorithms were tested on the subset site and the best two were implemented on the main dataset i.e. May 30, 2019 and April 11, 2019 dataset. The unsupervised classification showed results in the form of maps and therefore, it required a further validation by producing a confusion matrix which shows the overall accuracy of the method and class-wise balanced accuracy illustrating the number of pixels that were correctly classified and the number of pixels that were misclassified into other land cover classes.

3.2.2. Supervised Classification

The supervised classification also uses a stacked dataset consisting the five UAV multispectral bands which were stacked in the following order: blue band, green band, red band, red edge band and NIR band (refer Figure 4). In R 3.5.3, supervised classification was

performed using RStoolbox::superClass command which requires the user to input training and validation sample sets along with the response column which acts as a common reference point (R Core Team, 2013). This function allows the user to work with two algorithms: random forest (RF) and maximum likelihood (MLC) based on which the rest of the pixels' classes would be predicted.

The first step to begin with supervised classification was to create training and validation datasets corresponding to each dataset (i.e. May 30, 2019 and April 11, 2019 datasets) and to their respective land cover classes. Afterwards, these training and validation datasets were used as an input in the superClass function to train pixels and predict class of the pixels of the imageries. The function works based on the selected algorithm: rf or mlc. Both the algorithms were tested on May 30, 2019 and April 11, 2019 datasets. Supervised classification showed results in the form of maps along with confusion matrix that shows the overall accuracy of the method and class-wise balanced accuracy illustrating the number of pixels that were correctly classified and the number of pixels that were misclassified into other land cover classes.

3.2.3. Threshold Classification

Threshold classification was performed on all bands of the multispectral imageries for both datasets which helped to identify which band has more information on shadows. This method helped to identify the behaviour of shadows in different bands and the common spectral signature value for each band. The gray scale imageries stores pixel values based on the intensity of the pixels. Therefore, the gray scale imageries of each band would store values from 0 to 255 which mark the minimum – maximum range bracket, where 0 means black and 255 means white while the values in between gives different shades of gray. This method required the user to create pixel value range brackets corresponding to each land cover based on each bands' minimum-maximum range for May 30, 2019 and April 11, 2019 datasets.

In R 3.5.3, threshold classification method was applied as the user first identifies the land cover class ranges for each band and then save it in the form of a matrix so that the bands can be reclassified based on the corresponding range values from the matrix (R Core Team, 2013). In case the range bracket values don't have continuity even by a difference of 0.001, then the pixels with this undesignated value or range bracket would be treated as an

additional class so therefore, it is important that the range brackets should have continuity and covers all the pixel values.

The threshold classification results were displayed in the form of a map so therefore, it further required a validation showing the overall accuracy of the method and class-wise balanced accuracy illustrating the number of pixels that were correctly classified and the number of pixels that were misclassified into other land cover classes

3.2.4. Vegetation Indices Threshold Classification

The vegetation indices were calculated based on the formulas (refer Table 1) which gave minimum-maximum range brackets for each VI. The threshold classification was performed for the calculated VIs from the multispectral imageries for both the datasets which gave respective vegetation index values to the pixel. This method helped to identify the behaviour of shadows in different VIs and the common spectral value for CCCI, EVI, GCC and NDVI spectral values. The idea to identify shadows using the intensity values of pixels remained the same but the only difference would be the change in minimum-maximum range values of each VI as compared to the individual bands and the threshold ranges for shadows.

CCCI was calculated using two bands: red edge and NIR, EVI was calculated using three bands: blue, red and NIR, GCC was calculated using 3 bands: blue, green and red and NDVI was calculated using two bands: red and NIR (refer Table 1). This resulted in creation of single bands for the respective VIs.

In R 3.5.3, threshold classification method was applied to classify VIs to detect shadows. It allowed the user to identify the land cover class ranges for each VI band based on the calculated VIs and then save it in the form of a matrix so that the VI bands can be reclassified based on the corresponding threshold values. These ranges were derived from minimum-maximum band values for each VIs (R Core Team, 2013).

The VIs threshold classification results were generated in the form maps and therefore it also required validation by producing a confusion matrix, similar to the other methods to check the overall accuracy and class-wise balanced accuracy.

Chapter – 4

Results

This chapter deals with the outcome of all the shadow detection methods used for temporal datasets.

4.1. Unsupervised Classification

Clustering: The result of unsupervised classification for the subset of May 30, 2019 dataset for the clustering of pixels showed that Hartigan-Wong (HW) and Lloyd shared some similarities when the number of clusters increased from two clusters to ten clusters during the classification (refer Annexure 1 and 2). In both cases, the shadows could be observed from three clusters onwards but some parts of the other land covers were also detected in the same class. But when the classification was performed using four classes, the result gave a fair idea of the land cover of the study area (refer Map 4 and 5). The four classes depicted three land cover: shadows, forest and grassland which included information on the pathway. On increasing the number of classes from four to five or till seven, it was observed that the forest became fragmented but when the number of classes increased to eight till ten, the fragmentation for each class increased especially in the case of shadows (refer Annexure 1 and 2). Therefore, it was concluded that the number of classes that would be best suited was equivalent to the number of land cover classes that the user wants to detect. Hence, the May 30, 2019 dataset has used five classes while the April 11, 2019 dataset has used seven classes for each classification method.

Table 4: Confusion Matrix Unsupervised 30.05.2019 Subset (Source: Results derived in R 3.5.3, 2020 (bold values under class accuracy shows the accuracy of shadows (HW-2, Lloyd-1, Macqueen-1 and Forgy- 2)))

Hartigan-Wong 30.05.2019 Subset					Lloyd 30.05.2019 Subset				
	Reference					Reference			
Pred.	1 Gras sland	2 Shado ws	3 Fores t	4 Pathw ay	Pred.	1 Shado ws	2 Fores t	3 Grassl and	4 Pathwa y
1	300	12	98	300	1	293	7	0	0
2	0	288	4	0	2	0	176	0	2
3	0	0	179	0	3	7	91	300	298
4	0	0	19	0	4	0	26	0	0
Accu racy	0.772	0.978	0.798	0.4894	Accu racy	0.984	0.792	0.780	0.486

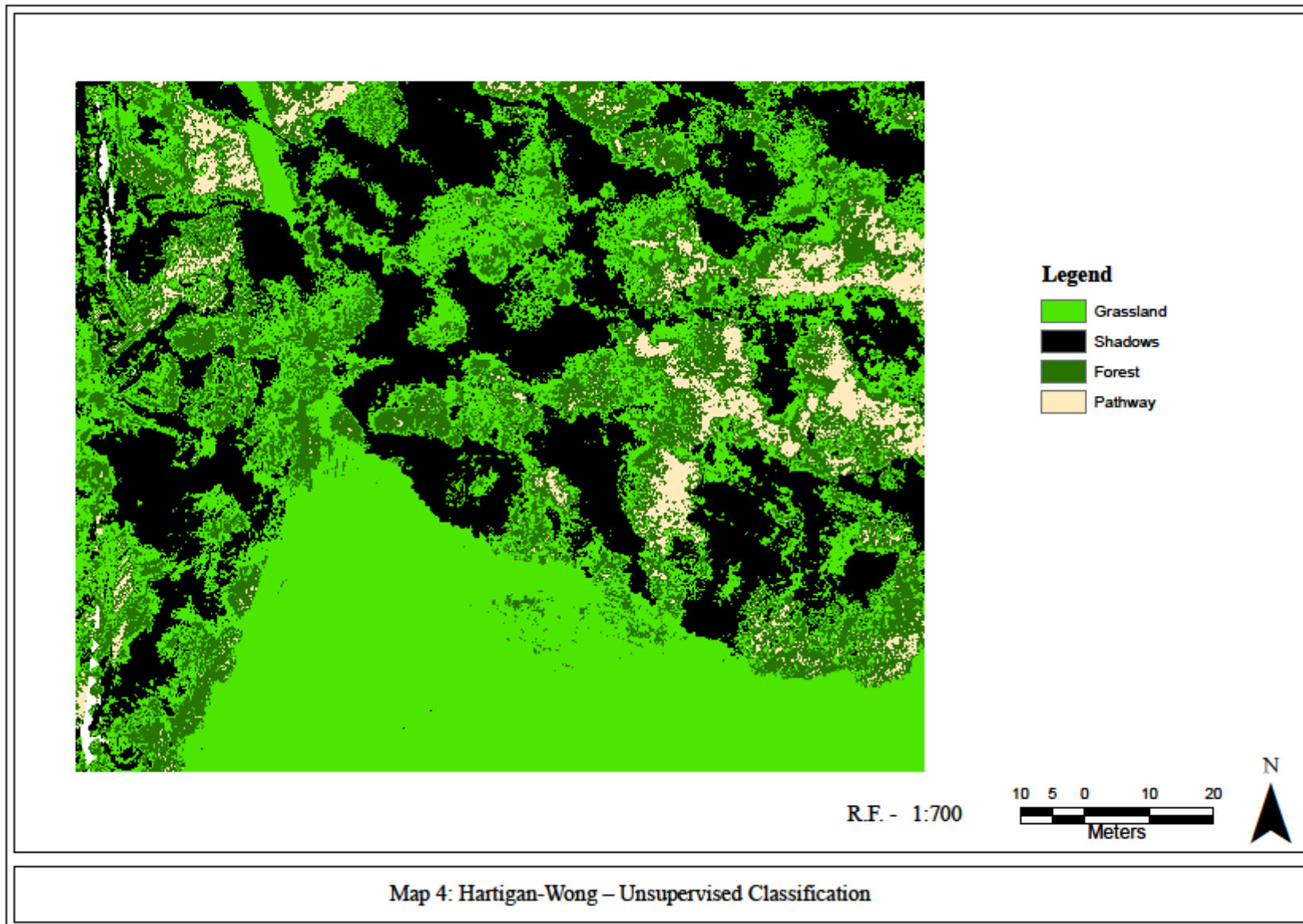
MacQueen 30.05.2019 Subset					Forgy 30.05.2019 Subset				
	Reference					Reference			
Pred.	1 Shadows	2 Pathway	3 Grassland	4 Forest	Pred.	1 Grassland	2 Shadows	3 Forest	4 Pathway
1	295	0	0	7	1	300	6	75	295
2	0	0	0	19	2	0	294	6	0
3	5	300	300	106	3	0	0	46	0
4	0	0	0	168	4	0	0	173	5
Accuracy	0.978	0.489	0.772	0.78	Accuracy	0.791	0.987	0.577	0.412

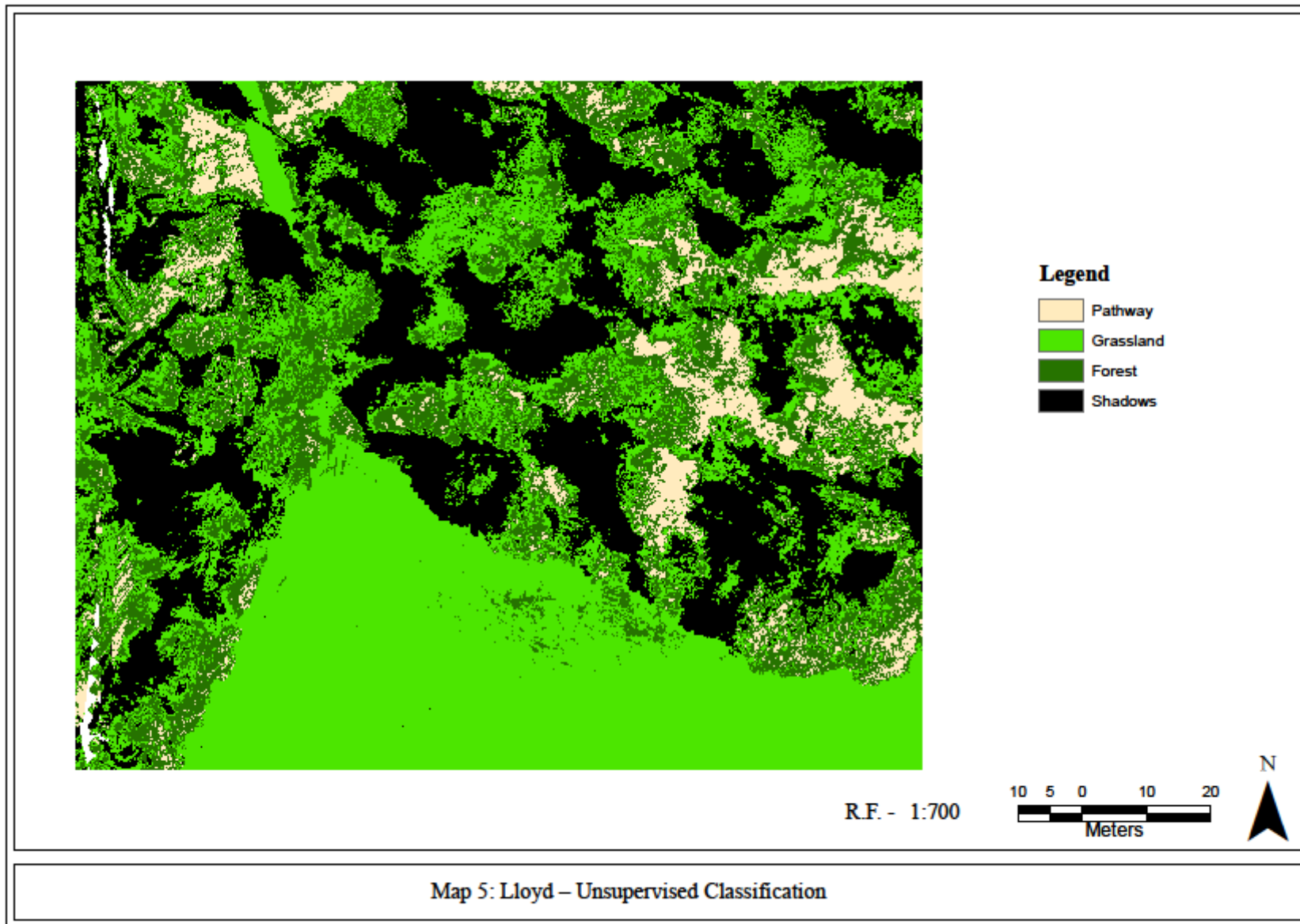
Algorithms: Comparing the four unsupervised classification algorithms, the confusion matrix (refer Table 4) shows that shadows in HW (class 2) and MacQueen (class 1) showed an accuracy of 0.978 while Lloyd (class 1) showed an accuracy of 0.984 and Forgy (class 2) showed an accuracy of 0.987. In all the four methods, grassland and pathway pixels were detected as one class and therefore, some other pixels which were detected as class four were assigned as the pathway class to identify the accuracy of the other classes.

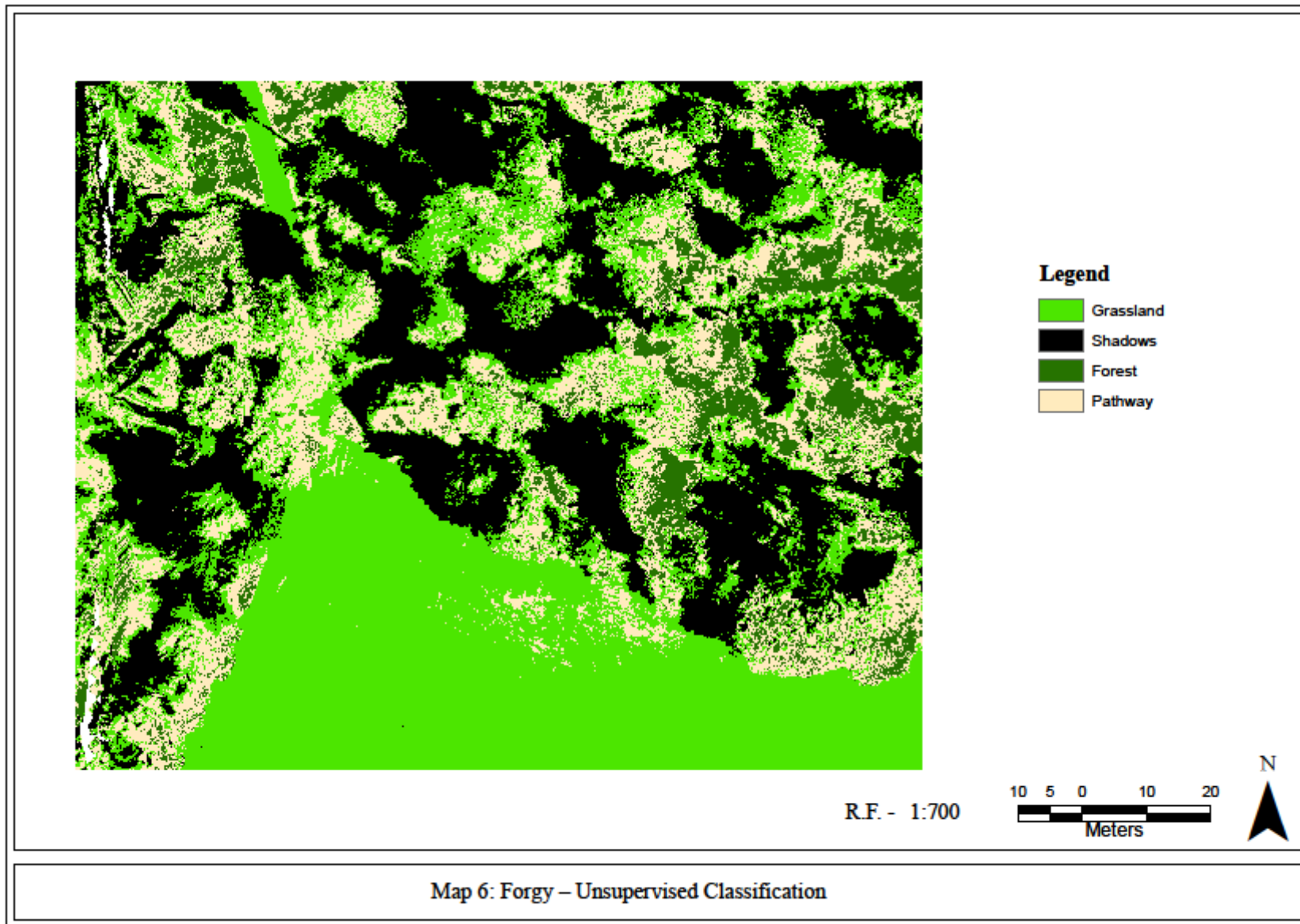
The HW method showed that some shadows were classified as grassland and some forest was classified as shadows (refer Map 4) which was least accurate in comparison to the other methods. Forgy and Macqueen showed similar results as only a few pixels of shadows were misclassified into other classes (refer Map 6 and 7).

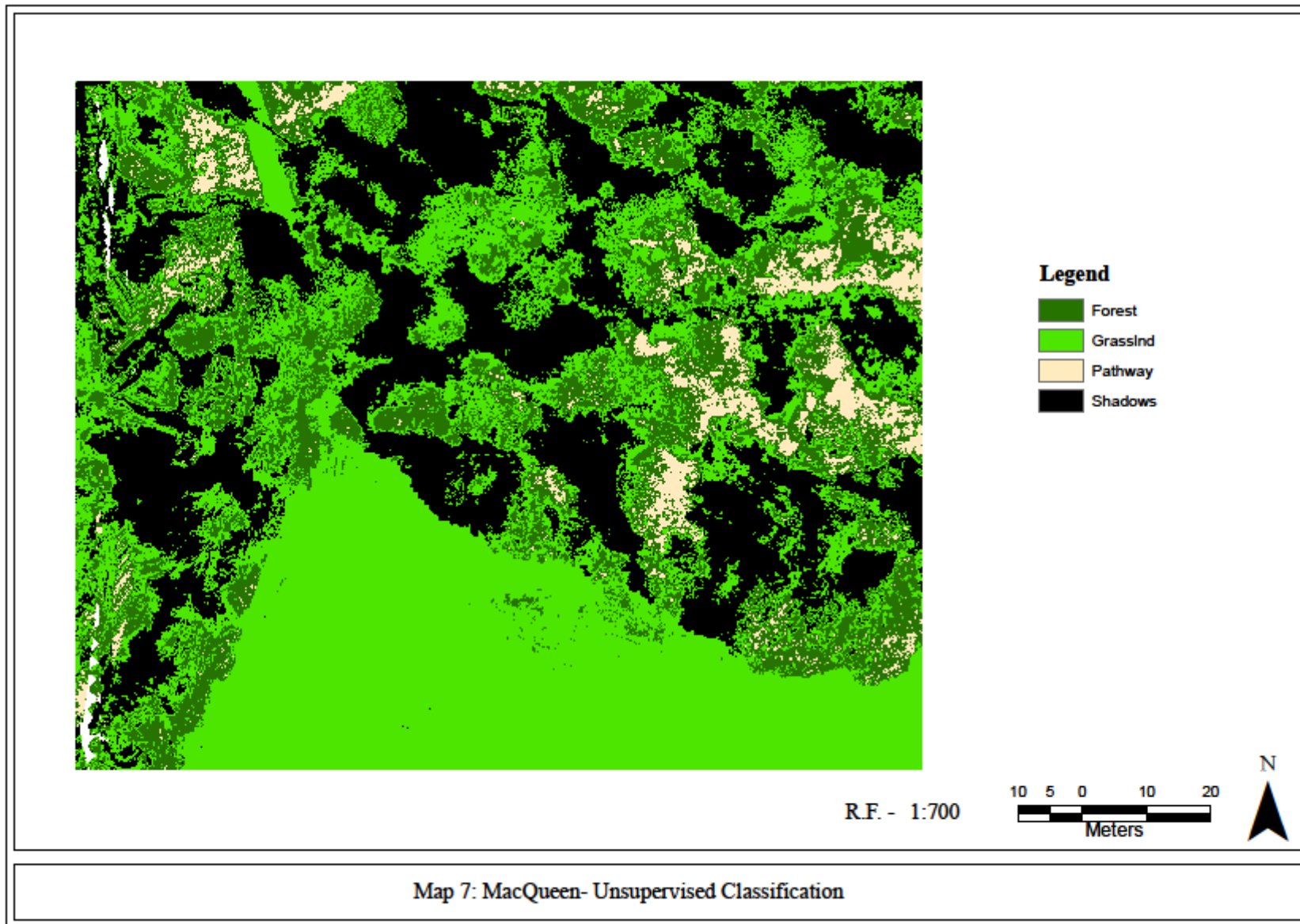
The overall accuracy of HW was found to be 0.639, the Macqueen method showed an accuracy of 0.636 and Lloyd showed an accuracy of 0.640 while Forgy showed the lowest overall accuracy of 0.538 amongst the four methods (refer Annexure 4). HW and Macqueen showed quite similar results for the overall accuracy but they showed a minor difference in the shadow class accuracy which can be treated negligible as well.

On the whole, all the four methods showed similar results but the minor difference in the overall accuracy and class-wise accuracy shortlisted HW and Lloyd methods of unsupervised classification. Also, these methods are quite commonly used for image classification and are often used as an alternative of k-means methods.









In the May 30, 2019 dataset, the HW and Lloyd method of unsupervised classification were used to detect shadows as one of the five land cover classes namely: shadows, forest, grassland, pathway and cropland (refer Map 8 and 9). Shadows were detected in class four in HW method and class five in Lloyd method (refer Table 5).

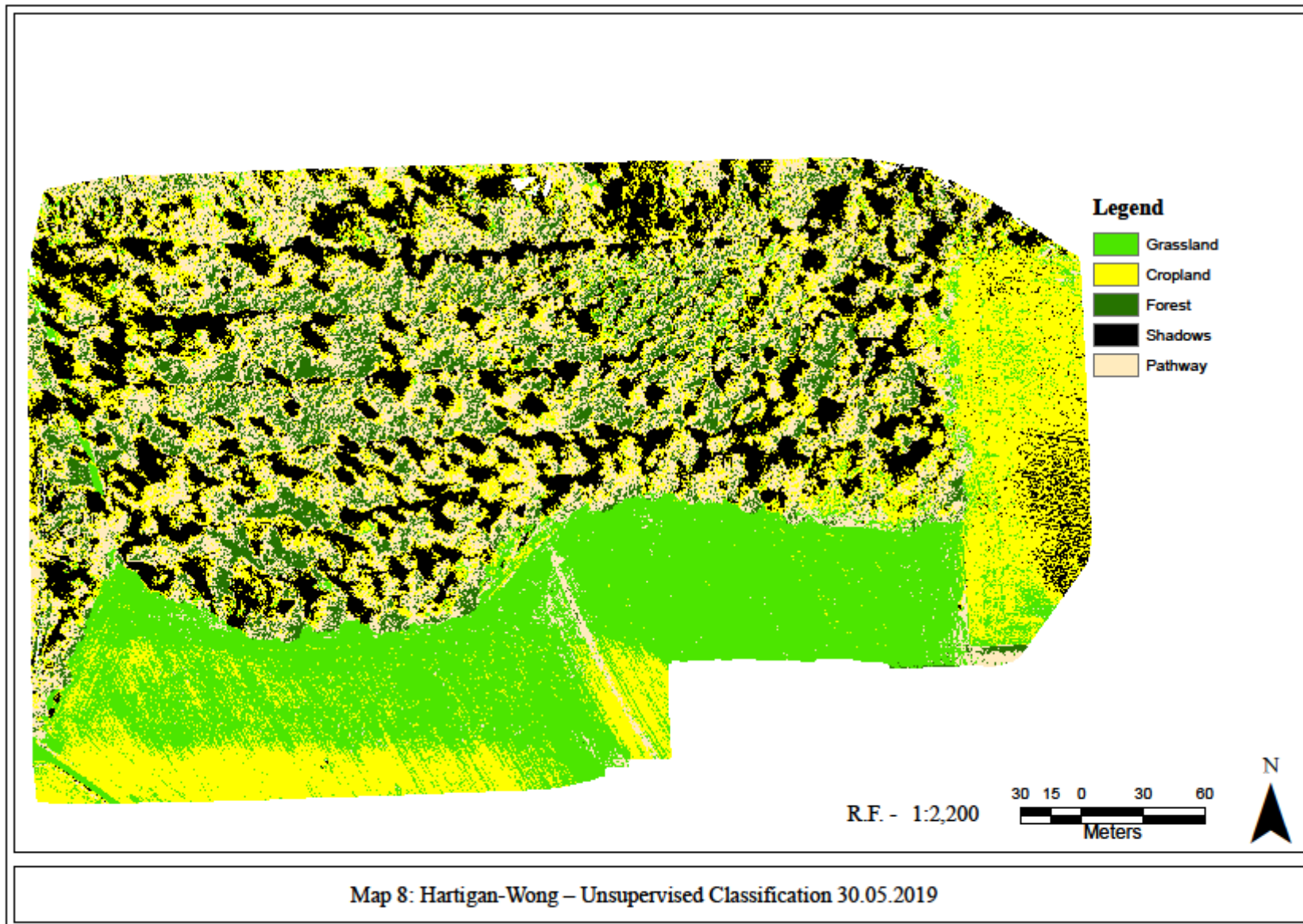
Table 5: Confusion Matrix Unsupervised 30.05.2019 (Source: Results derived in R 3.5.3, 2020 (bold values under class accuracy shows the accuracy of shadows))

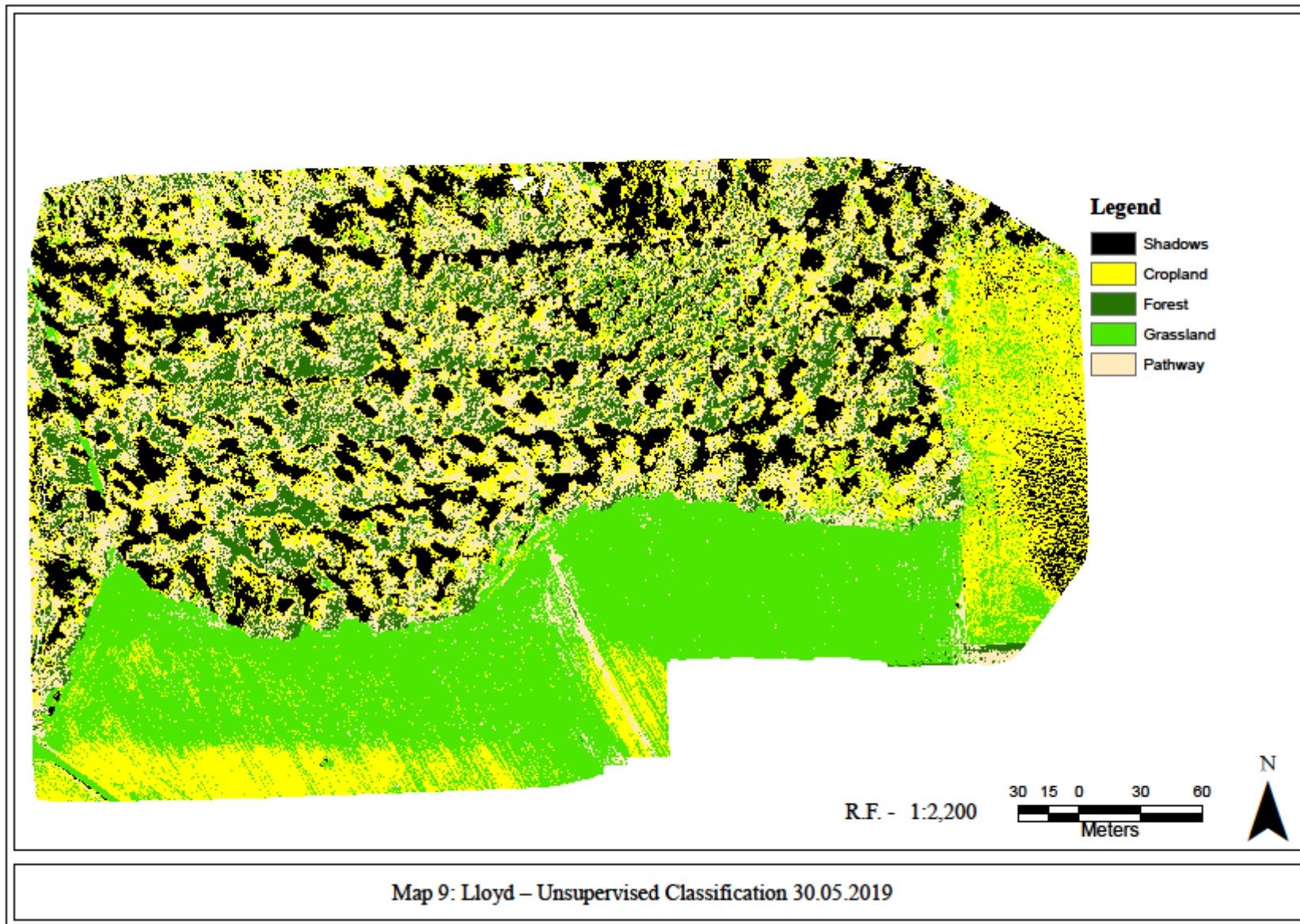
Hartigan-Wong 30.05.2019					
	Reference				
Prediction	1 Grassland	2 Cropland	3 Forest	4 Shadows	5 Pathway
1	718	173	16	0	846
2	221	757	196	46	1
3	15	0	227	0	0
4	0	66	14	954	0
5	46	4	547	0	2
Accuracy	0.725	0.818	0.612	0.967	0.427

Lloyd 30.05.2019					
	Reference				
Prediction	1 Pathway	2 Grassland	3 Forest	4 Cropland	5 Shadows
1	3	46	510	6	0
2	834	770	8	256	0
3	0	21	277	0	0
4	0	163	191	643	79
5	0	0	14	95	921
Accuracy	0.432	0.742	0.636	0.765	0.946

The result showed that the accuracy for shadows was high, 0.967 for HW while 0.946 for Lloyd. In both the methods, some pixels of cropland were detected as shadows but in the case of HW some pixels from other classes were detected as shadows (refer Table 5) while only some pixels of forest and cropland were misclassified as shadows in the case of Lloyd method. Shadows misclassification was seen more in Lloyd (refer Map 9) while misclassification of other classes as shadows was observed in HW (refer Map 8).

The overall accuracy of HW was found to be 0.548 while Lloyd showed an overall accuracy of 0.540. The difference in both the algorithms was minor which can be negligible (refer Annexure 4).





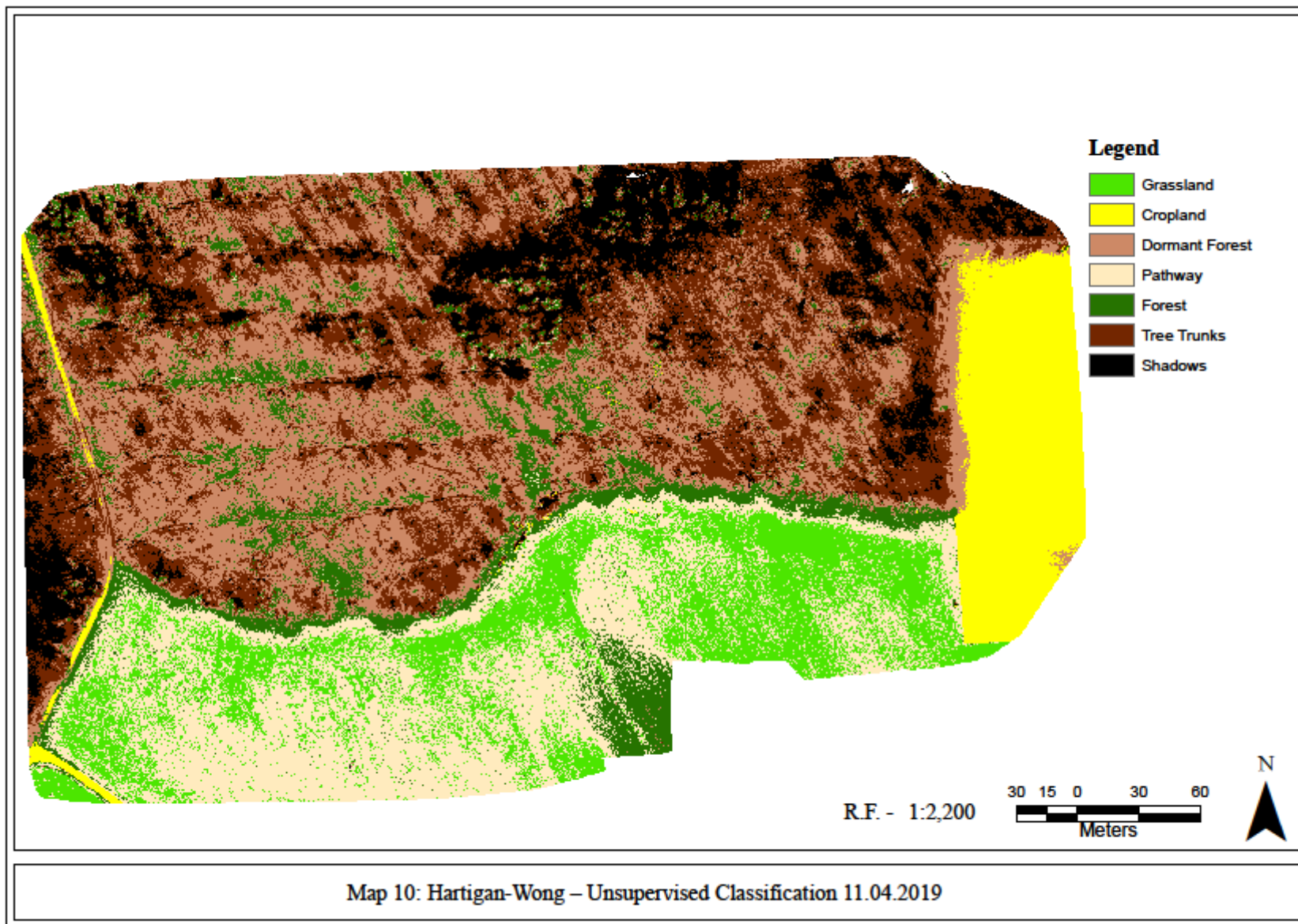
In the April 11, 2019 dataset, the HW and Lloyd methods of unsupervised classification were used to detect shadows as one of the seven land cover classes: shadows, forest, grassland, pathway, cropland, tree trunks and dormant forest. The result showed that shadows were detected in class 7 in HW method while for Lloyd it was detected in class 1 (refer Table 6).

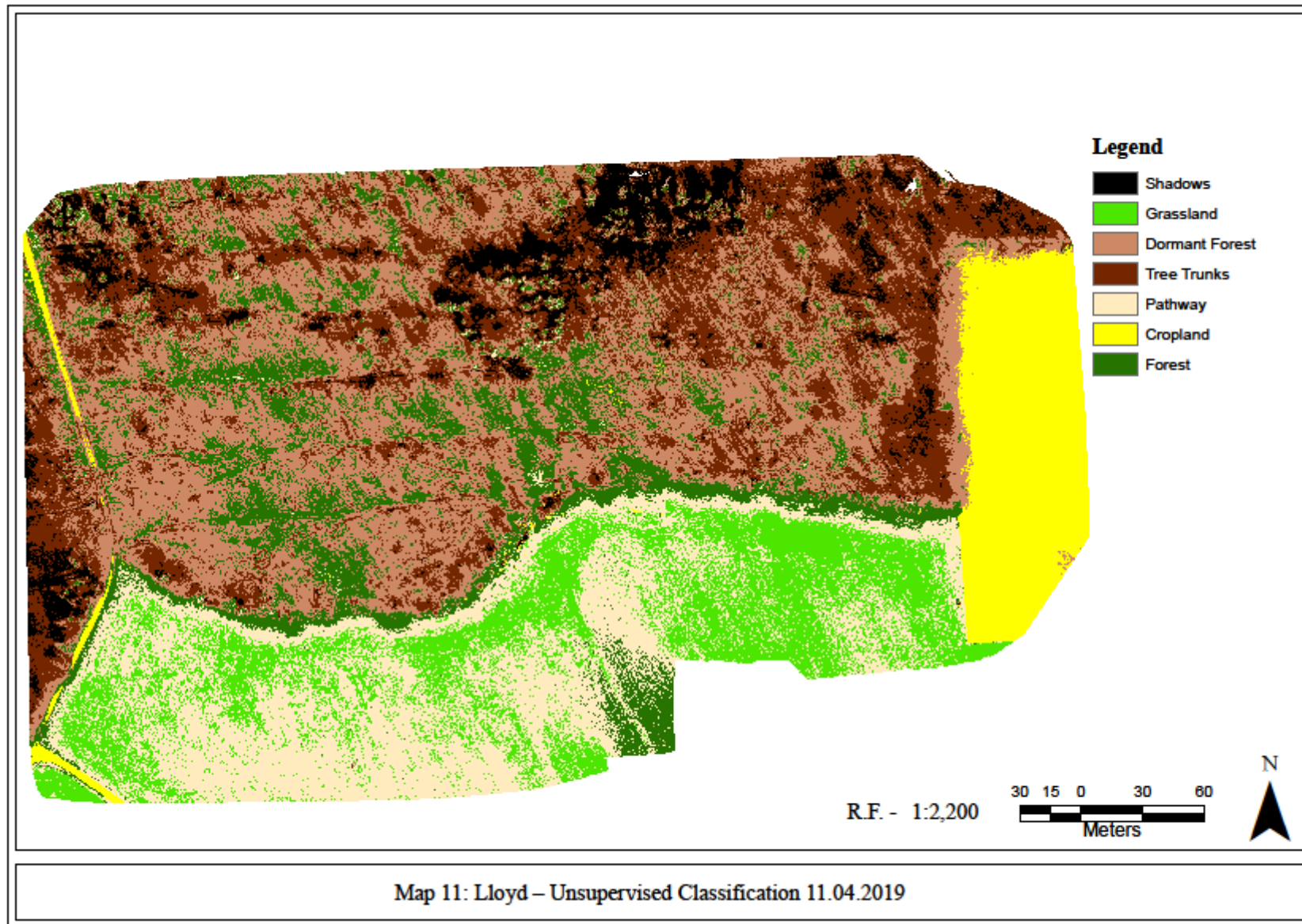
Table 6: Confusion Matrix- Unsupervised 11.04.2019 (Source: Results derived in R 3.5.3, 2020 (bold values under class accuracy shows the accuracy of shadows))

Hartigan-Wong 11.04.2019							
	Reference						
Prediction	1 Grassland	2 Cropland	3 Dormant Forest	4 Pathway	5 Forest	6 Tree Trunks	7 Shadows
1	558	0	0	0	9	0	0
2	0	928	0	830	0	23	0
3	0	72	654	142	241	290	104
4	433	0	0	0	59	0	0
5	9	0	142	17	413	78	1
6	0	0	204	11	213	329	390
7	0	0	0	0	65	280	505
Accuracy	0.778	0.893	0.756	0.459	0.686	0.596	0.724

Lloyd 11.04.2019							
	Reference						
Prediction	1 Shadows	2 Grassland	3 Dormant Forest	4 Tree Trunks	5 Pathway	6 Cropland	7 Forest
1	346	0	0	133	0	0	32
2	0	585	0	0	0	0	6
3	228	0	632	304	109	68	316
4	424	0	56	375	6	0	161
5	0	412	0	0	0	0	93
6	0	0	0	26	803	932	0
7	2	3	312	162	82	0	392
Accuracy	0.659	0.792	0.731	0.634	0.458	0.897	0.649

The results for the April 11, 2019 dataset showed that the shadows class for HW method showed an accuracy of 0.724 while Lloyd showed an accuracy of 0.659. In both the cases, some of the shadows pixels were misclassified as tree trunks and dormant forest but forest and tree trunks classes' pixels were also misclassified into shadow class (refer Map 10 and 11). HW showed an overall accuracy of 0.484 while Lloyd showed an overall accuracy of 0.466 (refer Annexure 4).





4.2. Supervised Classification

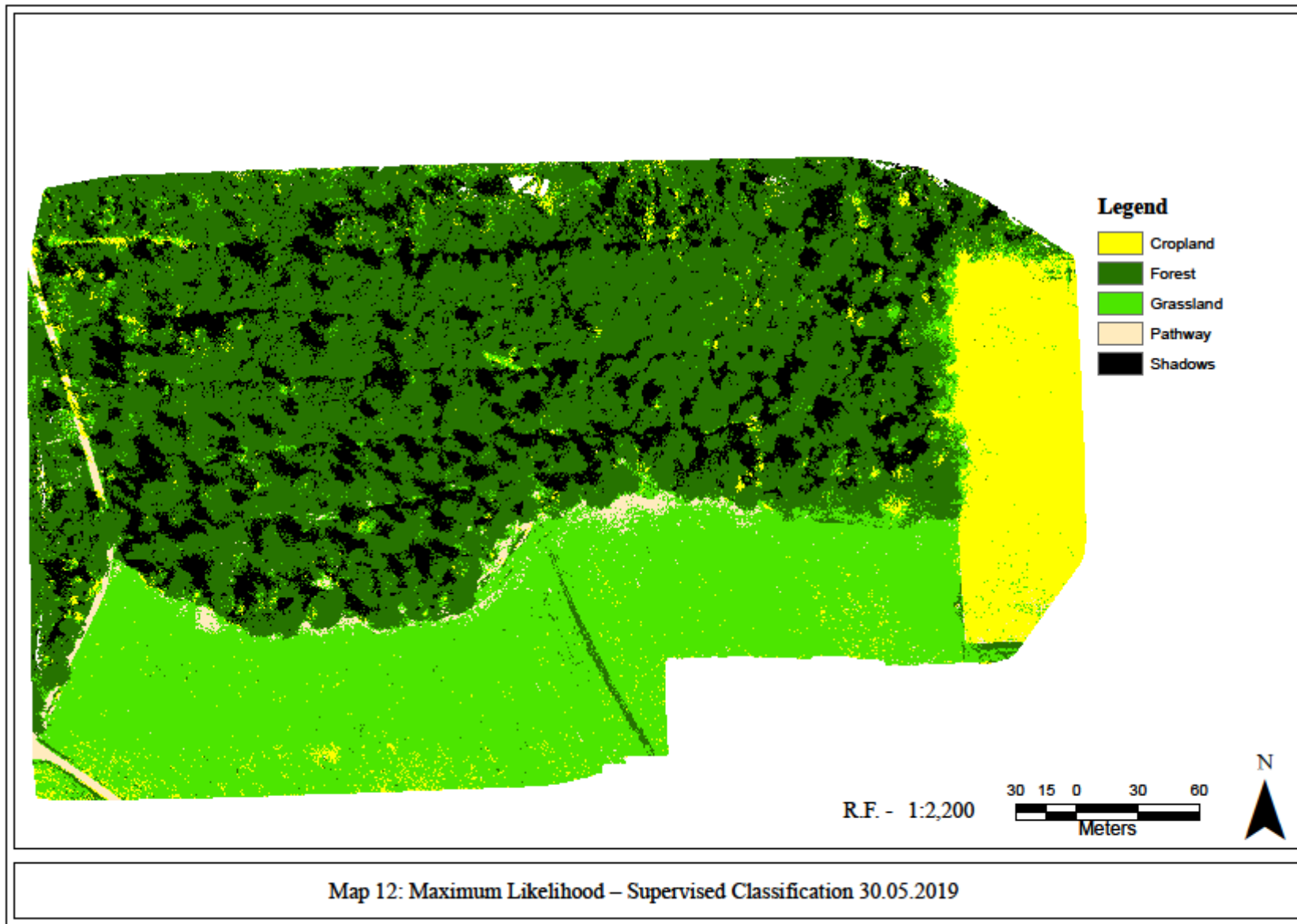
In the May 30, 2019 dataset, the land cover classes that were pre-defined were shadows, forest, grassland, pathway and cropland. Table 7 shows the result of MLC and RF methods which showed that the accuracy of detecting shadows was 0.996 for MLC and for RF, it was 0.999 because only a few shadow pixels were misclassified in maximum likelihood method. Both methods showed similar results in maps (refer Map 12-13) which proves to be right because the class-wise accuracy for shadows for both methods showed a similar pattern (refer Table 7). For maximum likelihood method only one forest pixel was misclassified as shadows class while in random forest method, three forest pixels were misclassified as shadows. This minor difference in both the methods was negligible.

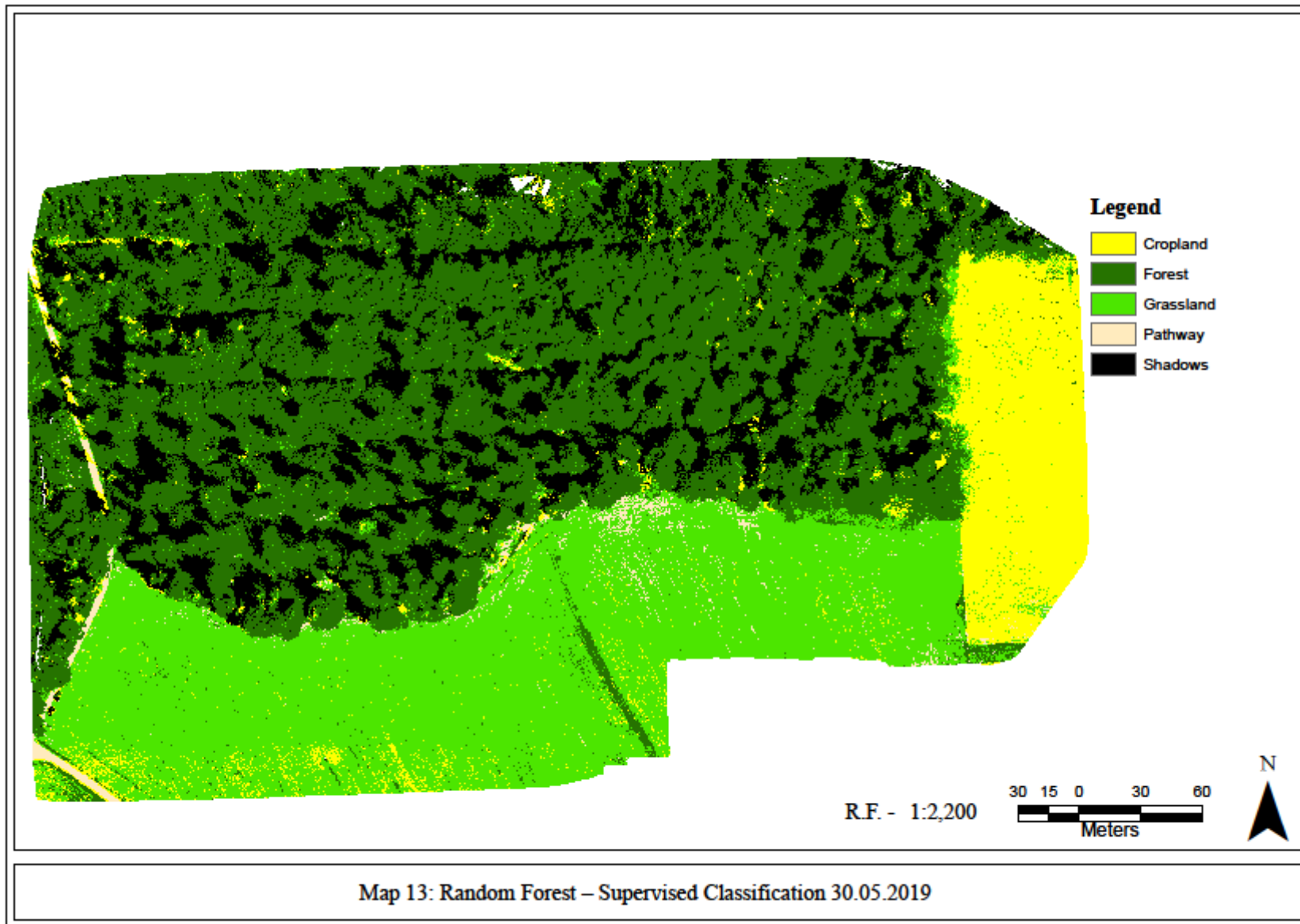
Table 7: Confusion Matrix Supervised 30.05.2019 (Source: Results derived in R 3.5.3, 2020 (bold values under class accuracy shows the accuracy of shadows))

Maximum Likelihood 30.05.2019					
	Reference				
Prediction	Cropland	Forest	Grassland	Pathway	Shadows
Cropland	992	1	6	0	0
Forest	0	987	2	0	4
Grassland	8	11	987	0	0
Pathway	0	0	5	763	0
Shadows	0	1	0	0	996
Accuracy	0.995	0.993	0.991	0.999	0.998

Random Forest 30.05.2019					
	Reference				
Prediction	Cropland	Forest	Grassland	Pathway	Shadows
Cropland	983	3	13	2	0
Forest	2	985	5	0	0
Grassland	15	9	970	0	0
Pathway	0	0	12	754	0
Shadows	0	3	0	0	1000
Accuracy	0.989	0.992	0.982	0.992	0.999

MLC showed an overall accuracy of 0.992 while RF showed an accuracy of 0.987. Both the methods showed a minor difference in the accuracy which was negligible (refer Annexure 4).





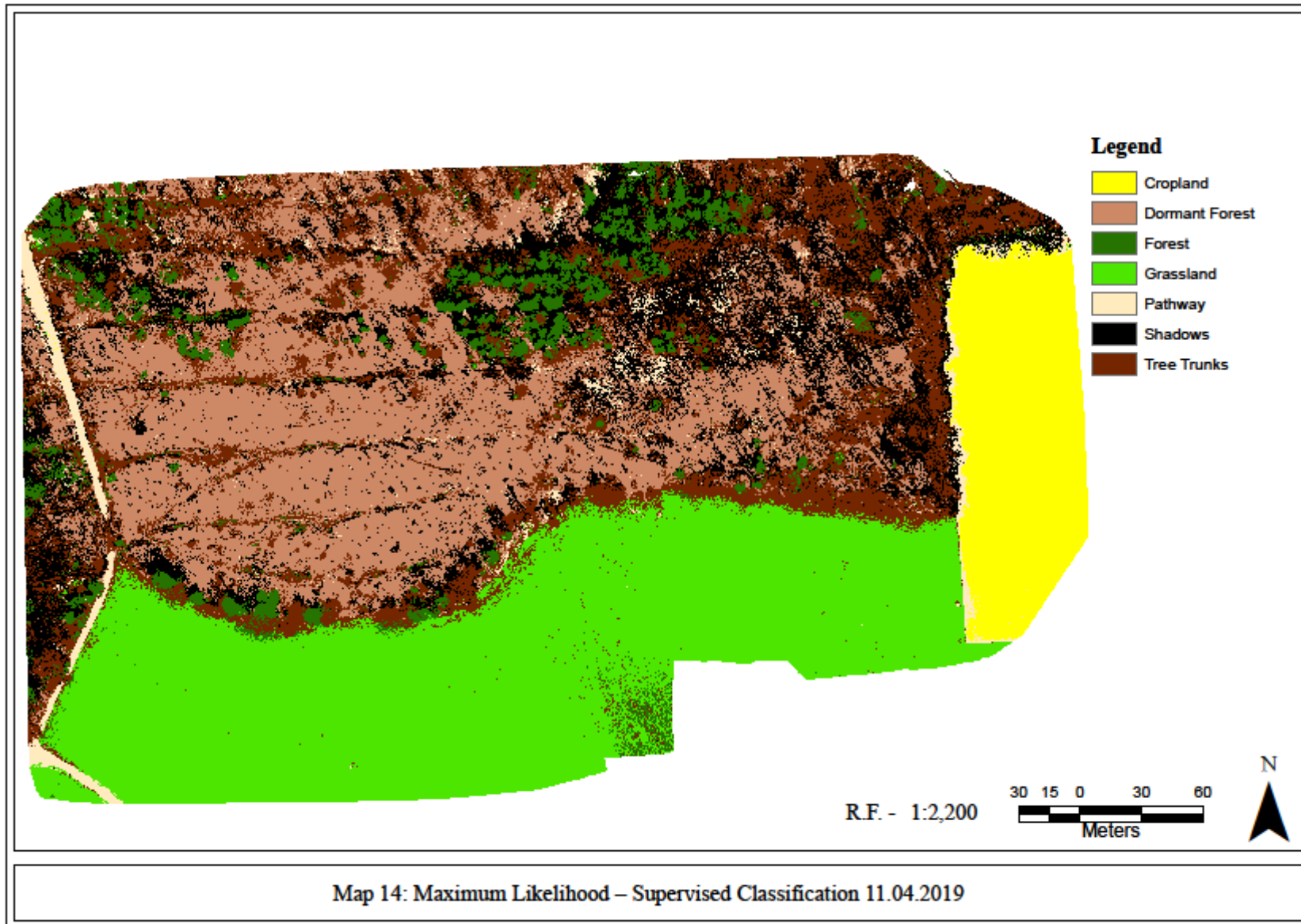
In the April 11, 2019 dataset, the land cover classes that were pre-defined were shadows, forest, grassland, pathway, cropland, tree trunks and dormant forest (refer Map 14). The results showed that the accuracy for shadows class was 0.766 for MLC method while 0.791 for random forest method. In both methods, dormant forest and tree trunks land cover pixels were misclassified as shadows while some of the shadows (refer Map 15) class pixels were misclassified into other classes except for cropland and grassland (refer Table 8)

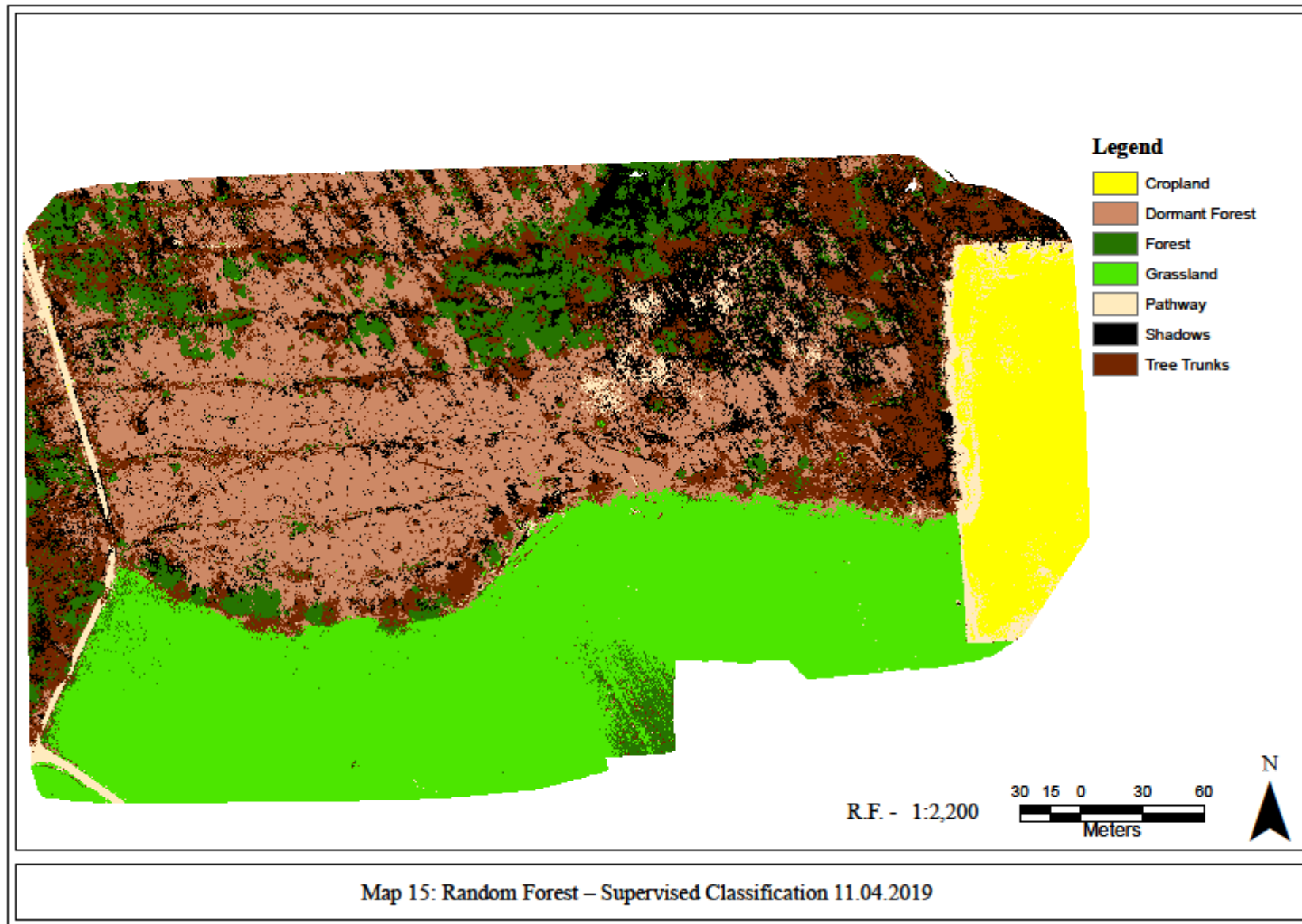
Table 8: Confusion Matrix - Supervised Classification 11.04.2019 (Source: Results derived in R 3.5.3, 2020 (bold values under class accuracy shows the accuracy of shadows))

Maximum Likelihood 11.04.2019							
	Reference						
Prediction	Cropland	Dormant Forest	Forest	Grassland	Pathway	Shadows	Tree Trunks
Cropland	962	0	0	0	3	0	0
Dormant Forest	0	875	0	0	0	230	39
Forest	0	0	959	44	0	0	15
Grassland	0	0	3	947	0	0	0
Pathway	38	1	0	0	768	1	0
Shadows	0	36	3	0	37	591	277
Tree Trunks	0	88	35	9	192	178	669
Accuracy	0.981	0.915	0.975	0.973	0.881	0.766	0.793

Random Forest 11.04.2019							
	Reference						
Prediction	Cropland	Dormant Forest	Forest	Grassland	Pathway	Shadows	Tree Trunks
Cropland	864	0	0	0	18	0	0
Dormant Forest	0	888	1	0	2	138	44
Forest	0	14	956	88	0	5	22
Grassland	0	0	0	906	0	0	0
Pathway	136	0	0	0	783	0	0
Shadows	0	55	3	0	116	632	131
Tree Trunks	0	43	40	6	81	225	803
Accuracy	0.931	0.929	0.967	0.953	0.880	0.791	0.869

MLC showed an overall accuracy of 0.824 while RF showed an accuracy of 0.833. Both the methods showed a minor difference in the accuracy which was negligible (refer Annexure 4).





4.3. Threshold Classification

In the May 30, 2019 dataset, the threshold brackets were created for five land cover classes: shadows, forest, grassland, pathway and cropland which were given class number one to five respectively.

The result showed that the shadows (in class 1) showed high accuracy of 0.979 for the blue band, 0.982 for the green band, 0.991 for the red band, 0.994 for the red edge band and 0.838 for the NIR band (refer Table 9). Green, red and red edge band showed least amount of misclassification for the shadows land cover class (refer Map 16-20).

Blue band showed an overall accuracy of 0.682 which was quite close the highest accuracy amongst all the bands. Green band showed an overall accuracy of 0.615. Red band showed an overall accuracy of 0.722 which was the highest amongst the all the bands. Red edge band displayed an accuracy of 0.587 while NIR band showed an accuracy of 0.504 which was observed to be the least amongst all the five bands (refer Annexure 4).

Table 9: Confusion Matrix – Threshold Classification 30.05.2019 (Source: Results derived in R 3.5.3, 2020 (bold values under class accuracy shows the accuracy of shadows)

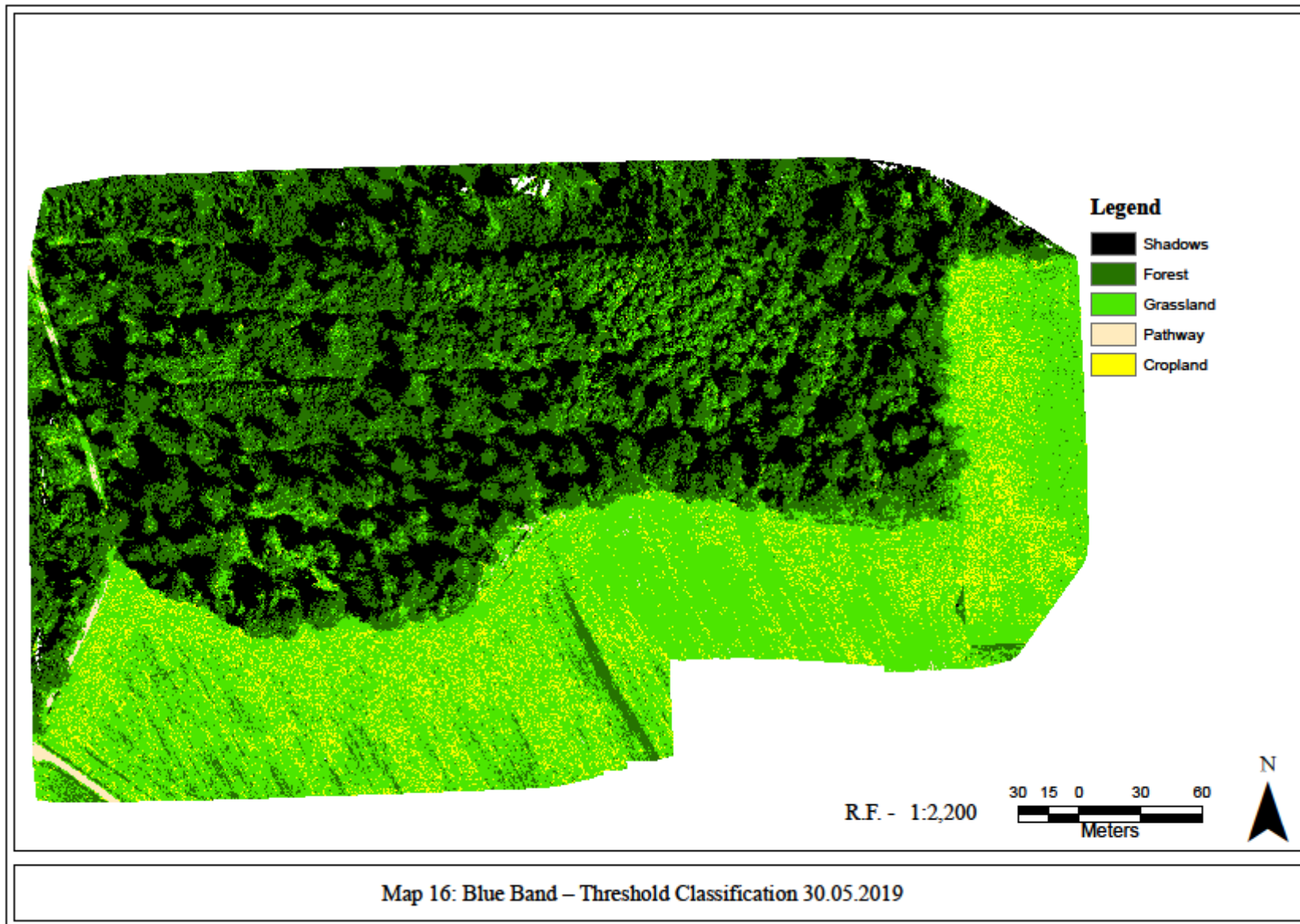
Blue Band 30.05.2019					
	Reference				
Prediction	1 Shadows	2 Forest	3 Grassland	4 Pathway	5 Cropland
1	496	65	0	0	0
2	4	386	46	0	2
3	0	49	376	125	418
4	0	0	0	353	0
5	0	0	78	0	80
Accuracy	0.979	0.873	0.726	0.869	0.560

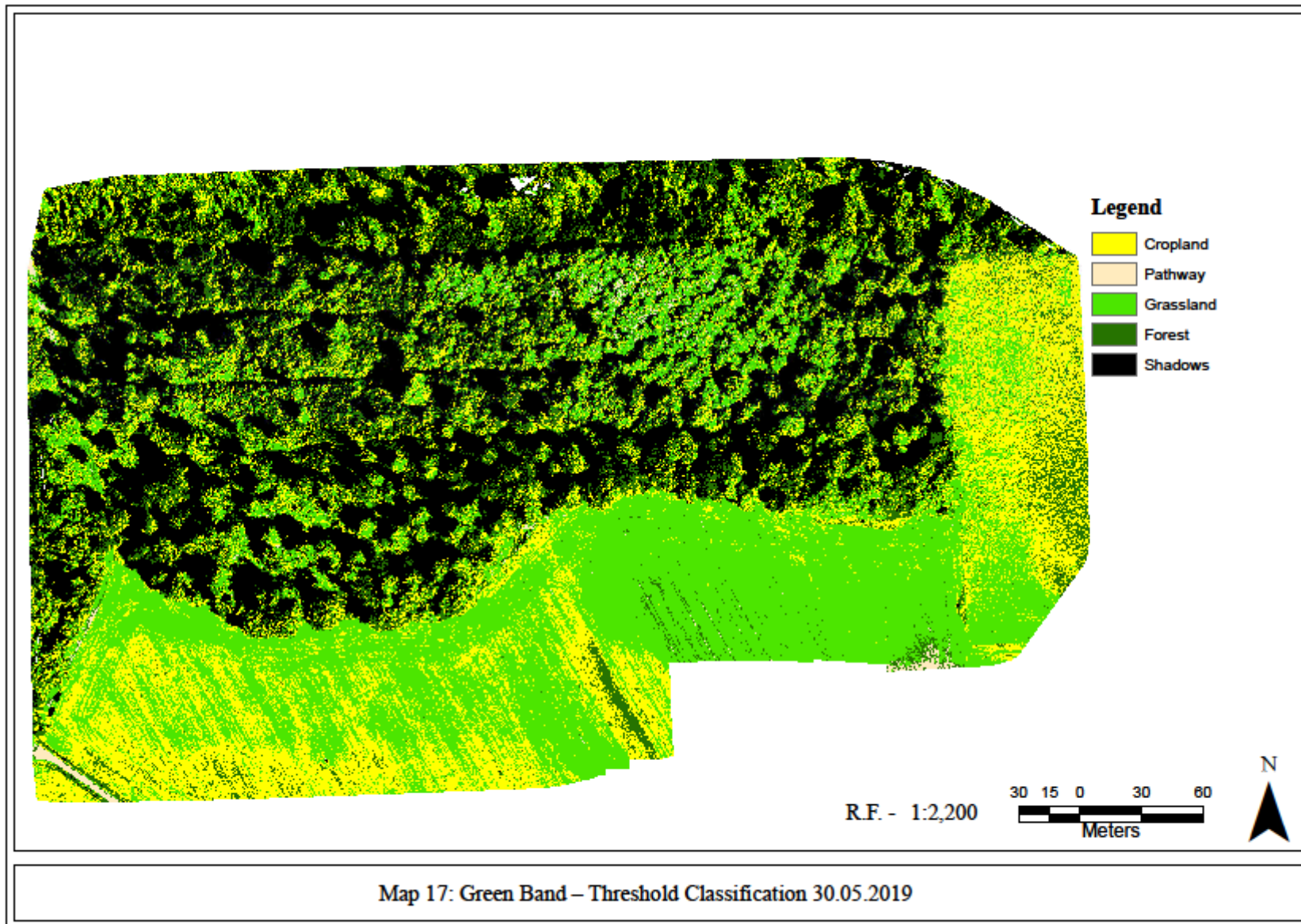
Green Band 30.05.2019					
	Reference				
Prediction	1 Shadows	2 Forest	3 Grassland	4 Pathway	5 Cropland
1	500	70	0	0	0
2	0	175	5	66	54
3	0	97	361	172	207
4	0	1	0	262	0
5	0	157	134	0	239
Accuracy	0.983	0.644	0.742	0.762	0.666

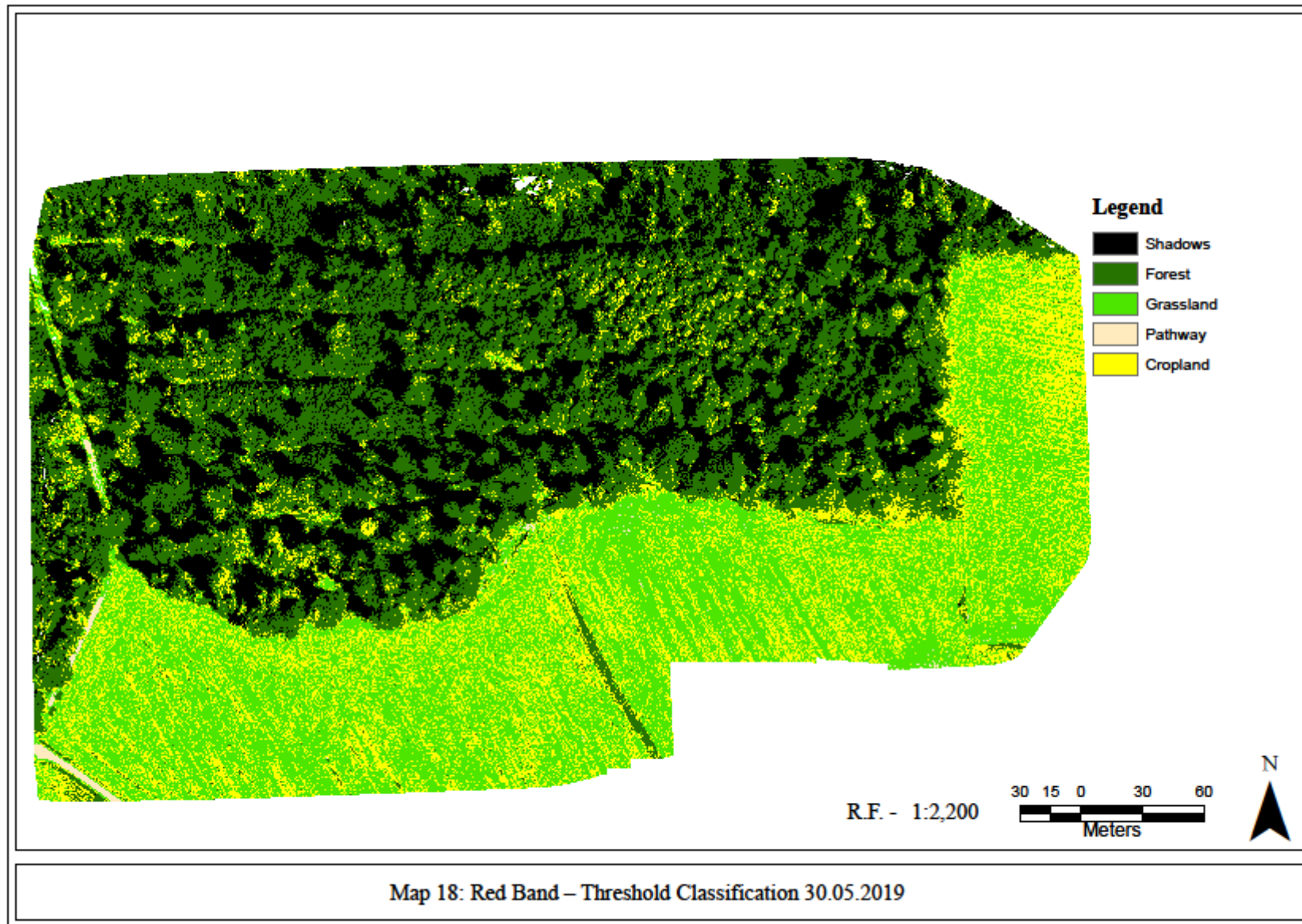
Red Band 30.05.2019					
	Reference				
Prediction	1 Shadows	2 Forest	3 Grassland	4 Pathway	5 Cropland
1	500	33	0	0	0
2	0	431	28	0	1
3	0	1	305	100	304
4	0	0	0	318	0
5	0	35	167	3	195
Accuracy	0.991	0.924	0.699	0.878	0.642

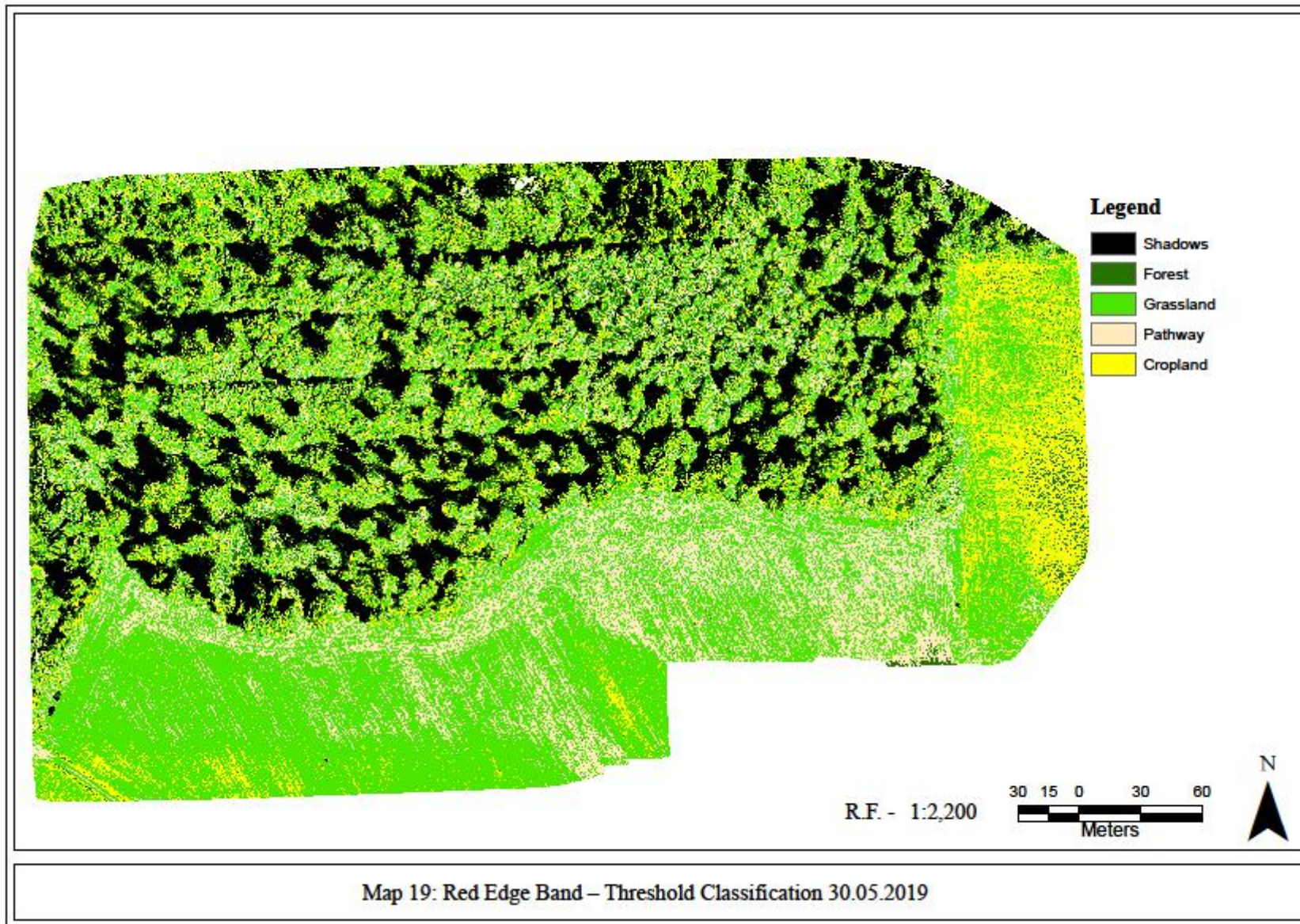
Red Edge Band 30.05.2019					
	Reference				
Prediction	1 Shadows	2 Forest	3 Grassland	4 Pathway	5 Cropland
1	496	9	0	0	0
2	4	55	0	2	25
3	0	216	371	176	235
4	0	110	123	322	17
5	0	110	6	0	223
Accuracy	0.994	0.547	0.714	0.759	0.694

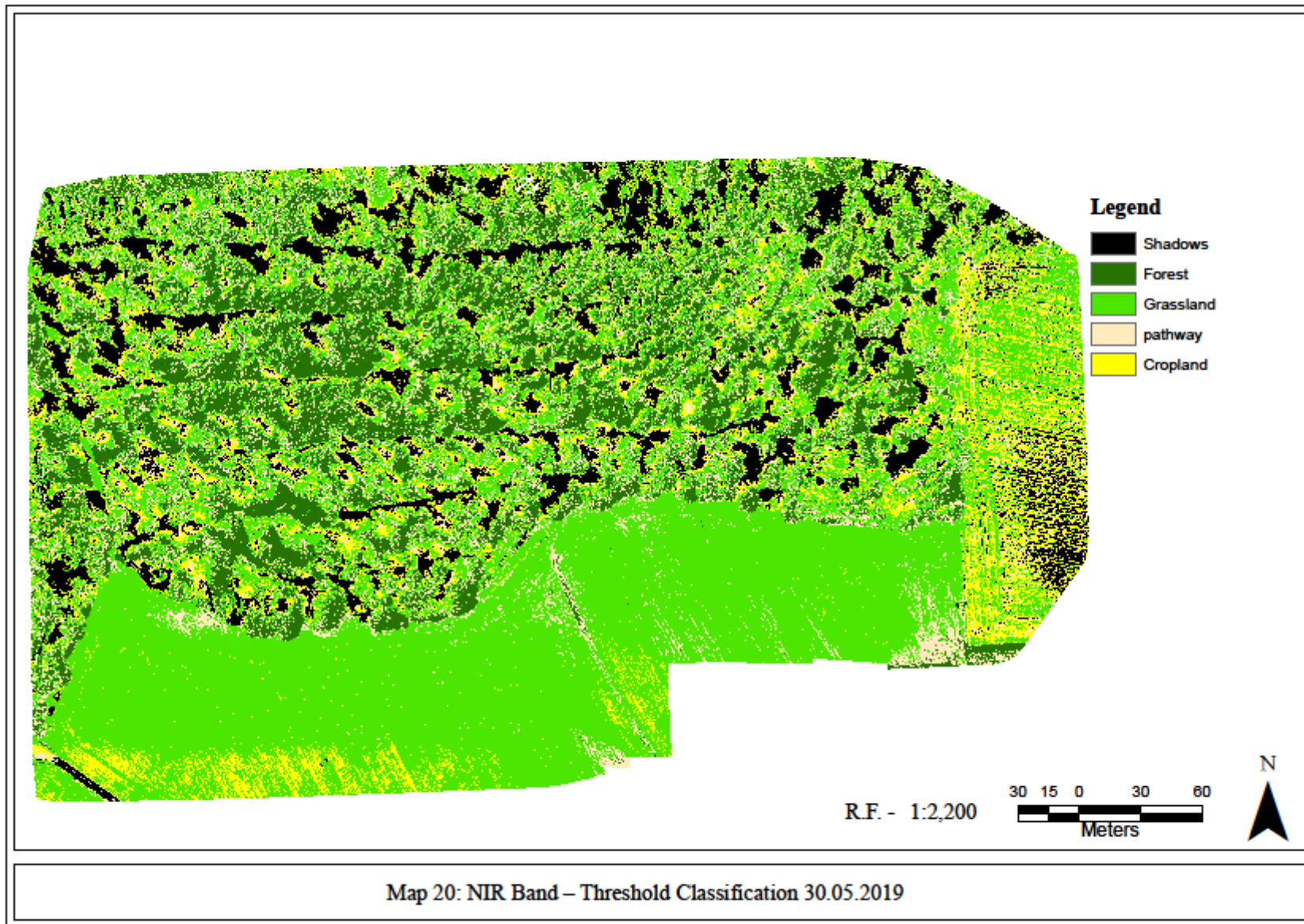
NIR Band 30.05.2019					
	Reference				
Prediction	1 Shadows	2 Forest	3 Grassland	4 Pathway	5 Cropland
1	362	0	0	46	51
2	0	214	20	0	0
3	42	164	423	340	185
4	50	110	24	83	86
5	46	12	33	31	178
Accuracy	0.838	0.709	0.740	0.515	0.648











In the April 11, 2019 dataset, the threshold brackets were created for seven land cover classes: shadows, forest, grassland, pathway, cropland, tree trunks and dormant forest which were given class number one to seven respectively (refer Map 21-25). It was observed that pixel values lying closer to the minimum range value for each band was the shadow class values. The result showed that the shadows were classified as class 1 for all the bands. The shadows showed an average level of accuracy of 0.51 for the blue band, 0.589 for the green band, 0.556 for the red band, 0.688 for the red edge band and 0.523 for the NIR band (refer Table 10). In all the bands, shadows pixels were misclassified as tree trunks and dormant forest (refer Map 21-25).

Table 10: Confusion Matrix – Threshold Classification 11.04.2019 (Source: Results derived in R 3.5.3, 2020 (bold values under class accuracy shows the accuracy of shadows))

Blue Band 11.04.2019							
	Reference						
Prediction	1 Shadow s	2 Forest	3 Grasslan d	4 Pathwa y	5 Croplan d	6 Tree trunks	7 Dorman t Forest
1	10	0	0	0	0	0	0
2	126	287	10	0	0	30	10
3	165	35	423	191	52	168	233
4	0	0	0	74	0	0	0
5	0	0	9	235	448	0	0
6	73	109	17	0	0	55	30
7	126	69	41	0	0	247	227
Accuracy	0.51	0.758	0.782	0.574	0.907	0.519	0.647

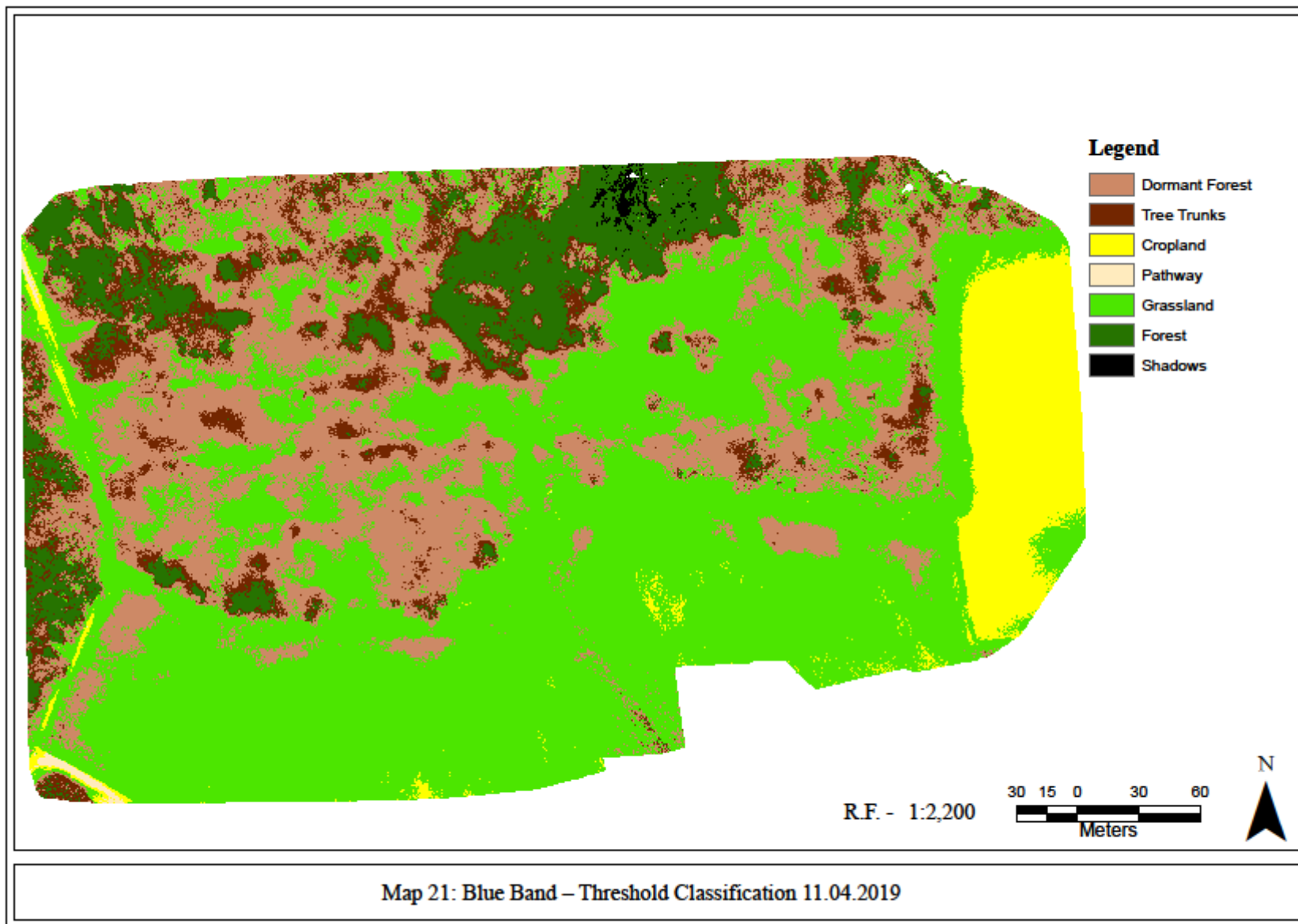
Green Band 11.04.2019							
	Reference						
Prediction	1 Shadow s	2 Forest	3 Grasslan d	4 Pathwa y	5 Croplan d	6 Tree trunks	7 Dorman t Forest
1	92	11	0	0	0	5	0
2	49	20	0	0	0	27	0
3	7	60	368	118	61	89	35
4	21	65	6	107	0	35	93
5	0	0	110	272	439	7	0
6	114	40	0	0	0	67	3
7	217	304	16	3	0	270	369
Accuracy	0.589	0.507	0.806	0.570	0.874	0.540	0.734

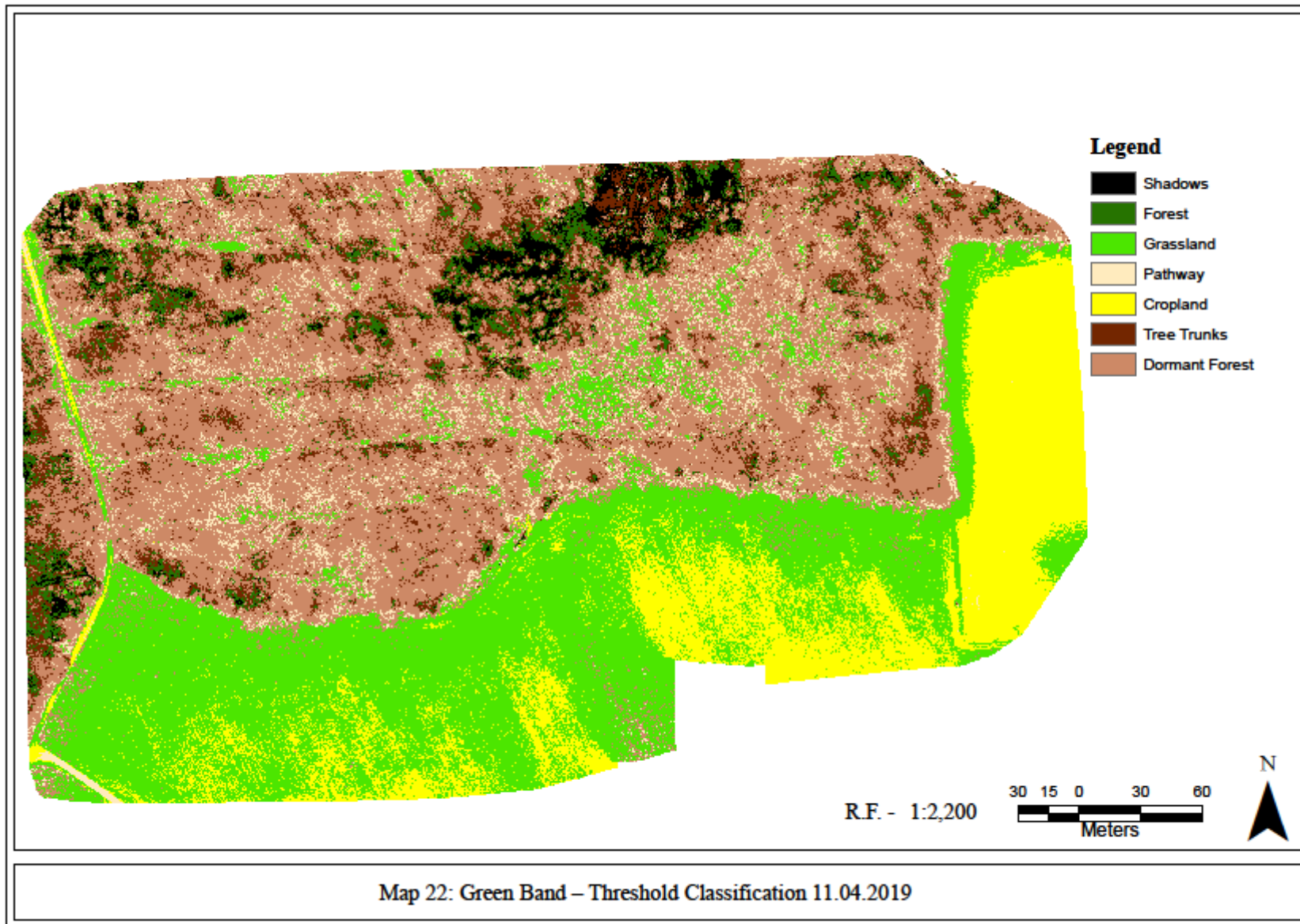
Red Band 11.04.2019							
	Reference						
Prediction	1 Shadow s	2 Forest	3 Grasslan d	4 Pathwa y	5 Croplan d	6 Tree trunks	7 Dorman t Forest
1	131	315	58	0	0	75	0
2	40	83	22	0	0	0	0
3	23	7	99	33	1	56	222
4	2	0	34	124	46	25	113
5	0	0	0	343	453	11	0
6	209	76	176	0	0	246	27
7	95	19	111	0	0	87	138
Accuracy	0.556	0.573	0.542	0.587	0.894	0.665	0.586

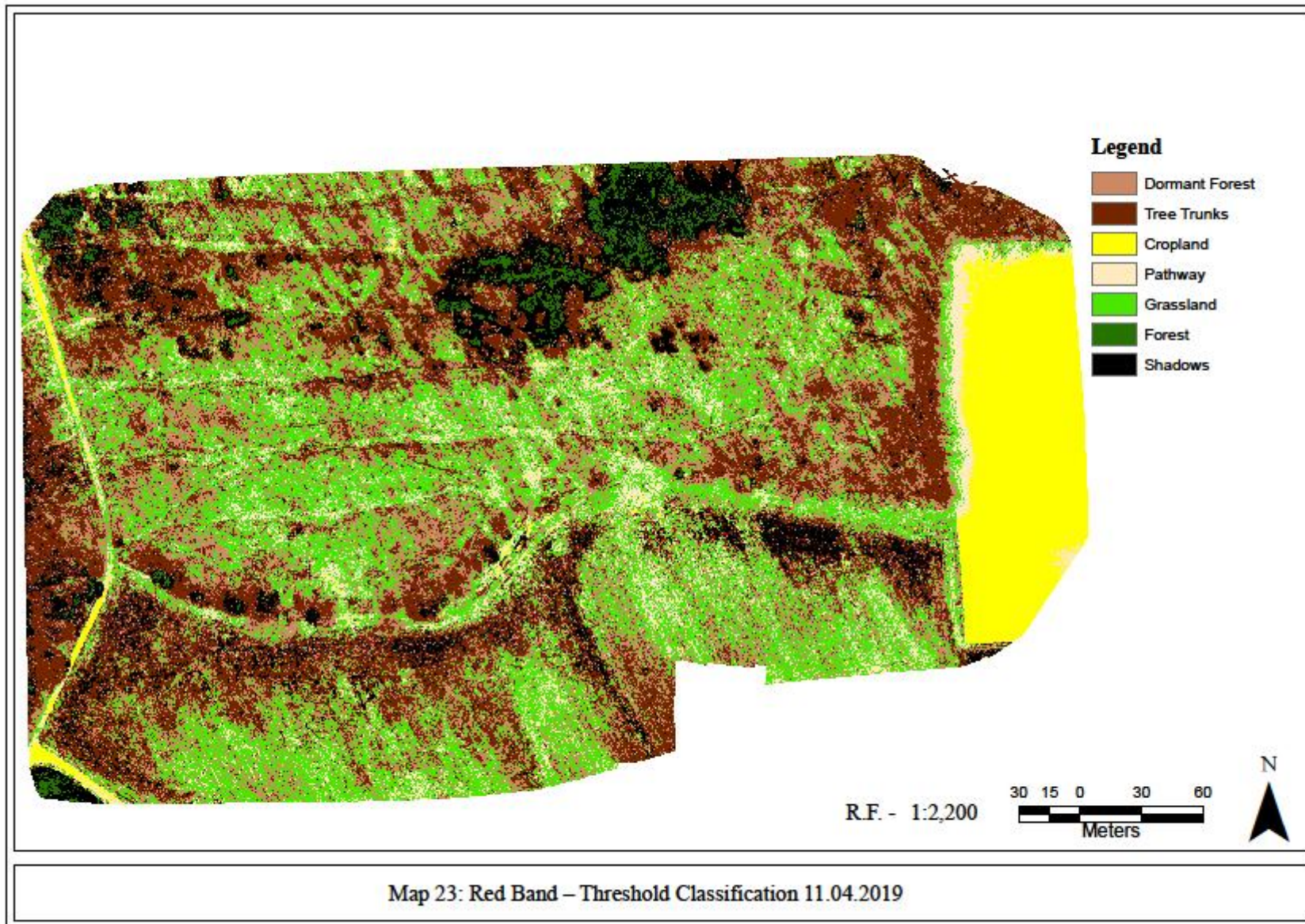
Red Edge Band 11.04.2019							
	Reference						
Prediction	1 Shadow s	2 Forest	3 Grasslan d	4 Pathwa y	5 Croplan d	6 Tree trunks	7 Dorman t Forest
1	204	32	0	0	0	67	0
2	171	154	0	22	1	155	165
3	0	9	212	230	193	12	8
4	2	62	40	95	25	42	70
5	0	2	240	101	253	5	0
6	103	71	0	1	0	118	8
7	20	170	8	51	28	101	249
Accuracy	0.688	0.568	0.637	0.555	0.695	0.586	0.686

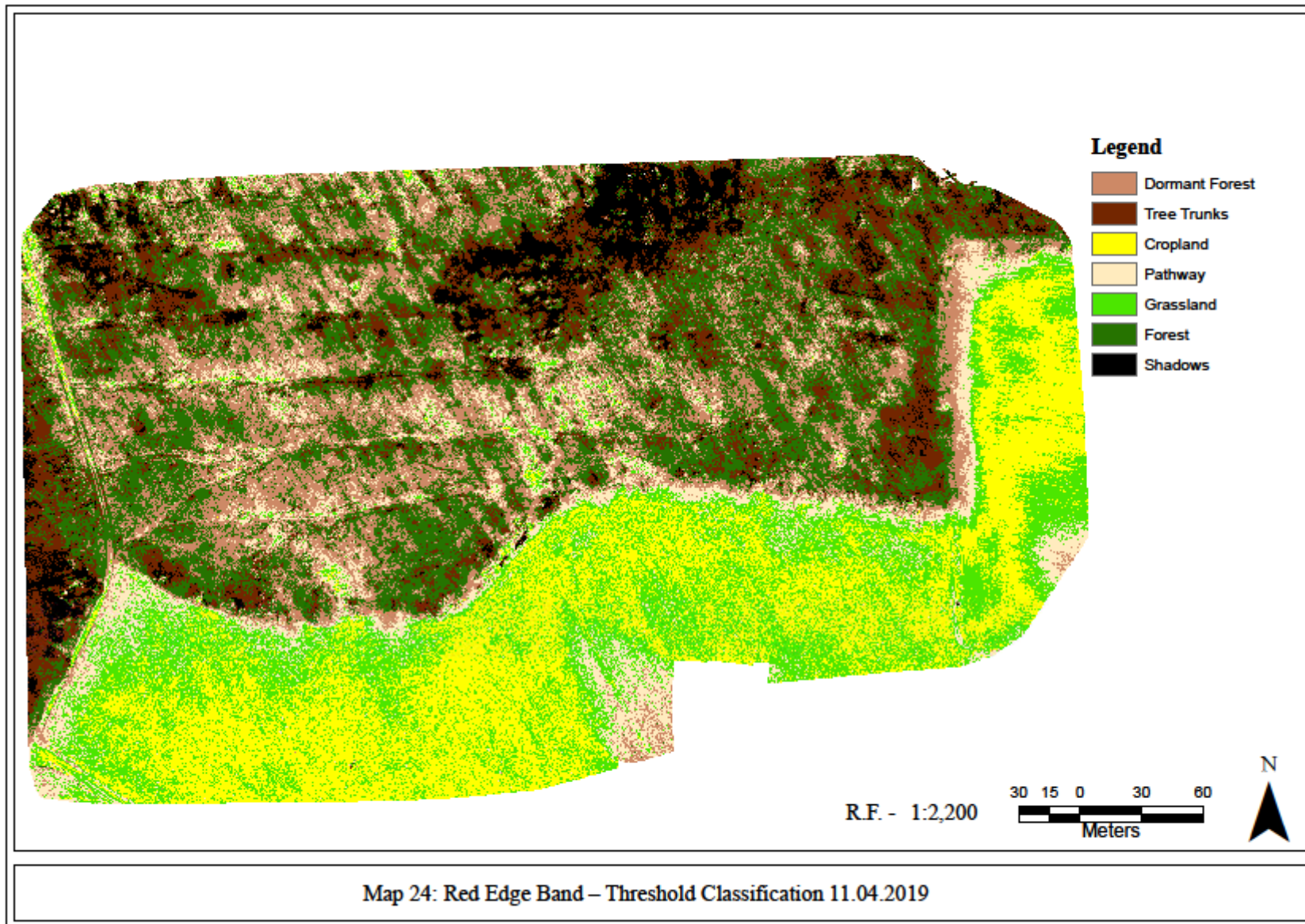
NIR Band 11.04.2019							
	Reference						
Prediction	1 Shadow s	2 Forest	3 Grasslan d	4 Pathwa y	5 Croplan d	6 Tree trunks	7 Dorman t Forest
1	24	0	0	0	0	4	0
2	0	32	32	1	0	0	0
3	0	173	468	56	0	12	17
4	7	121	0	157	208	92	162
5	104	139	0	263	238	169	302
6	135	4	0	0	0	73	0
7	230	31	0	23	54	150	19
Accuracy	0.523	0.527	0.925	0.559	0.575	0.550	0.437

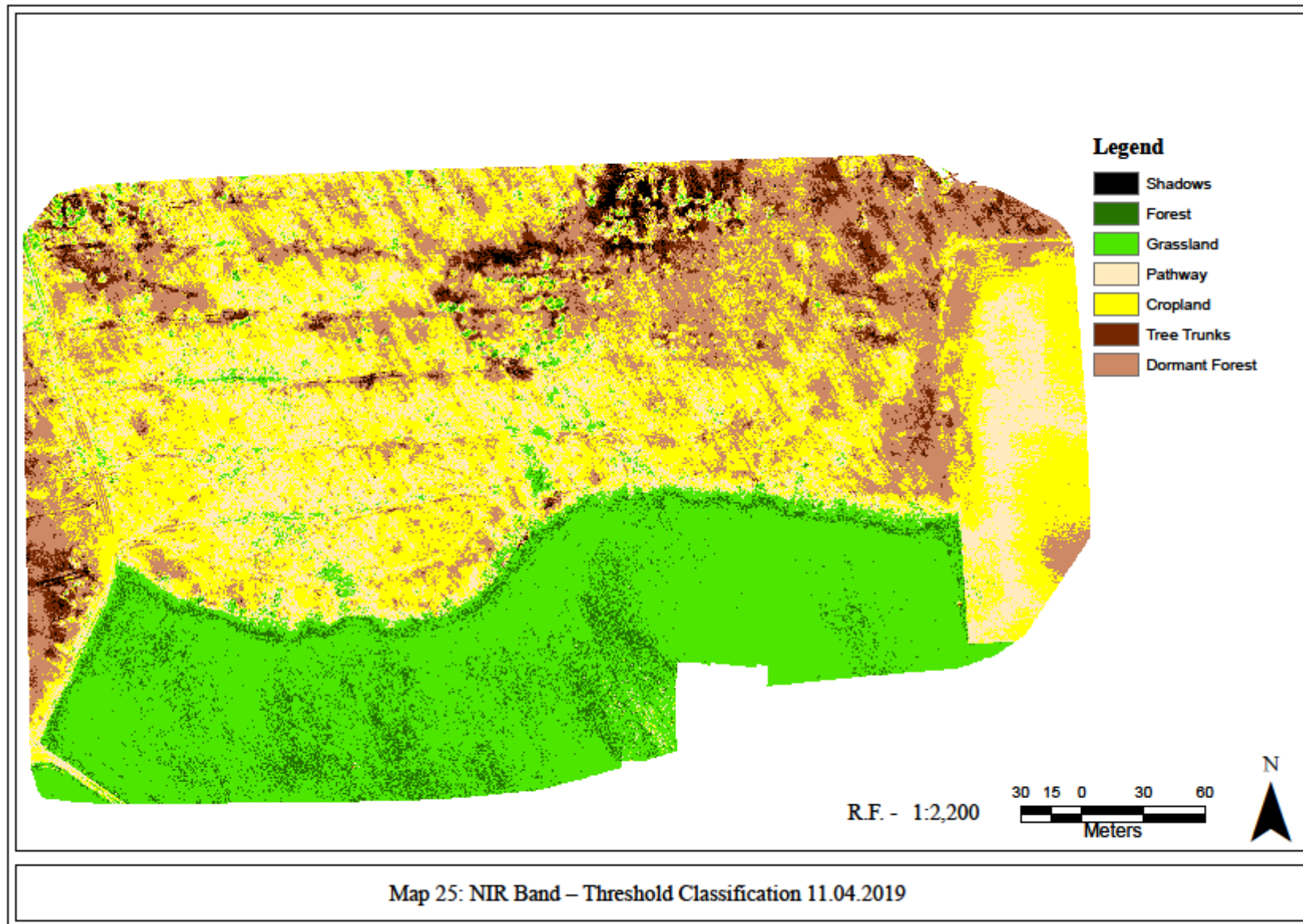
Overall accuracy: blue 0.435, green 0.418, red 0.364, red edge 0.367 and NIR 0.289.











4.4. Vegetation Indices Threshold Classification

It was observed that pixel values lying closer to the maximum range value for CCCI, GCC and NDVI bands were the shadow class values while it was opposite in the case of EVI where the shadows pixel value were closer to the lower range of the minimum-maximum values. Shadows were classified as class one for each band.

In the May 30, 2019 dataset, the threshold brackets were created for five land cover classes: shadows, forest, grassland, pathway and cropland which were given class number one to five respectively (refer Map 26 -29). The results showed that the shadows (in class 1) showed high accuracy of 0.922 for CCCI, 0.645 for EVI, 0.748 for GCC and 0.923 for NDVI (refer Table 11). The results also showed that shadows pixels were misclassified into other classes in all the VIs (refer Map 26-29). NDVI showed least amount of misclassification because shadows pixels were only misclassified as forest and only a few pixels of forest were misclassified as shadows (refer Map 29).

Table 11: Confusion Matrix – Vegetation Indices 30.05.2019 (Source: Results derived in R, 2020 (bold values under class accuracy shows the accuracy of shadows))

CCCI 30.05.2019					
	Reference				
Prediction	1 Shadows	2 Forest	3 Grassland	4 Pathway	5 Cropland
1	461	3	0	146	1
2	15	346	56	100	162
3	0	98	224	23	161
4	24	18	0	144	5
5	0	35	220	10	171
Accuracy	0.922	0.759	0.651	0.659	0.602

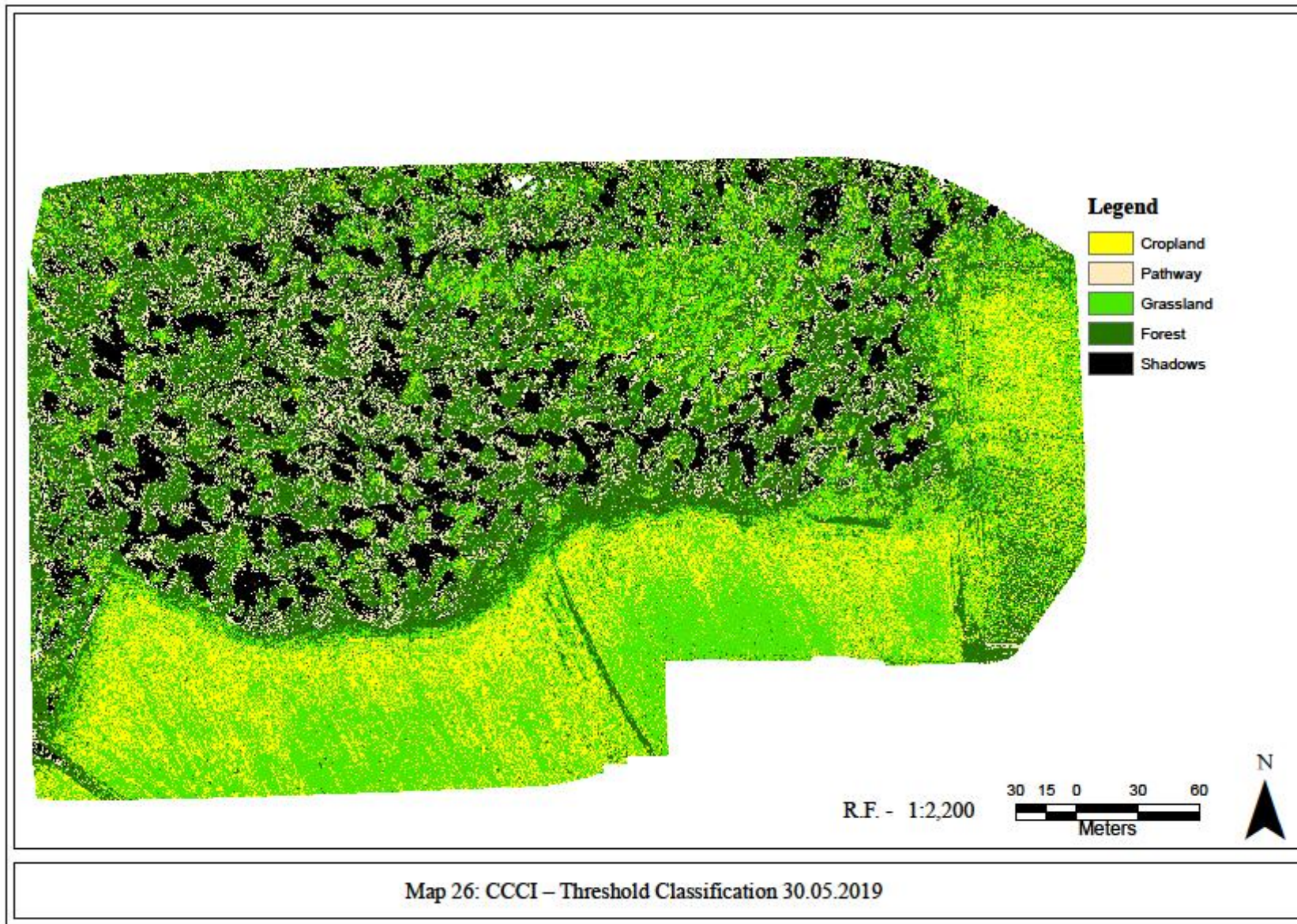
EVI 30.05.2019					
	Reference				
Prediction	1 Shadows	2 Forest	3 Grassland	4 Pathway	5 Cropland
1	257	0	125	93	207
2	1	376	37	0	4
3	124	67	275	21	129
4	81	0	1	284	109
5	37	57	62	1	51
Accuracy	0.645	0.865	0.685	0.808	0.510

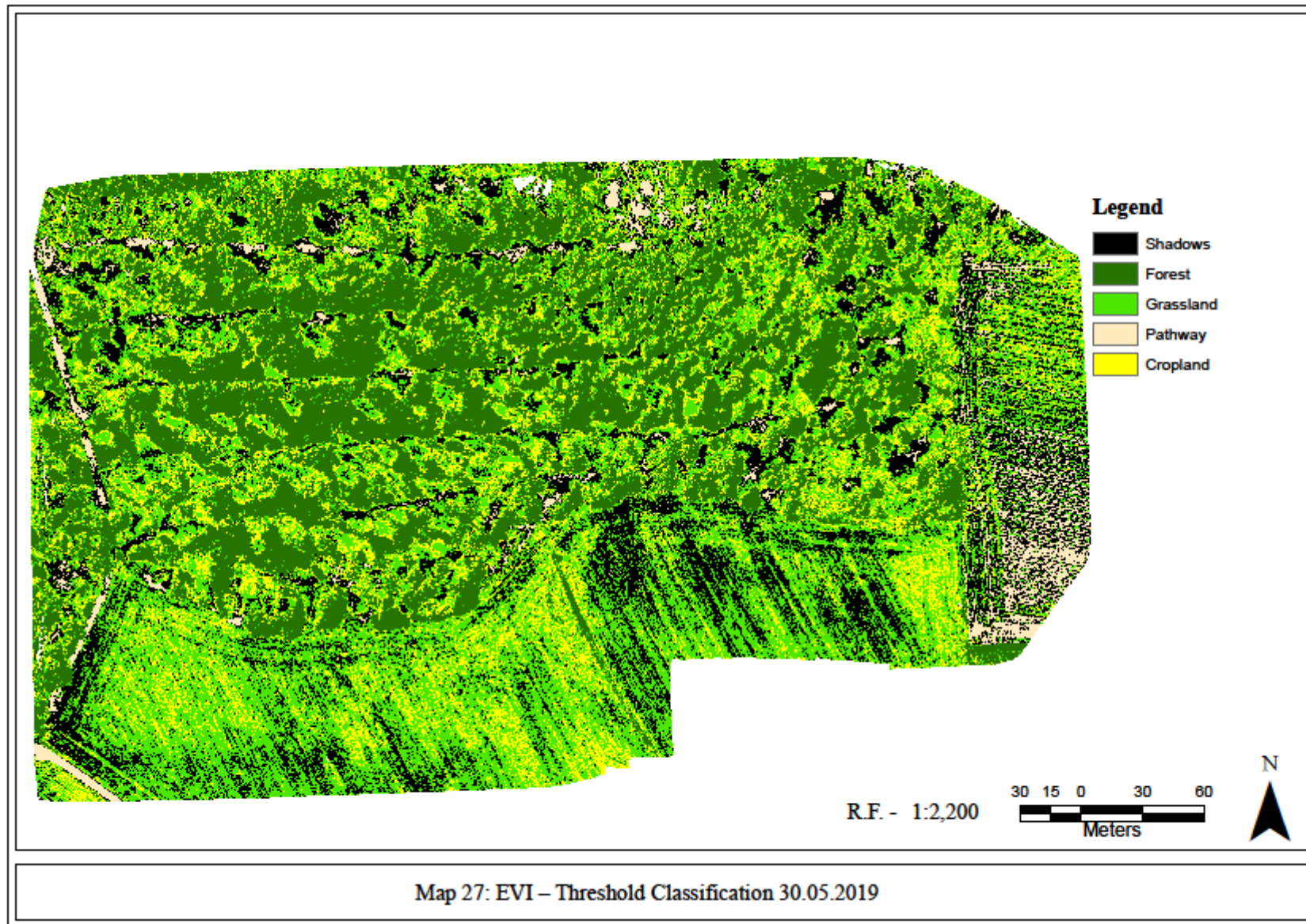
GCC 30.05.2019					
	Reference				
Prediction	1 Shadows	2 Forest	3 Grassland	4 Pathway	5 Cropland
1	300	122	35	0	42
2	14	369	23	0	0
3	141	6	211	4	192
4	0	0	0	365	14
5	45	3	231	57	252
Accuracy	0.7483	0.8594	0.62196	0.9249	0.6648

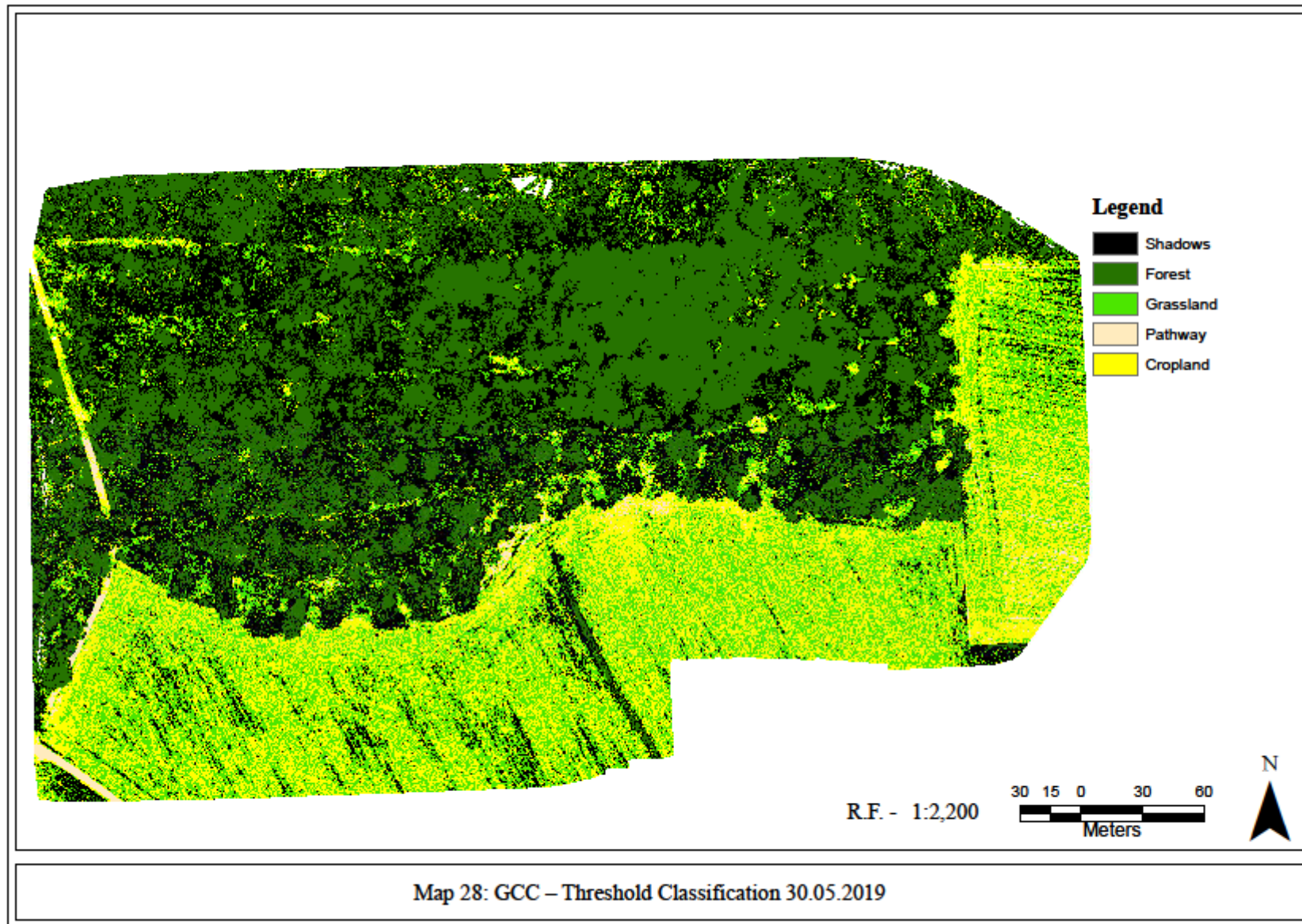
NDVI 30.05.2019					
	Reference				
Prediction	1 Shadows	2 Forest	3 Grassland	4 Pathway	5 Cropland
1	461	144	1	0	0
2	38	356	35	0	21
3	1	0	338	3	245
4	0	0	0	150	1
5	0	0	126	258	233
Accuracy	0.9231	0.8314	0.7729	0.68223	0.63253

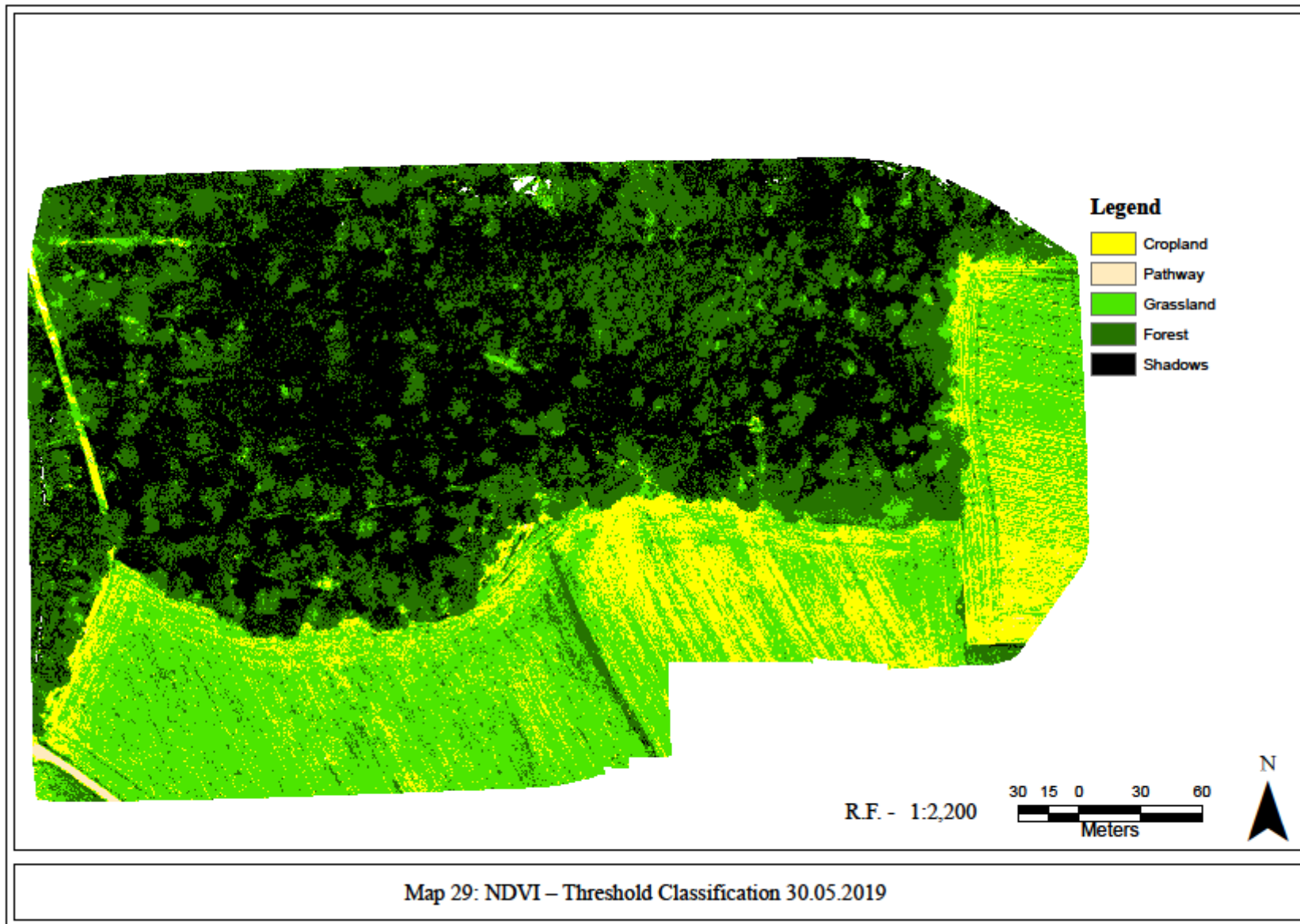
All the VIs showed an average overall accuracy for each band. CCCI showed an overall accuracy of 0.556 and EVI showed an overall accuracy of 0.518 which was least amongst all the indices. GCC showed an overall accuracy of 0.617 which was the second-highest while NDVI showed an accuracy of 0.638 which was the highest accuracy value amongst the four indices.

In the April 11, 2019 dataset, the threshold brackets were created for seven land cover classes: shadows, forest, grassland, pathway, cropland, tree trunks and dormant forest which were given class number one to seven respectively (refer map 30 – 33). The minimum and maximum values for each VI band were first identified and based on this; range brackets for shadow land cover classes were developed. It was observed that pixel values lying closer to the middle of the minimum – maximum range values for CCCI, EVI and NDVI bands were the shadow class values while in the case of GCC shadows class value range was distributed from lower range values to middle range of the GCC values.









Shadows were classified as class one for each VI. The results showed that shadows class had an accuracy of 0.549 for CCCI, 0.496 for EVI, 0.507 for GCC and 0.494 for NDVI (refer Table 12). The results showed that shadows pixels were misclassified into other classes in all the VIs. EVI showed that shadows class pixels were least misclassified as compared to the other VIs. The shadows were misclassified as tree trunks and dormant forest classes (refer Map 31). All the VIs showed that other land cover classes were misclassified as shadows class (refer Map 31-33).

Table 12: Confusion Matrix – Vegetation Indices 11.04.2019 (Source: Results derived in R 3.5.3, 2020 (bold values under class accuracy shows the accuracy of shadows))

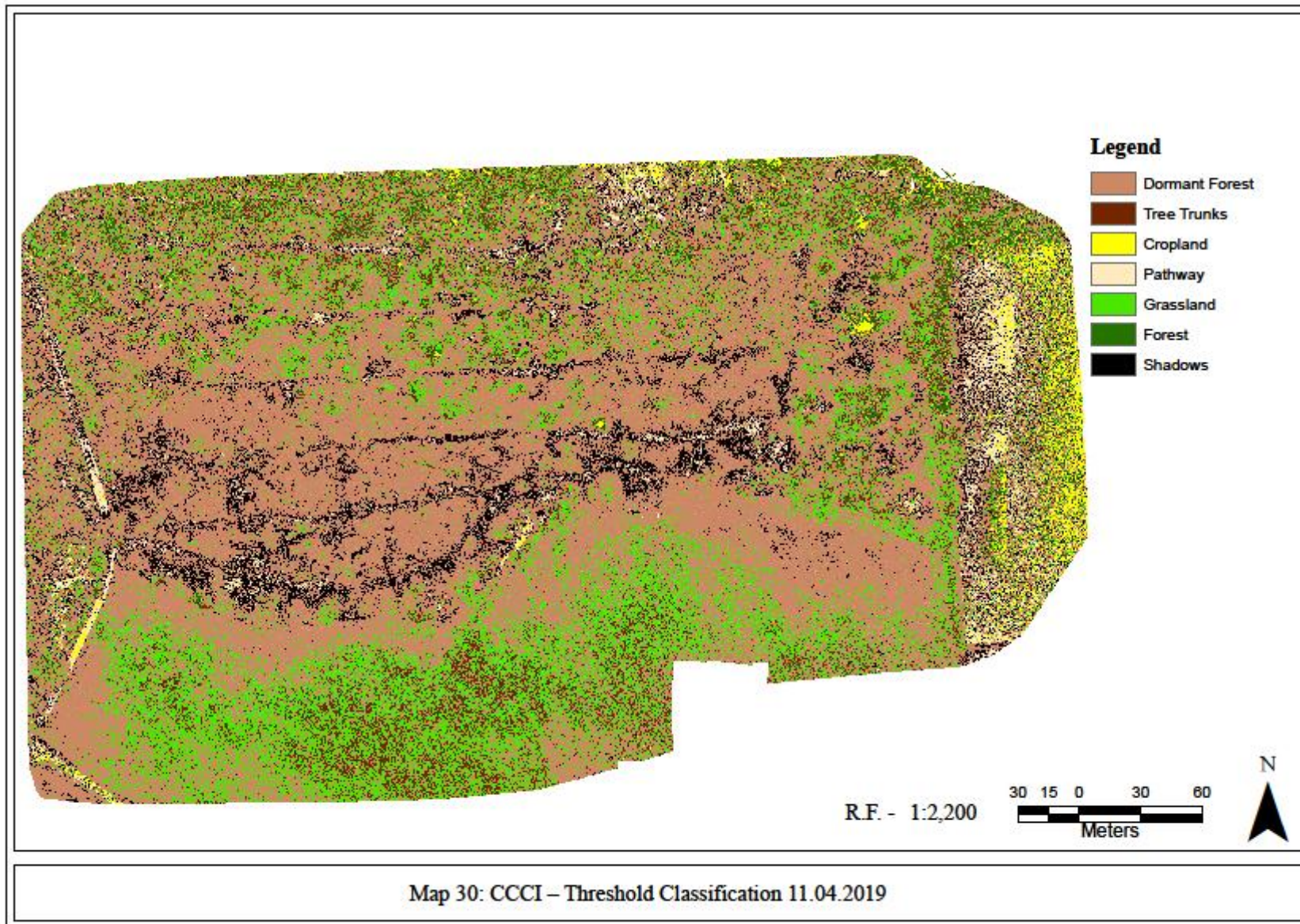
CCCI 11.04.2019							
	Reference						
Predictio n	1 Shadow s	2 Forest	3 Grasslan d	4 Pathwa y	5 Croplan d	6 Tree trunks	7 Dorman t Forest
1	98	9	8	101	60	19	100
2	8	77	0	4	52	43	3
3	52	105	174	14	43	99	13
4	72	0	0	178	38	10	7
5	2	28	0	72	84	31	0
6	26	49	62	6	28	74	15
7	242	232	256	125	193	224	362
Accuracy	0.549	0.559	0.620	0.657	0.562	0.543	0.650

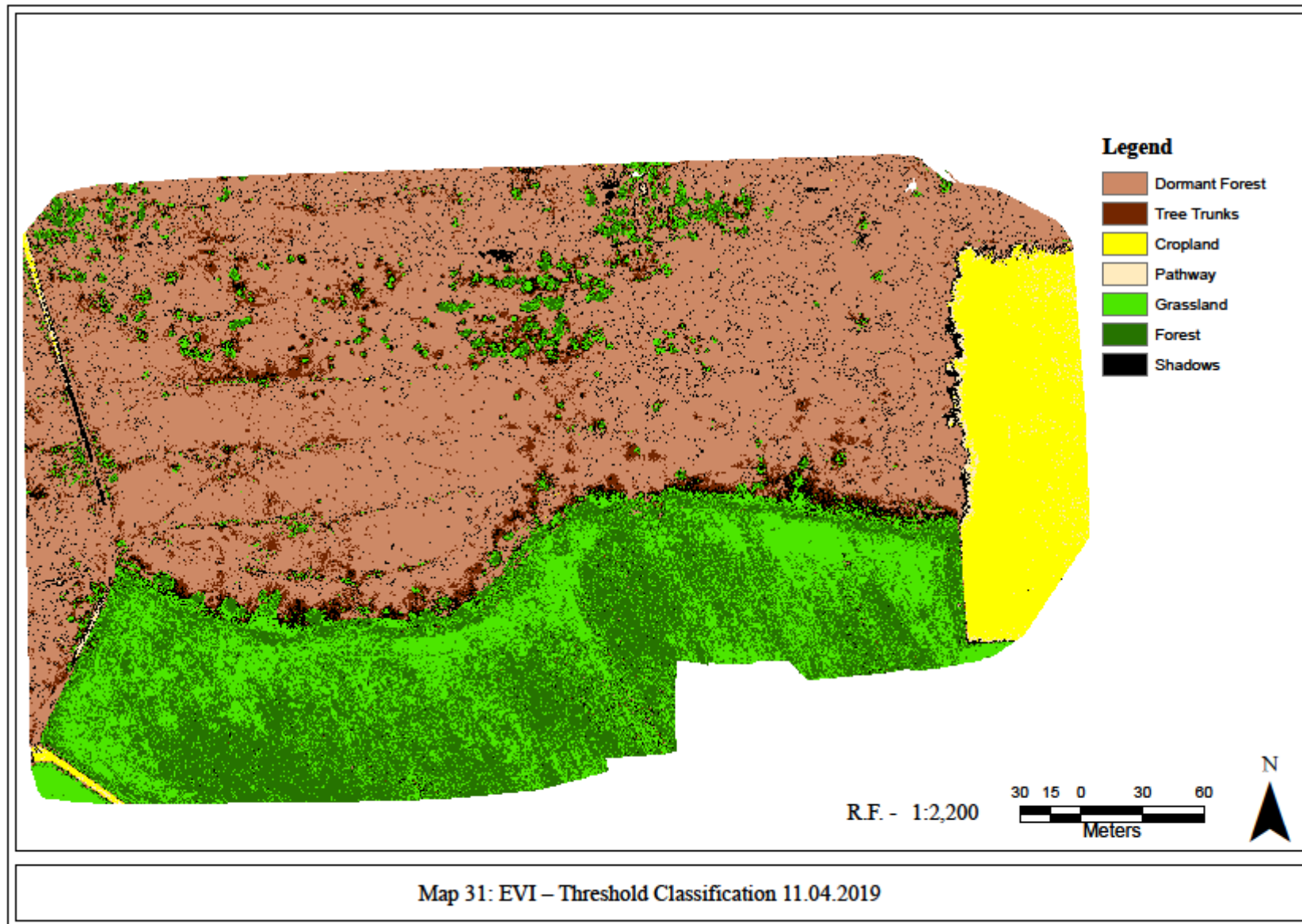
EVI 11.04.2019							
	Reference						
Predictio n	1 Shadow s	2 Forest	3 Grasslan d	4 Pathwa y	5 Croplan d	6 Tree trunks	7 Dorman t Forest
1	36	50	1	148	3	24	12
2	0	275	219	0	0	1	0
3	0	106	279	0	0	10	0
4	0	0	0	79	37	0	0
5	0	0	0	167	460	0	0
6	66	20	0	0	0	72	2
7	398	49	1	106	0	393	486
Accuracy	0.496	0.738	0.760	0.573	0.932	0.557	0.828

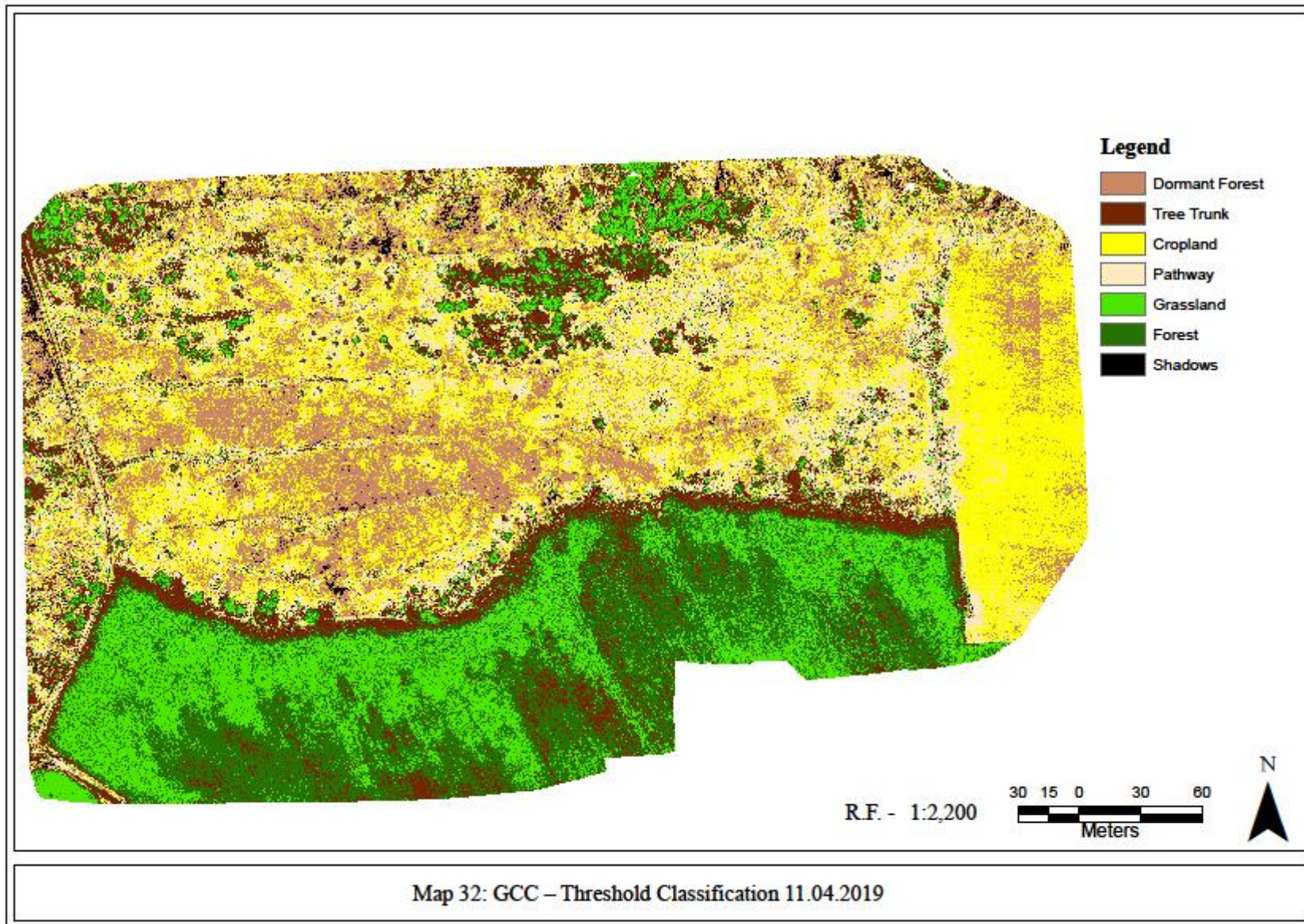
GCC 11.04.2019							
	Reference						
Predictio n	1 Shadow s	2 Forest	3 Grasslan d	4 Pathwa y	5 Croplan d	6 Tree trunks	7 Dorman t Forest
1	12	0	0	20	0	11	1
2	35	124	196	0	0	7	0
3	20	320	296	76	0	29	0
4	95	14	0	173	39	165	71
5	160	2	0	27	428	53	228
6	67	36	8	143	0	192	1
7	111	4	0	61	33	43	199
Accuracy	0.507	0.584	0.722	0.609	0.850	0.650	0.657

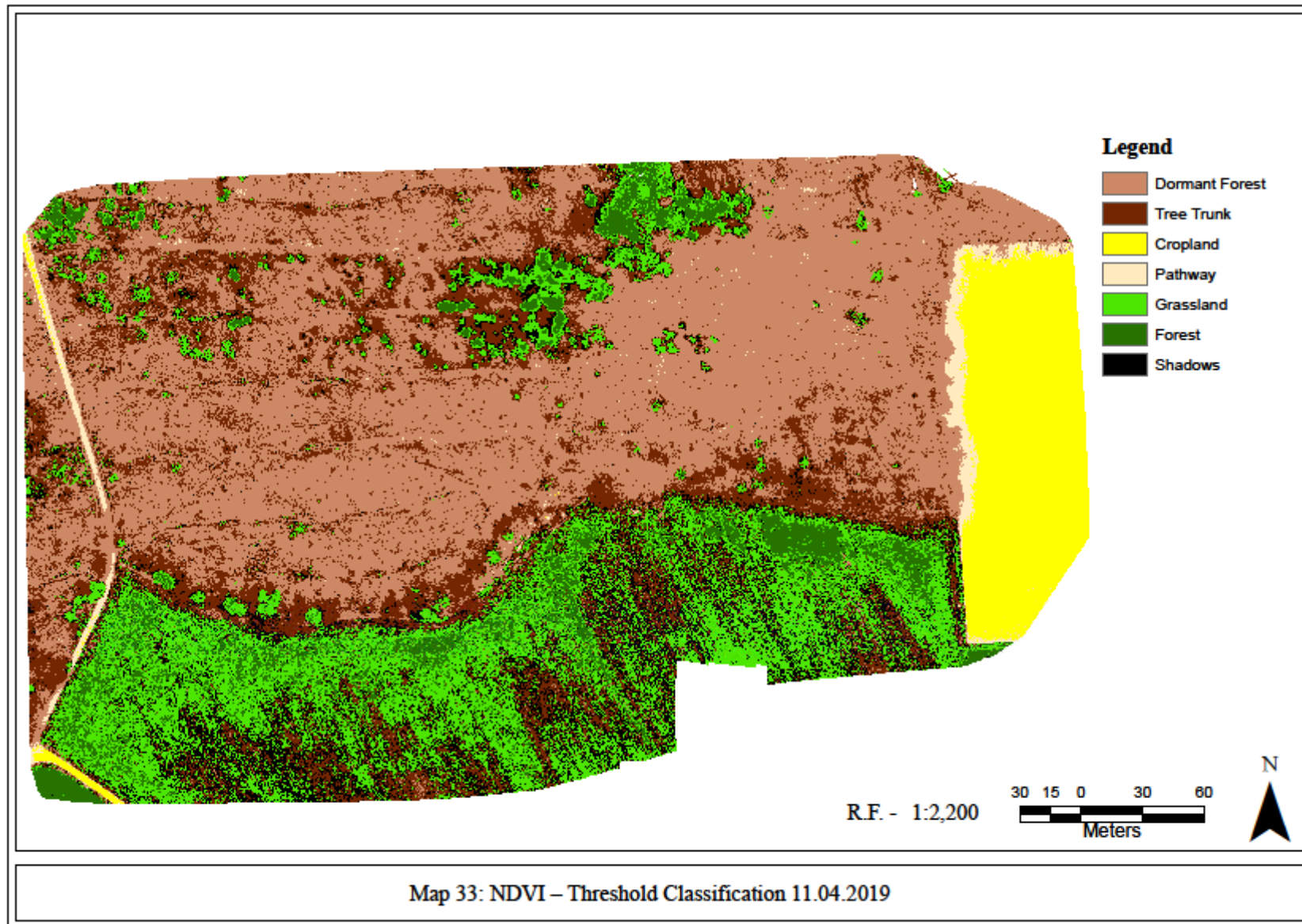
NDVI 11.04.2019							
	Reference						
Predictio n	1 Shadow s	2 Forest	3 Grasslan d	4 Pathwa y	5 Croplan d	6 Tree trunks	7 Dorman t Forest
1	14	34	73	0	0	16	0
2	51	232	107	0	0	0	0
3	68	188	272	0	0	2	0
4	0	0	0	243	31	12	0
5	0	0	0	222	469	0	0
6	143	27	48	0	0	240	25
7	224	19	0	35	0	230	475
Accuracy	0.494	0.706	0.729	0.736	0.932	0.670	0.890

CCCI showed an overall accuracy of 0.299 which was least amongst the four indices. EVI showed an overall accuracy of 0.482 which was the second highest while GCC showed an accuracy of 0.407. NDVI showed the highest value for the overall accuracy which was 0.556 (refer Annexure 4).









Chapter – 5

Discussion

This chapter reviews various shadow detection methods that were used for the May 30, 2019 and the April 11, 2019 datasets. It was observed that there were variations between these methods and also some variation were observed within each method. Hence, a conclusion could be drawn at the end of the discussion which method was better at detecting shadows.

The first thing that was observed was the difference in land cover classes for both the datasets. There were five classes in the May 30, 2019 dataset while seven classes were observed in the April 11, 2019 dataset because May marked the end of the spring season when the leaves were fully grown but in the case of April dataset, most of the forest was dormant and furthermore, tree trunks were lying across the forest stand. The variation in the land cover highlighted an issue related to the spectral signature overlap. The dormant forest and tree trunks land cover had similar spectral reflectance and the same was observed in the case of cropland and grassland land covers. In the April 11, 2019 dataset, it was observed that shadows were misclassified as dormant forest class while tree trunks and dormant forest class pixels were identified as shadows because there was a similarity in the spectral characteristics of these three land cover classes. But in the May 30, 2019 dataset, something similar yet different was observed as shadows were misclassified mostly with the forest class and vice versa. However, the misclassification for the May 30, 2019 dataset was minor which can easily be neglected.

The pattern and size of the shadows in the April dataset were quite different from that of May dataset because of the variation in the land cover and the stage of development of the forest stand. The April imagery had small cylindrical shaped shadows from southeast to northwest which were formed due to the axed tree trunks and leafless trees (deciduous trees). It showed small patches of shadows around small clusters of evergreen trees in the northwest, centre and fringes at the south of the forest stand. On the contrary, the May dataset showed big patches of shadows across the forest stand. The shadows in the deciduous forest segment were dense as compared to the shadows in the evergreen forest segment because the deciduous forest had broad leaves and had more foliage as compared to the evergreen trees which had small leaves and less foliage. Just because the May dataset showed bigger clusters of shadows in comparison to the April dataset, it became easier for unsupervised classification and threshold classification methods to detect shadows.

The unsupervised classification methods (HW and Lloyd) showed high accuracy in detecting shadow however the overall accuracy of the method was average. Though these methods were quite simple and easy but had its disadvantages as it required user to identify the right number of classes that could identify all the land covers including the shadows as one of the other classes. But it was observed that even if the desired number of classes were same as that of the number of the visible land cover classes in the imagery then also there was a tendency of misclassification of one or more classes. The fragmentation increased when the number of classes was more than the number of visible land covers classes in the imagery. It was observed that misclassification of the land cover classes in both the dataset was bound to occur because the short-range values couldn't cover one entire class e.g. unsupervised classification with ten clusters showed shadows distributed over two or three classes. But the longer range of values for a class misclassified other classes as shadows as it showed in the case of unsupervised classification with two clusters where the forest and grassland were misclassified as shadows along with the actual shadows. Enderle and Weih (2005) observed a similar pattern where the clusters showed spectral homogeneity which may not correspond with the information classes of interest. Furthermore, the relationship between the natural clustering and desired land cover classes were not always directly correlated.

The supervised classification methods (RF and MLC) were quite accurate as they showed high accuracy in detecting shadows and even showed a high level of accuracy for the overall method accuracy. Furthermore, it was less time consuming because the training and validation sample sets were created before initiating the process and once they were ready the rest of the method became a one-click method. This method proved to be quite an accurate method for both the datasets. All the other methods showed low accuracy for April dataset since the size of the shadows were small but supervised classification still produced a satisfactory result, better than unsupervised and threshold methods of classification as only a few patches of forest were misclassified as shadows. This might have been due to the precise selection of the sample training sites containing pure and natural spectral values for each land cover (Al Ajmi, 2009).

The threshold classification showed an average level of accuracy for class-wise accuracy and for the overall method accuracy as well. The time-consuming task in this method was to identify the threshold ranges for each class of each band of the UAV multispectral dataset. In the April dataset, the size of shadows was small and therefore, it took more time to identify its range brackets for each band and the spectral range was closer to the minimum value but it

was fragmented or disturbed by other classes like tree trunks and dormant forest. In the May dataset, the big cluster of shadows gave a clear spectral range brackets lying closer to the minimum value of each band and was easier to identify as compared to the April dataset. Threshold method relies on hit and trial method and therefore, it can be said that the time required to perform threshold method would increase if the area of the site increases or the size of the features for each class in the UAV imagery decreases in size. Hsieh et al. (2016) observed a similar response of shadows in his research where it showed that the pixel values of shadows were lower as compared to the non-shaded areas of the study area. It also showed that the pixel values of shadows decrease in the visible light due to scattering. A similar pattern was observed in another study where the spectral reflectance of the shaded leaves to the non-shaded leaves was compared. It showed that the non-shaded leaves showed low reflectance at blue and red regions of the spectrum but then it spiked at the green region and the reflectance remained at high value for NIR. The reflectance of the shaded leaves was lower for all the regions of the spectrum but a minor increase in the reflectance was observed at the NIR region (Zhang et al. 2015).

The spectral range bracket for shadows in the vegetation indices was difficult to identify because there were no land cover classes that were dedicated to shadows in CCCI, EVI and GCC, only some patches were visible in NDVI. CCCI could not detect all the shadows in the April dataset but a good amount of shadows were detected in the May dataset. Therefore, it can be said that CCCI could be sensitive to shadows only if there are big clusters of shadows in the imageries. EVI misclassified other classes as shadows since it could only detect a few patches of shadows in May dataset so therefore, EVI was not much affected by shadows. In the case of GCC, it only detected shadows which were at the fringes of the tree foliage or fringes of the cluster of trees for the May dataset but in the April dataset, it detected only a few small patches of shadows which were also not accurate. In the April dataset, NDVI couldn't detect small patches of shadows but in the May dataset, it misclassified some patches of the forest as shadows. Hence, it was easier to detect shadows in the calculated VIs for the May dataset as it contains big clusters of shadows as compared to the smaller cluster of shadows in the April dataset. The sensitive VIs were able to detect only a few patches of shadows in the May dataset even though it contained big clusters of shadows while the rest of the shadow patches were misinterpreted.

The threshold values of shadows for CCCI, GCC and NDVI were detected between the middle to maximum value ranges for the respective VIs bands' minimum-maximum range

except for EVI, where the pixel values for shadows were detected closer to the minimum VI band's minimum-maximum range. Zhang et al. (2015) shared similar results that the pixel values of shadows for the 11 out of 14 VIs showed high spectral values lying closer or higher than the non-shaded vegetation pixel values. In the case of NDVI, the shadows threshold values were detected closer to the higher values of the minimum-maximum range bracket which were found to be similar for this thesis as well.

Overall, less than 50% of the shadows were detected in the April dataset but more than 60% of the shadows were detected in the May dataset for all the VIs. Hence, it could be said that NDVI and CCCI were sensitive to shadows while EVI and GCC were not that sensitive to shadows and misinterpreted the information.

Chapter – 6

Conclusion

The objectives of the study were to compare the different methods to detect shadows in UAV multispectral imageries and identify VIs sensitivity to the shadows. To achieve these objectives, unsupervised classification, supervised classification, threshold classification for band and threshold classification for CCCI, EVI, GCC and NDVI methods were used for the spring temporal datasets. In this thesis, a clear methodology for each method was established so that the same methods can be reproduced to support researches on variation in phenology in the future.

Each method showed good accuracy in the results as it could produce maps in which shadows were detected as one of the visible land cover classes along with the other classes (shadows, forest, grassland, pathway, cropland, tree trunks and dormant forest). As discussed in results and discussion chapter, all the methods had its advantages and disadvantages in detecting shadows so it depends on the user's interest that which method would work best for his interest. The best method to detect shadows depends on a few factors such as the size of the study area, the amount of knowledge the user has or requires before starting the classification process, objectives of the study and manipulation of shadows to extract further information or remove it from the imageries and time constraints.

As for this study area, the best method to detect shadows was supervised classification because it showed high accuracy for shadow land cover class and for the overall method accuracy. Furthermore, this method consumed minimum amount of time in processing the results because it required minimum input to initiate the classification. It only required a training and validation sample set which trains and check the accuracy of the pixel classification. The supervised classification had in-built accuracy assessment to check overall accuracy and class-wise accuracy so it didn't require any additional efforts to check and compare the methods.

The second best method to detect shadows was unsupervised classification because it showed high accuracy for detecting shadows land cover class even though the overall method accuracy was at an average level. This method took some time to identify the best number of classes to detect visible land cover classes and shadows as one of them and also to identify which algorithm works best in the interest of the study. The unsupervised classification

doesn't have any in-built validation setup so it required an additional accuracy assessment to check overall accuracy of the method and class-wise accuracy.

CCCI and NDVI were more sensitive to shadows as compared to EVI and GCC. As the size of the shadows increased, CCCI and NDVI became more and more sensitive to shadows and GCC became slightly sensitive to it but EVI remained least affected.

This study helped to find the best method to detect shadows in UAV multispectral imageries and this information on shadows can further be explored because shadows contain incomplete spectral information of the land cover features. The researchers can further decide whether to extract information from shadows or remove it from the imagery.

The study also showed that supervised classification showed a high level of accuracy while the threshold classification showed a below average accuracy level so therefore, the future research may focus on integrating different methods to detect shadows in order to achieve better accuracy and better overall result.

The future studies can reproduce methodology of this study and estimate tree crowns and VI value for each tree crown for shaded and non-shaded areas which would provide insight in examining variation in vegetation phenology.

Bibliography

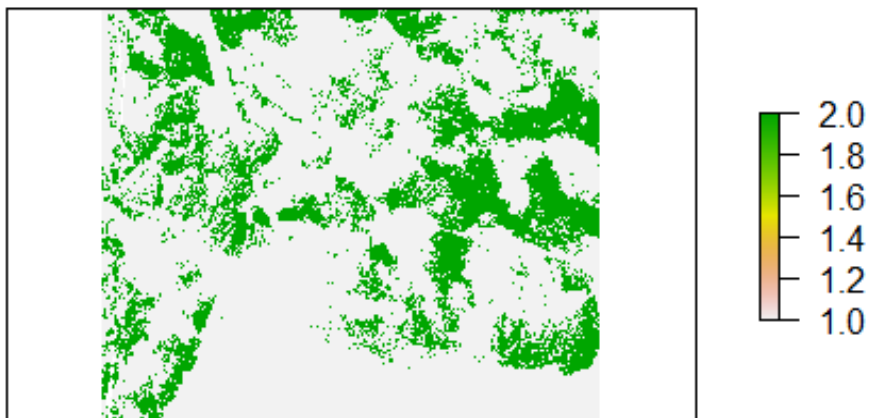
- Aboutalebi, A. Torres-Rua, A. McKee, M. and Kustas P, W. (2017). Evaluation of Different Shadow Detection Methods and Their Impact on Vegetation Indices and ET using UAV High-Resolution Imageries over Vineyards. Utah University, Fall Meeting. New Orleans.
- Al Ajmi, D. (2009). Remote Sensing: Fundamentals, Types and Monitoring Applications of Environmental Consequences of War. In Environmental Consequences of War and Aftermath (pp. 41-124). Springer, Berlin, Heidelberg.
- Berni, J. A. J., Zarco-Tejada, P. J., Suárez, L., González-Dugo, V., and Fereres, E. (2009). Remote Sensing of Vegetation from UAV Platforms Using Lightweight Multispectral and Thermal Imaging Sensors. Int. Arch. Photogramm. Remote Sens. Spatial Inform. Sci, 38(6), 6.
- Buisson, E., Alvarado, S. T., Le Stradic, S., and Morellato, L. P. C. (2017). Plant Phenological Research Enhances Ecological Restoration. Restoration Ecology, Wiley, 2017, 25 (2), pp.164 - 171.
- Enderle, D. I., and Weih Jr, R. C. (2005). Integrating supervised and unsupervised classification methods to develop a more accurate land cover classification. Journal of the Arkansas Academy of Science, 59(1), 65-73.
- Gilabert, M. A., González-Piqueras, J., Martínez, B., Maselli, F., Menenti, M., and Brivio, P. A. (2010). Theory and Applications of Vegetation Indices. Remote Sensing Optical Observations of Vegetation Properties, 1-43.
- Gordo, O., and Sanz, J. J. (2005). Phenology and Climate Change: A Long-Term Study in a Mediterranean Locality. Oecologia, 146(3), 484-495.
- Hsieh, Y. T., Wu, S. T., Chen, C. T., and Chen, J. C. (2016). Analyzing Spectral Characteristics of Shadow Area From Ads-40 High Radiometric Resolution Aerial Images. International Archives of the Photogrammetry, Remote Sensing and Spatial Information Sciences, 41.
- IDB, (n.d.). Index database: A database for remote sensing index, Retrieved from <https://www.indexdatabase.de>
- Landklif, (n.d.). LandKlif - Effects of climate change on biodiversity and ecosystem services in near-natural, agrarian and urban landscapes and strategies for the management of climate change. Retrieved from <https://www.bayklif.de/verbundprojekte/landklif/>
- Liu, H., Zhang, F., Zhang, L., Lin, Y., Wang, S., and Xie, Y. (2020). UNVI-Based Time Series for Vegetation Discrimination Using Separability Analysis and Random Forest Classification. Remote Sensing, 12(3), 529.

- Neto, P., and (Pix4D), B. (n.d.). Menu Process Processing Options... 1. Initial Processing General. Retrieved September 13, 2020, from <https://support.pix4d.com/hc/en-us/articles/202557759-Menu-Process-Processing-Options-1-Initial-Processing-General>
- Nord, E. A., and Lynch, J. P. (2009). Plant Phenology: A Critical Controller of Soil Resource Acquisition. *Journal of experimental botany*, Volume 60, Issue 7, May 2009, Pages 1927–1937.
- Pons, X., and Padró, J. C. (2019, July). An Empirical Approach on Shadow Reduction of UAV Imagery in Forests. In *IGARSS 2019-2019 IEEE International Geoscience and Remote Sensing Symposium* (pp. 2463-2466). IEEE.
- R Core Team (2013). R: A language and environment for statistical computing. R Foundation for Statistical Computing, Vienna, Austria. URL <http://www.R-project.org/>.
- Richardson, A. D., Hufkens, K., Milliman, T., and Frolking, S. (2018). Intercomparison of Phenological Transition Dates Derived from the PhenoCam Dataset V1. 0 and MODIS Satellite Remote Sensing. *Scientific reports*, 8(1), 1-12.
- Sanin, A., Sanderson, C., and Lovell, B. C. (2012). Shadow Detection: A Survey and Comparative Evaluation of Recent Methods. *Pattern recognition*, 45(4), 1684-1695.
- Sarabandi, P., Yamazaki, F., Matsuoka, M., and Kiremidjian, A. (2004, September). Shadow Detection and Radiometric Restoration in Satellite High Resolution Images. In *IGARSS 2004. 2004 IEEE International Geoscience and Remote Sensing Symposium* (Vol. 6, pp. 3744-3747). IEEE
- Shahtahmassebi, A., Yang, N., Wang, K., Moore, N., and Shen, Z. (2013). Review of Shadow Detection and De-Shadowing Methods in Remote Sensing. *Chinese Geographical Science*, 23(4), 403-420.
- Shi, W., and Li, J. (2012). Shadow Detection in Color Aerial Images Based on HSI Space and Color Attenuation Relationship. *EURASIP Journal on Advances in Signal Processing*, 2012(1), 141.
- Slonim, N. Aharoni, E. and Crammer, K., (August 2013) Hartigan's K-Means Versus Lloyd's K-Means – Is It Time for a Change? *Proceedings of the Twenty-Third International Joint Conference on Artificial Intelligence*, Beijing, China, AAAI Press / International Joint Conferences on Artificial Intelligence
- St Peter, J., Hogland, J., Hebblewhite, M., Hurley, M. A., Hupp, N., and Proffitt, K. (2018). Linking Phenological Indices from Digital Cameras in Idaho and Montana to MODIS NDVI. *Remote Sensing*, 10(10), 1612

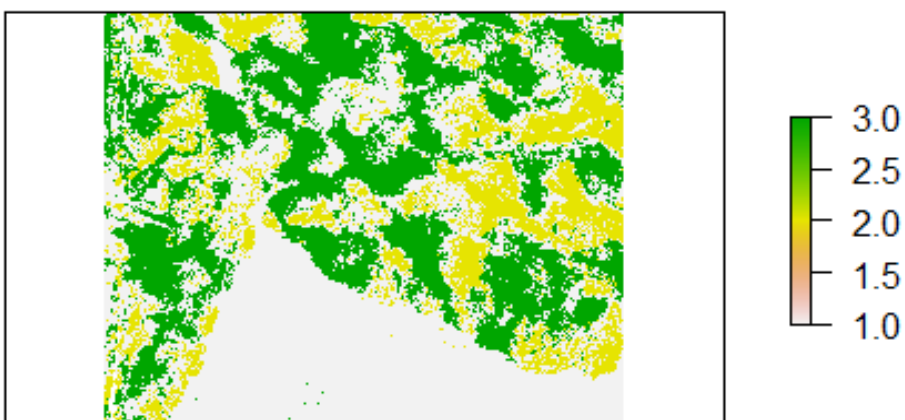
- Van der Maarel, E., (Eds.). (2005). *Vegetation Ecology* (1st ed.). United Kingdom, Blackwell Science ltd.
- Wan, L., Li, Y., Cen, H., Zhu, J., Yin, W., Wu, W., and He, Y. (2018). Combining UAV-Based Vegetation Indices and Image Classification to Estimate Flower Number in Oilseed Rape. *Remote Sensing*, 10(9), 1484
- Wang, Q., Yan, L., Yuan, Q., and Ma, Z. (2017). An Automatic Shadow Detection Method for VHR Remote Sensing Orthoimagery. *Remote Sensing*, 9(5), 469.
- Wegmann, M., Leutner, B., and Dech, S., (2016). *Remote Sensing and GIS for Ecologists: Using Open Source Software*. Exeter: Pelagic Publishing, UK.
- Zhang, H. Sun, K. and Wenzhuo, L. (2014) Object-Oriented Shadow Detection and Removal from Urban High-Resolution Remote Sensing Images, *IEEE Transactions on Geoscience and Remote Sensing*, 52(11):6972-6982
- Zhang, L., Sun, X., Wu, T., and Zhang, H. (2015). An analysis of shadow effects on spectral vegetation indexes using a ground-based imaging spectrometer. *IEEE Geoscience and Remote Sensing Letters*, 12(11), 2188-2192.

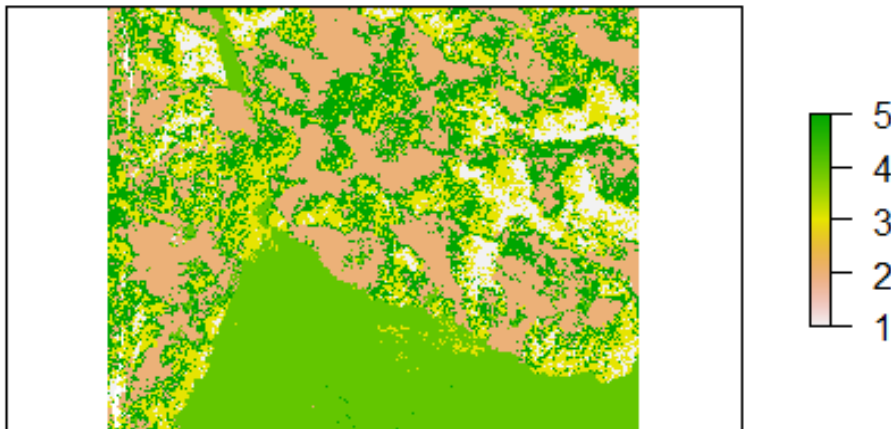
Annexure 1:
Unsupervised Hartigan-Wong Clusters

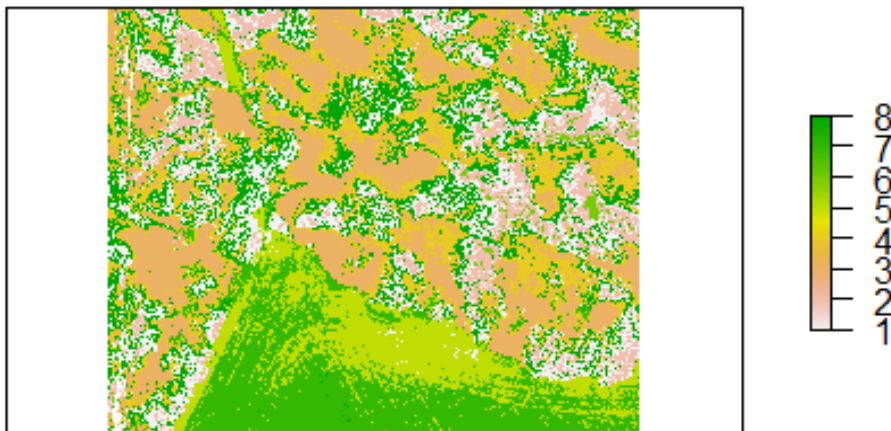
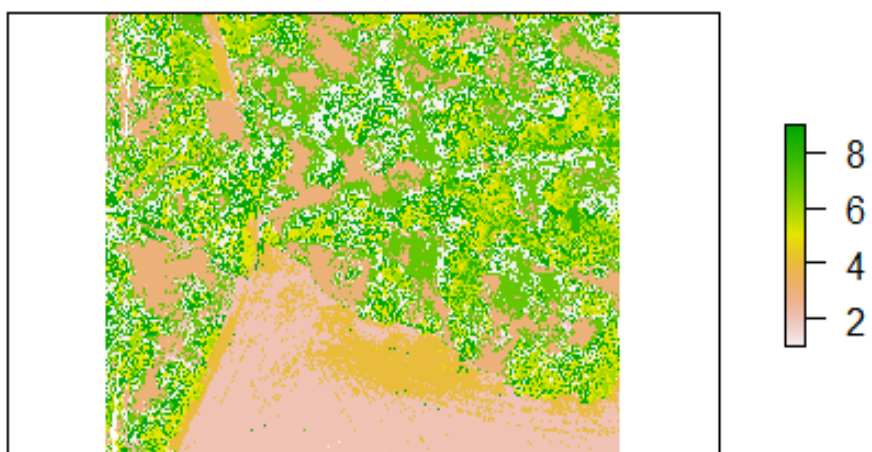
30.05.2019 Subset Hartigan-Wong_2



30.05.2019 Subset Hartigan-Wong_3

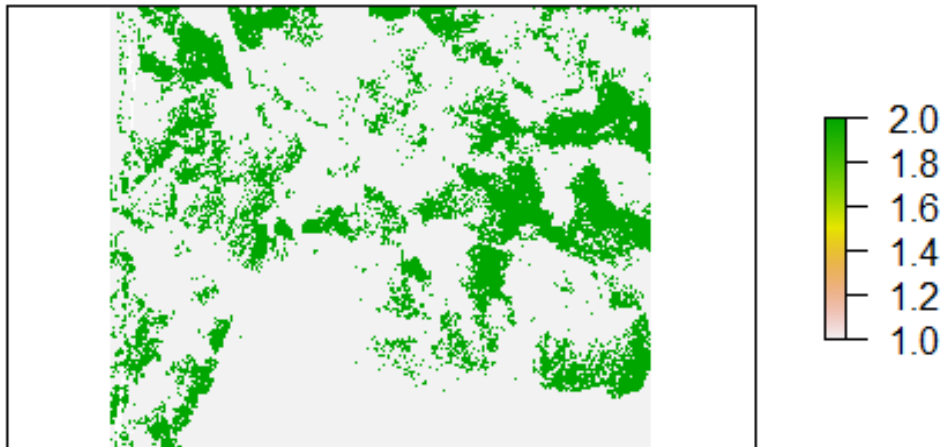


30.05.2019 Subset Hartigan-Wong_5**30.05.2019 Subset Hartigan-Wong_6****30.05.2019 Subset Hartigan-Wong_7**

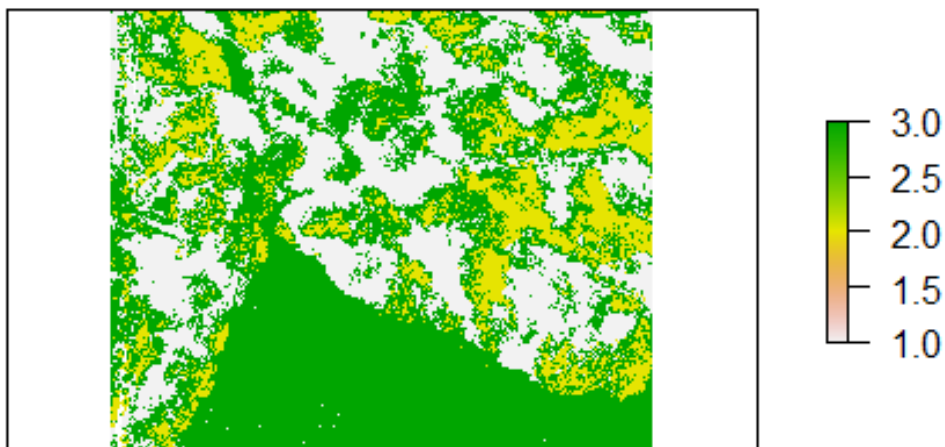
30.05.2019 Subset Hartigan-Wong_8**30.05.2019 Subset Hartigan-Wong_9****30.05.2019 Subset Hartigan-Wong_10**

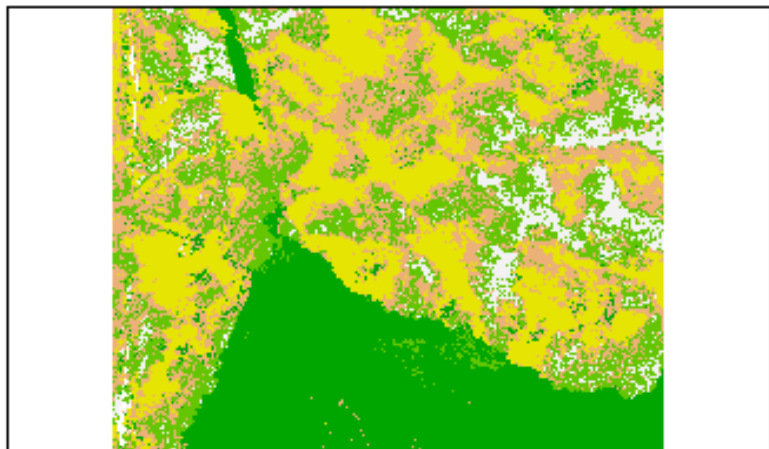
Annexure 2:
Unsupervised Lloyd Clusters

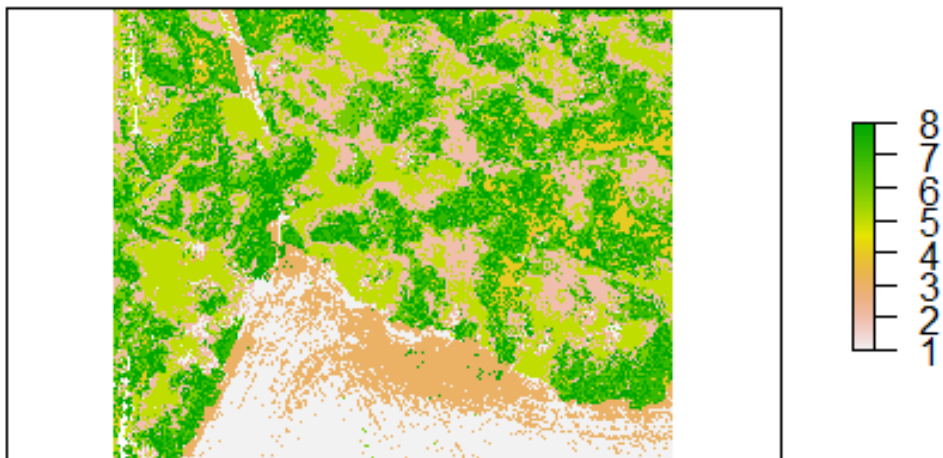
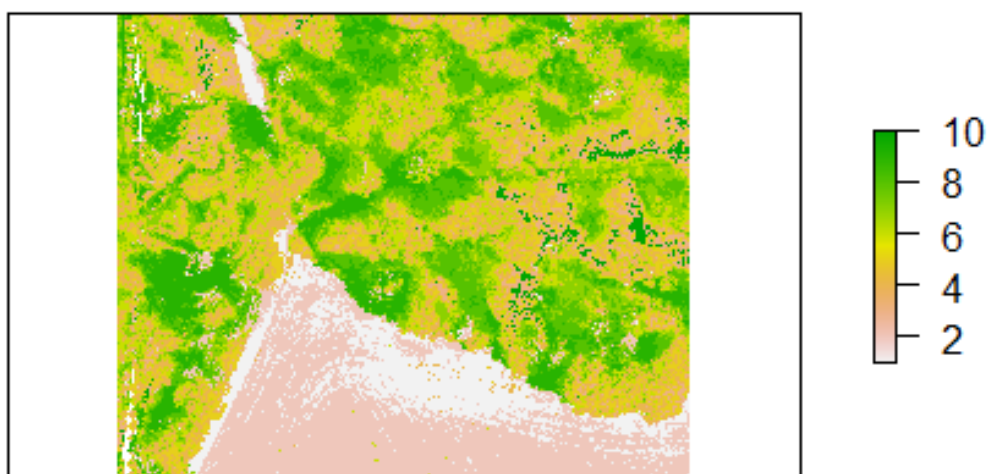
30.05.2019 Subset Lloyd_2



30.05.2019 Subset Lloyd_3



30.05.2019 Subset Lloyd_5**30.05.2019 Subset Lloyd_6****30.05.2019 Subset Lloyd_7**

30.05.2019 Subset Lloyd_8**30.05.2019 Subset Lloyd_9****30.05.2019 Subset Lloyd_10**

Annexure 3:
Area of the Samples

Table I: Area of the Samples for Training and Validation Dataset (in sqm) (Own Illustration, ArcMap)

Class	Land cover	Training Samples			Validation Samples		
		30 May Subset	30-May	11-April	30 May Subset	30-May	11-April
1	Shadows	35.56	93.97	19.82	18.19	99.42	9.65
2	Forest	42.88	119.82	27.50	24.23	109.24	8.71
3	Grassland	34.20	211.38	252.46	21.94	274.32	329.24
4	Pathway	7.70	21.89	58.48	7.14	24.04	21.99
5	Cropland	0	150.48	140.64	0	180.61	101.90
6	Tree Trunks	0	0	15.32	0	0	15.66
7	Dormant Forest	0	0	44.43	0	0	27.12
Total Area		120.35	597.54	558.65	71.50	687.63	514.26

Annexure 4:
Overview of Accuracy of Shadow Detection Methods

Table II: Overview of Accuracy of subset of 30.05.2019

	Unsupervised				Supervised		Threshold					Vegetation Indices			
	HW	Lloyd	Forgy	MacQueen	MLC	RF	Blue	Green	Red	Red Edge	NIR	CCCI	EVI	GCC	NDVI
Shadows	0.9778	0.9844	0.9867	0.9878	0.9690	0.9993	0.9880	0.9877	0.9827	0.9770	0.6997	0.9270	0.5703	0.7223	0.9510
Forest	0.7983	0.7922	0.5767	0.7800	0.9732	0.9800	0.9337	0.8207	0.9350	0.6673	0.6900	0.5773	0.8467	0.7867	0.9280
Grassland	0.7722	0.7800	0.7911	0.7717	0.9350	0.9590	0.9590	0.9100	0.9470	0.8463	0.6683	0.8983	0.6777	0.8933	0.9567
Pathway	0.4894	0.4856	0.4122	0.4894	0.9882	0.9957	0.9580	0.9443	0.9713	0.8253	0.4300	0.5000	0.9267	0.9630	0.9310
Overall	0.6392	0.6408	0.5375	0.6358	0.9758	0.9752	0.9395	0.8735	0.9385	0.7435	0.4330	0.5885	0.6330	0.7620	0.9125

Table III: Overview of Accuracy 30.05.2019

	Unsupervised		Supervised		Threshold					Vegetation Indices			
	HW	Lloyd	MLC	RF	Blue	Green	Red	RedEdge	NIR	CCCI	EVI	GCC	NDVI
Shadows	0.9666	0.9463	0.9979	0.9996	0.9796	0.9825	0.9914	0.9938	0.8377	0.9220	0.6451	0.7483	0.9231
Forest	0.6116	0.6358	0.9927	0.9927	0.8729	0.6438	0.9235	0.5473	0.7090	0.7594	0.8649	0.8594	0.8314
Grassland	0.7245	0.7419	0.9910	0.9910	0.7264	0.7420	0.6996	0.7143	0.7402	0.6507	0.6852	0.6220	0.7729
Pathway	0.4266	0.4315	0.9994	0.9994	0.8692	0.7618	0.8777	0.7595	0.5155	0.6585	0.8081	0.9249	0.6822
Cropland	0.8182	0.7651	0.9951	0.9951	0.5603	0.6663	0.6416	0.6940	0.6475	0.6021	0.5097	0.6648	0.6325
Overall	0.54820	0.54040	0.99200	0.98650	0.6824	0.6148	0.7224	0.5868	0.5040	0.5555	0.5181	0.6171	0.6379

Table IV: Overview of Accuracy 11.04.2019

	Unsupervised		Supervised		Threshold					Vegetation Indices			
	HW	Lloyd	MLC	RF	Blue	Green	Red	RedEdge	NIR	CCCI	EVI	GCC	NDVI
Shadows	0.7238	0.6593	0.7661	0.7906	0.5100	0.5893	0.5563	0.6875	0.5233	0.5485	0.4963	0.5067	0.4935
Forest	0.6859	0.6492	0.9746	0.9672	0.7577	0.5073	0.5727	0.5683	0.5265	0.5587	0.7383	0.5843	0.7057
Grassland	0.7783	0.7920	0.9732	0.9530	0.7823	0.8063	0.5420	0.6367	0.9250	0.6196	0.7597	0.7218	0.7290
Pathway	0.4590	0.4579	0.8807	0.8802	0.5740	0.5703	0.5873	0.5548	0.5587	0.6568	0.5728	0.6090	0.7358
Cropland	0.8929	0.6492	0.9808	0.9305	0.9073	0.8742	0.8940	0.6950	0.5752	0.5622	0.9322	0.8497	0.9320
Tree Trunks	0.5963	0.6336	0.7927	0.8686	0.5168	0.5408	0.6647	0.5875	0.5498	0.5430	0.5573	0.6495	0.6995
Dormant Forest	0.7563	0.7306	0.9151	0.9286	0.6465	0.7340	0.5860	0.6860	0.4377	0.6499	0.8282	0.6570	0.8903
Overall	0.4839	0.4660	0.8244	0.8331	0.4354	0.4177	0.3640	0.3671	0.2889	0.2993	0.4820	0.4069	0.5557

Declaration of Originality

I declare that this thesis is my own work and that, to the best of my knowledge, it contains no material previously published, or substantially overlapping with material submitted for the award of any other degree at any institution, except where due acknowledgment is made in the text.

Sukhveen Kaur

15.09.2020